Supporting Information for

Universal Host Materials for Red, Green and Blue High-Efficiency Single-Layer Phosphorescent Organic Light-Emitting Diodes

Fabien Lucas,[a] Cassandre Quinton,[a] Sadiara Fall,[b] Thomas Heiser,[b] Denis Tondelier,[c] Bernard Geffroy,[c,d] Nicolas Leclerc,[e] Joëlle Rault-Berthelot,[a] and Cyril Poriel[a*]

Table des matières

1 General experimental methods

1.1 Synthesis

All manipulations of oxygen and moisture-sensitive materials were conducted with a standard Schlenk technique. All glassware was kept in an oven at a temperature of 80°C. Argon atmosphere was generated by three repetitive cycles of vacuum/Argon using a schlenck ramp. Commercially available reagents and solvents were used without further purification other than those detailed below. THF was obtained through a PURE SOLV™ solvent purification system. Light petroleum refers to the fraction with bp 40-60°C. Analytical thin layer chromatography was carried out using aluminum backed plates coated with Merck Kieselgel 60 GF254 and visualized under UV light (at 254 and 360 nm). Flash chromatography was carried out using Teledyne Isco CombiFlash® Rf 400 (UV detection 200-360nm), over standard silica cartridges (Redisep® Isco or Puriflash® columns Interchim). ^{1}H and ^{13}C NMR spectra were recorded using Bruker 300 MHz instruments (^{1}H frequency, corresponding ^{13}C frequency: 75 MHz); chemical shifts were recorded in ppm and J values in Hz. The residual signals for the NMR solvents used are 5.32 ppm (proton) and 53.84 ppm (carbon) for CD_2Cl_2.[1] In the ^{13}C NMR spectra, signals corresponding to C, CH, CH_2 or CH_3 groups, assigned from DEPT experiment, are noted. The following abbreviations have been used for the NMR assignment: s for singlet, d for doublet, t for triplet, q for quadruplet and m for multiplet. High resolution mass spectra were recorded at the Centre Régional de Mesures Physiques de l'Ouest (CRMPO-Rennes) on a Thermo Ficher Q-Exactive instrument or a Bruker MaXis 4G or a Bruker Ultraflex III.

1.2 Spectroscopic studies

Cyclohexane (spectroscopic grade, Acros), 2-MeTHF (Anhydrous, >99 %, Sigma Aldrich), 1 N solution of sulfuric acid in water (Standard solution, Alfa Aesar) and quinine sulfate dihydrate (99+%, ACROS organics) were used without further purification.

UV-visible spectra were recorded using an UV-Visible spectrophotometer SHIMADZU UV-1605. Molar extinction coefficients (ε) were calculated from the gradients extracted from the plots of absorbance *vs* concentration with five solutions of different concentrations for each sample.

Emission spectra and phosphorescence decay were recorded with a HORIBA Scientific Fluoromax-4 equipped with a Xenon lamp. Singlet and triplet energy levels were calculated from the onset of the fluorescence spectrum at RT and from the maximum of the first phosphorescence emission peak at 77 K respectively. Conversion in electron-volt was obtained with the following formula: $E_{S\,or\,T}(eV) = \frac{hc}{\lambda}$ with h = 6.62607×10^{-34} J.s, C = 2.99792×10^{17} nm.s^{-1} and 1 J = 1.60218×10^{-19} eV. This equation can be simplified as:l

$$E_{S\,or\,T}(eV) = \frac{1239.84}{\lambda}$$ with λ formulated in nm.

Quantum yields in solution (øsol) were calculated relative to quinine sulfate (øref = 0.546 in H_2SO_4 1 N). øsol was determined according to the following equation,

$$\phi sol = \phi ref \times \frac{Grad_s}{Grad_r} \times \left(\frac{\eta_s}{\eta_r}\right)^2$$

where subscripts *s* and *r* refer respectively to the sample and reference, *Grad* is the gradient from the plot of integrated fluorescence intensity *vs* absorbance, η is the refracting index of the solvent (η_s = 1.426 for cyclohexane). Five solutions of different concentration (A < 0.1) of the sample and five solutions of the reference (quinine sulfate) were prepared. The integrated area of the fluorescence peak was plotted against the absorbance at the excitation wavelength for both the sample and reference. The gradients of these plots were then injected in the equation to calculate the reported quantum yield value for the sample.

Low temperature (77 K) measurements were performed in 2-MeTHF which freezes as a transparent glassy matrix. Measurements were carried in a singleblock quartz tube containing the solution, which was placed in an oxford Optistat Cryostat cooled with liquid nitrogen.

Infrared spectra were recorded on a Bruker Vertex 7 0 using a diamond crystal MIRacle ATR (Pike).

1.3 Electrochemical studies

Electrochemical experiments were performed under argon atmosphere using a Pt disk electrode (diameter 1 mm). The counter electrode was a vitreous carbon rod. The reference electrode was either a silver wire in a 0.1 M $AgNO_3$ solution in CH_3CN for the studies in oxidation or a Silver wire coated by a thin film of AgI (silver(I)iodide) in a 0.1 M Bu_4NI solution in DMF for the studies in reduction. Ferrocene was added to the electrolyte solution at the end of a series of experiments. The ferrocene/ferrocenium (Fc/Fc^+) couple served as internal standard. The three electrodes cell was connected either to a PAR Model 273 potentiostat/galvanostat (PAR, EG&G, USA) monitored with the ECHEM Software for **SPA-2,7-F(POPh$_2$)$_2$** and **SPA-F** or to a potentiostat/galvanostat (Autolab/PGSTAT101) monitored with the Nova 2.1 Software for **SPA-3,6-F(POPh$_2$)$_2$** and **SPA-2-FPOPh$_2$**. Activated Al_2O_3 was added in the electrolytic solution to remove excess moisture. For a further comparison of the electrochemical and optical properties, all potentials are referred to the SCE electrode that was calibrated at –0.405 V *vs.* Fc/Fc^+ system. Following the work of Jenekhe,[2] we estimated the electron affinity (EA) or lowest unoccupied molecular orbital (LUMO) and the ionization potential (IP) or highest occupied molecular orbital (HOMO) from the redox data. The LUMO level was calculated from: LUMO (eV) = -[E_{onset} (vs SCE) + 4.4] in the case of reversible wave or from LUMO (eV) = -[E_{onset}^{red} (vs SCE) + 4.4] in the case of irreversible wave. Similarly the HOMO level was calculated from: HOMO (eV) = -[E_{onset} (vs SCE) + 4.4] in the case of reversible wave or from HOMO (eV) = -[E_{onset}^{ox} (vs SCE) + 4.4] in the case of irreversible wave, based on an SCE energy level of 4.4 eV relative to the vacuum. The electrochemical gap was calculated from: ΔE^{el} =|HOMO-LUMO| (in eV).

1.4 Molecular modelling

Full geometry optimization of the ground state and frequency calculations were performed with Density Functional Theory (DFT)[3, 4] using the hybrid Becke 3 parameters exchange functional[5-7] and the Lee-Yang-Parr non-local correlation functional[8] (B3LYP) implemented in the Gaussian 16 program suite[9] using the 6-31G(d,p) basis set and the default convergence criterion implemented in the program. Transition diagrams were obtained through TD-DFT calculations performed using the B3LYP functionals and the 6-311+G(d,p) basis set on the geometry of S0. Figures were generated with GaussView 6.0 and Gauss Sum 3.0. Geometry optimization of the first excited triplet state (T1) was performed using Time-Dependent Density Functional Theory (TD-DFT) calculations using the B3LYP functional and the 6-311+G(d,p) basis set. Spin

density (SD) representation was obtained through TD-DFT calculations performed using the B3LYP functional and the extended 6-311+G(d,p) basis set and a triplet spin on the previously optimized geometry of T1. T1 to S0 energy transition (ET) was calculated from the difference between the total energy of the molecule in its respective excited triplet state (found trough TD-DFT, B3LYP 6-311+G(d,p)) and its ground singlet state (found through DFT, B3LYP 6-311+G(d,p)) in their optimized geometries.

1.5 Thermal analysis

Thermal Gravimetric Analysis (TGA) was carried out by using a Q50 apparatus of TA instruments at the Ecole Nationale Supérieure de Chimie de Rennes for **SPA-F** or a Mettler-Toledo TGA-DSC-1 apparatus at Institut des Sciences Chimiques de Rennes for **SPA-2,7-F(POPh$_2$)$_2$**, and **SPA-2-FPOPh$_2$** or Q50 apparatus of TA instruments at the Institut de Chimie et Procédés pour l'Energie, l'Environnement et la Santé de Strasbourg for **SPA-3,6-F(POPh$_2$)$_2$** TGA curved were measured at 10°C/min from 30°C to 1000°C under a nitrogen flux. Differential Scanning Calorimetry (DSC) was carried out by using a NETZSCH DSC 200 F3 instrument equipped with an intracooler at Institut des Sciences Chimiques de Rennes. DSC traces were measured at 10°C/min, 2 heating/cooling cycles were successively carried out under a nitrogen flux.

1.6 Device fabrication and characterization

Single layer phosphorescent organic light emitting diodes (SL-PhOLEDs)

The structure of the SL device is the following: ITO/PEDOT:PSS (40 nm)/Emissive layer *host:guest 10 %* (100 nm)/LiF (1.2 nm)/Al (100 nm). In this device, ITO/PEDOT:PSS (Poly(3,4-ethylenedioxythiophene)-poly(styrenesulfonate)) is used as the anode and a thin film of lithium fluoride covered with aluminum is the cathode. The devices have been fabricated onto patterned ITO coated glass substrates from XinYan Tech (thickness: 100 nm and sheet resistance: less of 20 W/m). The organic materials are deposited onto the ITO anode by sublimation under high vacuum (< 10^{-6} Torr) at a rate of 0.2 – 0.3 nm/s. The entire device is fabricated in the same run without breaking the vacuum. In this study, the thicknesses of the different organic layers were kept constant for all the devices. The active area of the devices defined by the overlap of the ITO anode and the metallic cathode was 0.3 cm². The current-voltage-luminance (I-V-L) characteristics of the devices were measured with a regulated power supply (Laboratory Power Supply EA-PS 3032-10B) combined with a multimeter and a 1 cm^2 area silicon calibrated photodiode (Hamamatsu). The spectral emission was recorded with a SpectraScan PR650 spectrophotometer. All the measurements were performed at room temperature and at ambient atmosphere with no further encapsulation of devices.

Space-charged limited current (SCLC) diodes

<u>*Solution preparation conditions:*</u> All four investigated molecules were dissolved in chloroform ($CHCl_3$) to form solutions with same concentrations of 30 mg/ml. Well-sealed vials with prepared solutions were left stirring at room temperature for at least 3 hours prior to spin-coating.

<u>*Fabrication of hole-only space-charge limited current (SCLC) diodes:*</u> Indium-tin oxide (ITO) coated glass was used as a substrate. A sequential cleaning of the substrates in soap water, distilled water, acetone and isopropanol (15 min for each step) using ultrasonic bath was performed. A thin, highly conductive poly(ethylenedioxythiophene):polystyrene sulfonate

(PEDOT:PSS) layer was spin-coated onto pre-cleaned ITO and used as a bottom electrode. Then samples were transferred into a nitrogen-filled glove box system and thermally annealed at 140°C for 30 min. After that, all the investigated layers were spin-coated at 600 rpm for 80 sec to obtain homogeneous thin films. Spin-coated samples were placed into a vacuum chamber and left overnight under high vacuum ($\approx 5\times10^{-7}$ mbar). SCLC devices were completed by sequential thermal evaporation of MoO_3 (7nm) and Ag (250 nm) layers.

Fabrication of electron-only space-charge limited current (SCLC) diodes: Identical ITO substrates and cleaning conditions were applied as for hole-only samples (see above). A thin ZnO layer (20-25 nm) was spin-coated onto pre-cleaned ITO and thermally annealed at 110°C for 15 min and used as a bottom contact. After deposition of the molecules by spin-coating and placing into a vacuum chamber, devices were completed by a sequential evaporation of Ca (20 nm) and Al (300 nm) as a top contact.

SCLC diode current-voltage characteristics were measured, inside the glove-box, using Keithley semiconductor characterization system 4200. The active-layer thicknesses were measured after SCLC characterization using a profilometer.

2 Synthetic procedures

General procedure for the brominated spiro platform synthesis

1st step: The halogen derivative (1.0 eq) was dissolved in dry THF under argon and the mixture was cooled to -78°C. *n*-BuLi (2.5M in hexanes, 1.2 eq) was then added dropwise and the resulting mixture was stirred for 30 min. The fluorenone derivative (1.0 eq) was dissolved under argon in dry THF at -78°C and added dropwise to the reaction mixture and stirred for 30 additional minutes. Then, the reaction was allowed to warm up to room temperature under stirring overnight. Solvent was removed under reduced pressure and the crude was dried under vacuum at 60°C for 2 hours.

2nd step: Without further purification, the crude was dissolved in acetic acid and hydrochloric acid was added under stirring. The reaction mixture was refluxed for 5 hours under stirring.

After cooling to room temperature, water was added to the reaction mixture. The precipitate was filtered off and then dissolved in CH_2Cl_2. The organic layer was washed with water and dried over $MgSO_4$. Solvent was then removed under reduced pressure. A hot saturated solution of the crude in $CHCl_3$ was prepared and the product was precipitate by adding MeOH. This was repeated several times. Product was finally dried under vacuum at 40°C overnight.

10-phenyl-10H-spiro[acridine-9,9'-fluorene] [SPA-F]

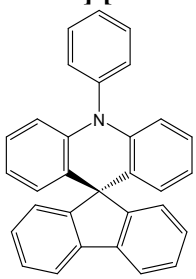

The *title compound* was synthesized using the general procedure for the brominated spiro platform synthesis.

1st step: 2-Bromotriphenylamine (2.00 g, 6.17 mmol, 1.0 eq) in THF (35 mL), *n*-BuLi (2.50 M in hexanes, 2.96 mL, 7.40 mmol, 1.2 eq) and fluorenone (1.11 g, 6.17 mmol, 1.0 eq) in THF (20 mL).
2nd step: acetic acid (50 mL) and hydrochloric acid (5 mL).
After purification, a white solid was obtained (2.06 g, 5.06 mmol); yield 82%. ^{1}H NMR (300 MHz, CD_2Cl_2): δ 7.84 (d, J = 7.5 Hz, 2H), 7.74 (t, J = 7.8 Hz, 2H), 7.60 (t, J = 7.5 Hz, 1H), 7.55 – 7.49 (m, 2H), 7.41 (t, J = 7.5 Hz, 4H), 7.34 – 7.26 (m, 2H), 6.97 – 6.88 (m, 2H), 6.56 (t, J = 7.5 Hz, 2H), 6.41 – 6.34 (m, 4H) ppm. ^{13}C NMR (75 MHz, CD_2Cl_2): δ 157.01 (2C), 141.84 (2C), 141.45 (C), 139.66 (2C), 131.53 (4CH), 128.93 (CH), 128.77 (2CH), 128.11 (2CH), 127.86 (2CH), 127.65 (2CH), 125.96 (2CH), 125.18 (2C), 120.82 (2CH), 120.46 (2CH), 115.19 (2CH), 57.26 (C) ppm. IR (ATR, platinum): 3073, 3020, 2604, 1960, 1909, 1591, 1569, 1501, 1479, 1450, 1331, 1296, 1271, 1171, 1153, 1125, 1100, 1074, 1063, 1022, 1006, 988, 940, 927, 904, 895, 863, 846, 745, 735, 697, 651, 638, 622, 543, 526, 458, 417 cm^{-1}. HRMS (ASAP, 180 °C): Found $[M+H]^+$ 408.1744; $C_{31}H_{22}N$ required 408.1747. m.p.: 280 °C.

2-Bromo-10-phenyl-10H-spiro[acridine-9,9'-fluorene] [SPA-2-FBr]

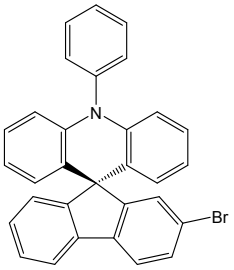

The *title compound* was synthesized using the general procedure for the brominated spiro platform synthesis.

1st step: 2-Bromotriphenylamine (2.00 g, 9.26 mmol, 1.2 eq) in dry THF (88 mL), *n*-BuLi (2.50 M in hexanes, 3.71 mL, 9.26 mmol, 1.2 eq), 2-Bromofluorenone (3.00 g, 7.72 mmol, 1.0 eq) in dry THF (40 mL).
2nd step: acetic acid (100 mL) and hydrochloric acid (10 mL)
After purification a white solid was obtained (3.57 g yield 95 %);^{1}H NMR (300 MHz, CD_2Cl_2) δ 7.86 – 7.81 (m, 1H), 7.79 – 7.70 (m, 3H), 7.65 – 7.49 (m, 5H), 7.46 – 7.38 (m, 2H), 7.36 – 7.29 (m, 1H), 6.95 (td, J = 8.5, 7.1, 1.6 Hz, 2H), 6.59 (td, J = 7.5, 1.3 Hz, 2H), 6.43 – 6.35 (m, 4H).^{13}C NMR (75 MHz, CD_2Cl_2) δ 158.99 (C), 156.91 (C), 141.71 (2C), 141.30 (C), 138.80 (C), 138.56 (C), 131.56 (2CH), 131.49 (2CH), 131.31 (CH), 129.27 (CH), 129.23 (CH), 129.00 (CH), 128.30 (CH), 127.96 (2CH), 127.91 (2CH), 126.07 (CH), 124.23 (2C), 122.16 (C), 121.96 (CH), 120.94 (2CH), 120.57 (CH), 115.38 (2CH), 57.34 (C). IR (ATR, platinum) : 1610, 1590, 1571, 1508, 1497, 1475, 1446, 1403, 1386, 1323, 1307, 1291, 1269, 1259, 1220, 1160.20, 1099, 1073, 1059, 1022, 1004, 950, 941, 926, 902, 879, 869, 839, 816, 775, 752, 740, 729, 709, 699, 675, 660, 646, 638, 623, 573, 542, 529, 496, 479, 429, 418 cm^{-1}. HRMS (MALDI, DCTB): Found $[M^{+\cdot}]$ 485.078; $C_{31}H_{20}N^{79}Br$ required 485.07736 m.p.: 262 °C

2,7-dibromo-10-phenyl-10H-spiro[acridine-9,9'-fluorene] [SPA-2,7-FBr$_2$]

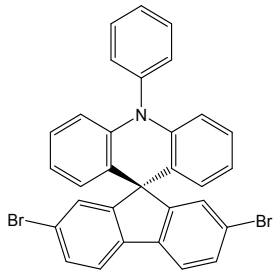

The *title compound* was synthesized using the general procedure for the brominated spiro platform synthesis.

1st step: 2-Bromotriphenylamine (0.500 g, 1.54 mmol, 1.0 eq) in dry THF (10 mL), *n*-BuLi (2.50 M in hexanes, 0.740 mL, 1.85 mmol, 1.2 eq), 2,7-Dibromofluorenone (0.520 g, 1.54 mmol, 1.0 eq) in dry THF (15 mL).
2nd step: acetic acid (20 mL) and hydrochloric acid (2 mL)
After purification a white solid was obtained (0.650 g, 1.12 mmol); yield 72%. ^{1}H NMR (300 MHz, CD_2Cl_2): δ 7.78 – 7.66 (m, 4H), 7.64 – 7.57 (m, 1H), 7.57 – 7.44 (m, 6H), 6.96 (ddd, J = 8.5, 7.2, 1.6 Hz, 2H), 6.60 (td, J = 7.5, 1.2 Hz, 2H), 6.37 (ddd, J = 7.7, 4.5, 1.4 Hz, 4H) ppm. ^{13}C NMR (75 MHz, CD_2Cl_2): δ 158.89 (2C), 141.57 (2C), 141.14 (C), 137.69 (2C), 131.58 (2CH), 131.52 (2CH), 131.44 (2CH), 129.38 (2CH), 129.06 (2CH), 128.16 (2CH), 128.07 (CH), 123.23 (2C), 122.66 (2C), 122.06 (2CH), 121.03 (2CH), 115.55 (2CH), 57.37 (C) ppm. IR (ATR, platinum): 1591, 1571, 1501, 1478, 1445, 14085, 1394, 1332, 1307, 1270, 1246, 1170, 1162, 1154, 1101, 1074, 1059, 1026, 1005, 967, 951, 940, 926, 899, 876, 848, 838, 809, 773, 742, 723, 670, 673, 660, 638, 623, 546, 537, 506, 465, 451, 435, 422 cm^{-1}. HRMS (ASAP, 220 °C): Found $[M+H]^+$ 563.9959; $C_{31}H_{20}NBr_2$ required 56.9957. m.p.: 344 °C

3,6-dibromo-10-phenyl-10H-spiro[acridine-9,9'-fluorene] [SPA-3,6-FBr$_2$]

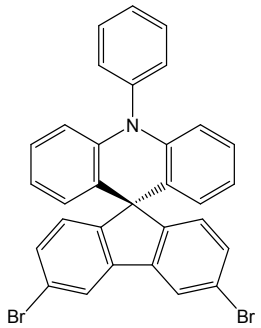

The *title compound* was synthesized using the general procedure for the brominated spiro platform synthesis with a small modification. In this particular case, this is the organo-lithium which is added dropwise onto the fluorenone.

1st step: 2-Bromotriphenylamine (1.15 g, 3.55 mmol, 1.2 eq) in dry THF (40 mL), *n*-BuLi (2.50 M in hexanes, 1.42 mL, 3.55 mmol, 1.2 eq), 2-Bromofluorenone (1.00 g, 2.96 mmol, 1.0 eq) in dry THF (600 mL).
2nd step: acetic acid (100 mL) and hydrochloric acid (10 mL)
After purification a white solid was obtained (1.48 g yield 86 %); ^{1}H NMR (300 MHz, CD_2Cl_2): δ 7.94 (s, 2H), 7.73 (t, J = 7.7 Hz, 2H), 7.64 – 7.57 (m, 1H), 7.50 – 7.41 (m, 4H), 7.34 – 7.19 (m, 2H), 7.07 – 6.86 (m, 3H), 6.57 (t, J = 7.5, 1.3 Hz, 2H), 6.36 (d, J = 7.9 Hz, 3H). ^{13}C NMR

(75 MHz, CD_2Cl_2): δ 156.11 (2C), 141.68 (2C), 140.52 (2C), 132.27 (2CH), 131.57 (2CH), 131.42 (2CH), 129.63 (C) 129.05 (CH), 128.05 (2CH), 127.79 (2CH), 127.71 (2CH), 123.94 (2CH), 123.57 (2C), 122.18 (2C), 120.99 (2CH), 115.42 (2CH), 56.91 (C). IR (ATR, platinum): 1708, 1606, 1590, 1571, 1499, 1475, 1448, 1416, 1403, 1391, 1324, 1271, 1268, 1211, 1197, 1164, 1117, 1100, 1073, 1058, 1025, 943, 924, 906, 896, 869, 847, 826, 812, 772, 750, 737, 721, 698, 676, 660, 633, 622, 592, 567, 548, 528, 478, 469, 431 cm^{-1}. HRMS (MALDI, DCTB): Found [$M^{+\cdot}$] 562.989; $C_{31}H_{20}N^{79}Br_2$ required 562.98787 m.p.: 317 °C

General procedure for the incorporation the diphenyl phosphine oxide groups

1st step: The brominated spiro platform derivative (1.0 eq) was dissolved in dry THF under argon. The reaction mixture was then cooled to -78°C and *n*-BuLi (2.50 M in hexanes, 2.4 eq) was added dropwise. The reaction mixture was stirred for 2 hours at -78°C. Chlorodiphenylphosphine (2.5 eq) was then added and the resulting mixture was stirred for 2 additional hours at -78°C. The reaction mixture was finally allowed to warm up to room temperature overnight under stirring. The reaction mixture was quenched with few drops of absolute ethanol and concentrated under reduced pressure. The crude product was dissolved in CH_2Cl_2. The organic layer was washed with water, brine, dried over $MgSO_4$ and filtered. Solvent was removed under reduce pressure and dried under vacuum at 60°C for 5 hours.

2nd step: Without any further purification, the crude was dissolved in CH_2Cl_2 and H_2O_2 (35 wt. % in water) was added to the mixture which was stirred overnight at room temperature. The organic layer was washed several times with water and dried over $MgSO_4$. Solvent was then evaporated under reduced pressure and the crude was purified with flash chromatography on silica gel.

Diphenyl(10-phenyl-10H-spiro[acridine-9,9'-fluoren]-2'-yl)phosphine oxide [SPA-2-FPOPh$_2$]

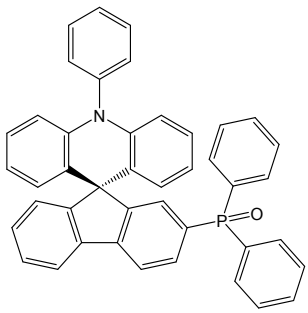

The *title compound* was synthesized using the general procedure for the incorporation of the diphenylposphine oxide groups.

1st step: **SPA-2-FBr** (0.500 g, 1.03 mmol, 1.0 eq), *n*-BuLi (2.50 M in hexanes, 0.62 mL, 1.54 mmol, 1.5 eq) and Chlorodiphenylphosphine (0.570 g, 0.28 mL, 1.75 mmol, 1.5 eq) in dry THF (47 mL).
2nd step: CH_2Cl_2 (50 mL) and H_2O_2 (5 mL, 35 wt. % in water).
After purification flash chromatography on silica gel [column condition: silica cartridge (40 g); solid deposit on Celite®; $\lambda_{detection}$: (254 nm, 280 nm); CH_2Cl_2/CH_3OH (98:2) at 40 mL/min] a white solid was obtained (0.46 g, 73 %); ^1H NMR (300 MHz, CD_2Cl_2) δ 7.90 (d, J = 7.8 Hz 2H), 7.81 (d, J = 11.8 Hz, 1H), 7.72 – 7.33 (m, 17H), 7.32 – 7.26 (m, 2H), 6.94 (dt, J = 8.5, 7.1,

1.7 Hz, 2H), 6.59 (dt, J = 7.5, 1.3 Hz, 2H), 6.39 (dd, J = 7.7, 1.6 Hz, 2H), 6.33 (d, J = 8.4, 1.2 Hz, 2H). ^{13}C NMR (75 MHz, $CDCl_3$): δ 156.95 (C), 156.79 (C), 156.62 (C), 143.29 (C), 143.25 (C), 141.84 (C), 141.13 (C), 138.56 (C), 134.25 (C), 133.51 (C), 132.88 (C), 132.40 (2CH), 132.27 (2CH), 132.18 (CH), 132.14 (CH), 131.45 (2CH), 131.43 (CH), 130.00 (CH), 129.70 (2CH), 129.57 (CH), 128.90 (2CH), 128.75 (2CH), 128.41 (CH), 127.87 (2CH), 127.36 (2CH), 126.20 (CH), 124.43 (C), 121.32 (CH), 120.88 (2CH), 120.54 (CH), 120.36 (CH), 115.27 (2CH) , 57.54 (C) ^{31}P NMR (121 MHz, CD_2Cl_2): δ 27.11 ppm IR (ATR, platinum) 1640, 1610, 1590, 1569, 1501, 1477, 1447, 1437, 1400, 1332, 1320, 1296, 1272, 1187, 1160, 113, 1120, 1105, 1081, 1072, 1058, 1024, 1004, 946, 923, 900, 854, 838, 792, 778, 758 749, 735, 724, 707, 698, 668, 653, 641, 623, 595, 555, 540, 518, 506, 488, 478, 469, 450, 424 cm^{-1}. HRMS (MALDI, DCTB): Found $[M+H]^+$ 608.216; $C_{43}H_{30}NOP$ required 608.21378 m.p.: 290 °C

(10-phenyl-10H-spiro[acridine-9,9'-fluorene]-2',7'-diyl)bis(diphenylphosphineoxide) [SPA-2,7-F(POPh$_2$)$_2$]

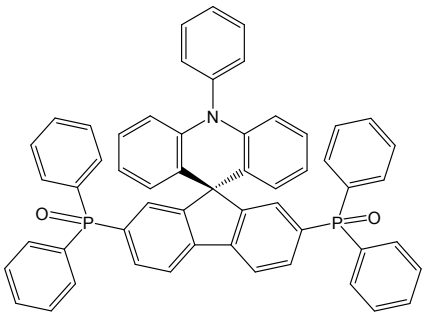

The *title compound* was synthesized using the general procedure for the incorporation of the diphenylposphine oxide groups.

1st step: **SPA-2,7-FBr$_2$** (1.00 g, 1.77 mmol, 1.0 eq), *n*-BuLi (2.50 M in hexanes, 1.7 mL, 4.25 mmol, 2.4 eq) and chlorodiphenylphosphine (0.980 g, 0.82 mL, 4.42 mmol, 2.5 eq) in dry THF (80 mL).
2nd step: CH_2Cl_2 (30 mL) and H_2O_2 (3 mL, 35 wt. % in water).
After purification flash chromatography on silica gel [column condition: silica cartridge (40 g); solid deposit on Celite®; $\lambda_{detection}$: (254 nm, 280 nm); CH_2Cl_2/CH_3OH (97:3) at 40 mL/min], a white solid solid was obtained (1.13 g, 1.40 mmol); yield 79 %. ^{1}H NMR (300 MHz, CD_2Cl_2): δ 7.94 (dd, *J* = 7.9, 2.3 Hz, 2H), 7.82 (d, *J* = 11.6 Hz, 2H), 7.73 – 7.47 (m, 17H), 7.41 (td, *J* = 7.6, 2.7 Hz, 8H), 7.04 (d, *J* = 7.3 Hz, 2H), 6.94 (ddd, *J* = 8.4, 7.2, 1.6 Hz, 2H), 6.60 (td, *J* = 7.5, 1.2 Hz, 2H), 6.38 (dd, *J* = 7.8, 1.5 Hz, 2H), 6.29 – 6.24 (m, 2H). ^{13}C NMR (75 MHz, CD_2Cl_2): δ 156.55 (C), 156.38 (C), 142.02 (C), 141.74 (2C), 140.65 (C), 134.70 (C), 133.63 (2C), 133.34 (C), 132.41 (2CH), 132.32 (4CH), 132.29 (2CH), 132.25 (3C), 132.19 (2CH), 131.36 (2CH), 131.23 (2CH), 129.80 (CH), 129.66 (CH), 128.94 (4CH), 128.78 (4CH), 128.05 (2CH), 126.76 (2CH), 123.61 (2C), 121.44 (CH), 121.26 (CH), 120.90 (2CH), 115.28 (2CH), 57.73 (C) ppm. ^{31}P NMR (121 MHz, CD_2Cl_2): δ 27.11 ppm. IR (ATR platinum): 3370, 3041, 1592, 1501, 1478, 1448, 1438, 1396, 1333, 1313, 1269, 1187, 1164, 1120, 1103, 1085, 1073, 1058, 1026, 1000, 962, 946, 933, 870, 847, 760, 750, 724, 709, 696, 663, 651, 641, 624, 566, 540, 518, 485 cm^{-1}. HRMS (ASAP, 320 °C): Found $[M+H]^+$, 808.2525; $C_{55}H_{40}NO_2P_2$ required 808.2529. m.p.: 303 °C.

(10-phenyl-10H-spiro[acridine-9,9'-fluorene]-3',6'-diyl)bis(diphenylphosphine oxide) [SPA-3,6-F($POPh_2$)$_2$]

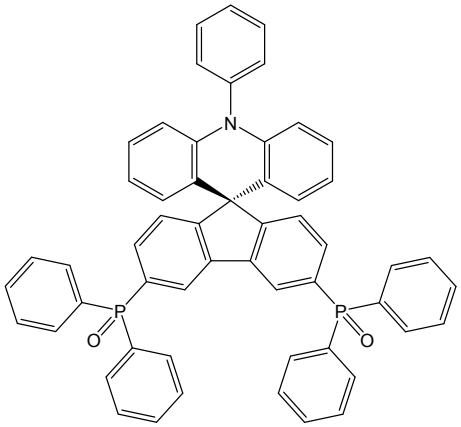

The *title compound* was synthesized using the general procedure for the incorporation of the diphenylposphine oxide groups.

1st step: **SPA-3,6-FBr$_2$** (0.250 g, 0.442 mmol, 1.0 eq), *n*-BuLi (2.50 M in hexanes, 0.42 mL, 1.06 mmol, 2.4 eq) and chlorodiphenylphosphine (0.244 g, 0.20 mL, 1.11 mmol, 2.5 eq) in dry THF (20 mL)
2nd step: CH_2Cl_2 (20 mL) and H_2O_2 (2 mL, 35 wt. % in water).
After purification flash chromatography on silica gel [column condition: silica cartridge (40 g); solid deposit on Celite®; $\lambda_{detection}$: (254 nm, 280 nm); CH_2Cl_2/CH_3OH at 40 mL/min using a gradient from 100% to 95 % during 30 min]a white solid solid was obtained (0.160 g, 0.198 mmol); yield 44 %. ^{1}H NMR (300 MHz, CD_2Cl_2): δ 8.14 (d, J = 11.8 Hz, 2H), 7.80 – 7.67 (m, 10H), 7.62 – 7.39 (m, 18H), 6.95 (dt, J = 7.2, 1.6 Hz, 3H), 6.59 (dt, J = 7.5, 1.2 Hz, 2H), 6.47 – 6.24 (d, J = 6 Hz, 4H) ppm. ^{13}C NMR (75 MHz, CD_2Cl_2): δ 159.96 (C), 159.92 (C), 141.78 (2C), 141.08 (C), 139.21 (C), 139.02 (C), 133.95 (C), 133.92 (2C), 133.22 (CH), 133.07 (CH), 132.59 (C), 132.55 (2C), 132.45 (4CH), 132.40 (2CH), 132.36 (2CH), 132.32 (4CH), 131.56 (2CH), 131.36 (2CH), 129.08 (4CH), 129.06 (CH), 128.92 (4CH), 128.18 (2CH), 127.85 (2CH), 126.23 (CH), 126.05 (CH), 124.73 (CH), 124.59 (CH), 123.57 (2C), 121.09 (2CH), 115.45 (2CH), 57.76 (C) ppm. ^{31}P NMR (121 MHz, CD_2Cl_2) 27.61 ppm. IR (ATR, platinum): 1591, 1572, 1501, 1480, 1448, 1437, 1389, 1333, 1312, 1289, 1271, 1182, 1160, 1120, 1105, 1073, 1058, 1027, 999, 944, 906, 849, 828, 782, 746, 726, 713, 695, 662, 641, 624, 586, 561, 534, 522, 506, 480, 451, 435, 421 cm^{-1}. HRMS (MALDI, DCBT): found $[M+H]^+$ 808.255; $C_{55}H_{40}NO_2P_2$ required 808.24506 m.p.: 320 °C

3 Thermal properties

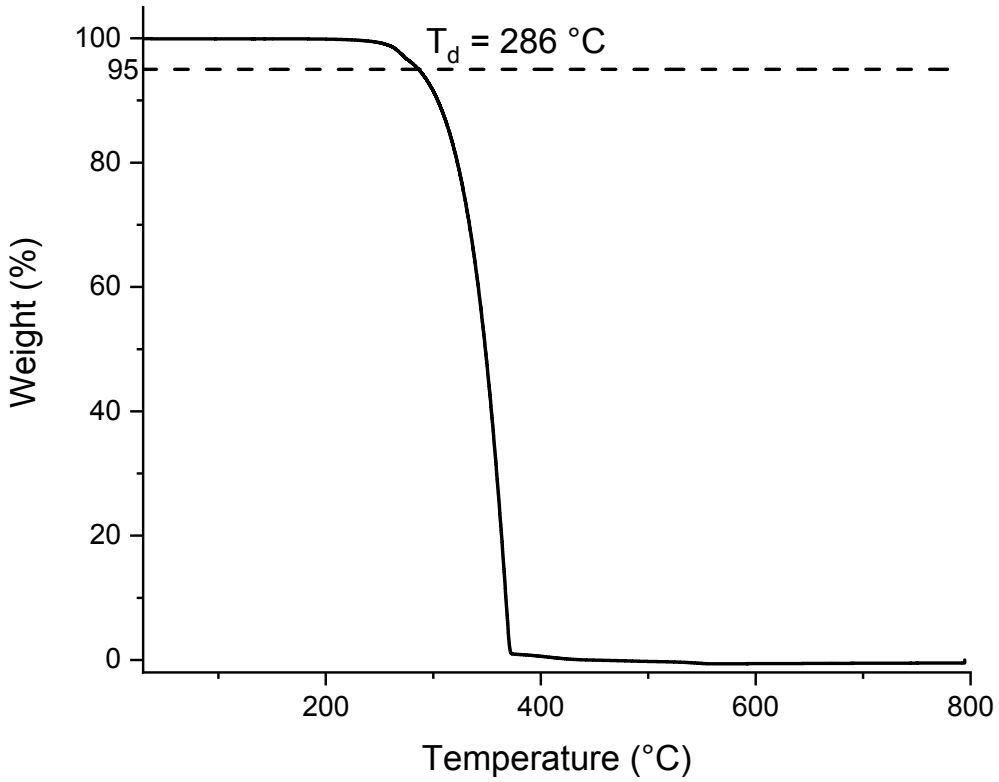

*Figure S 1 TGA trace of **SPA-F***

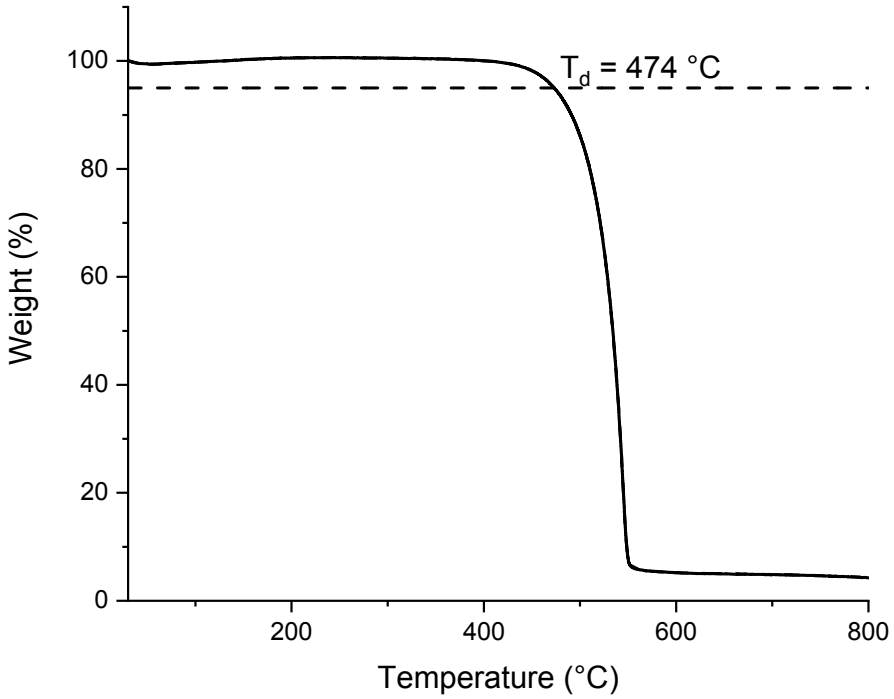

Figure S 2 TGA trace of ***SPA-2,7-F(POPh$_2$)$_2$***

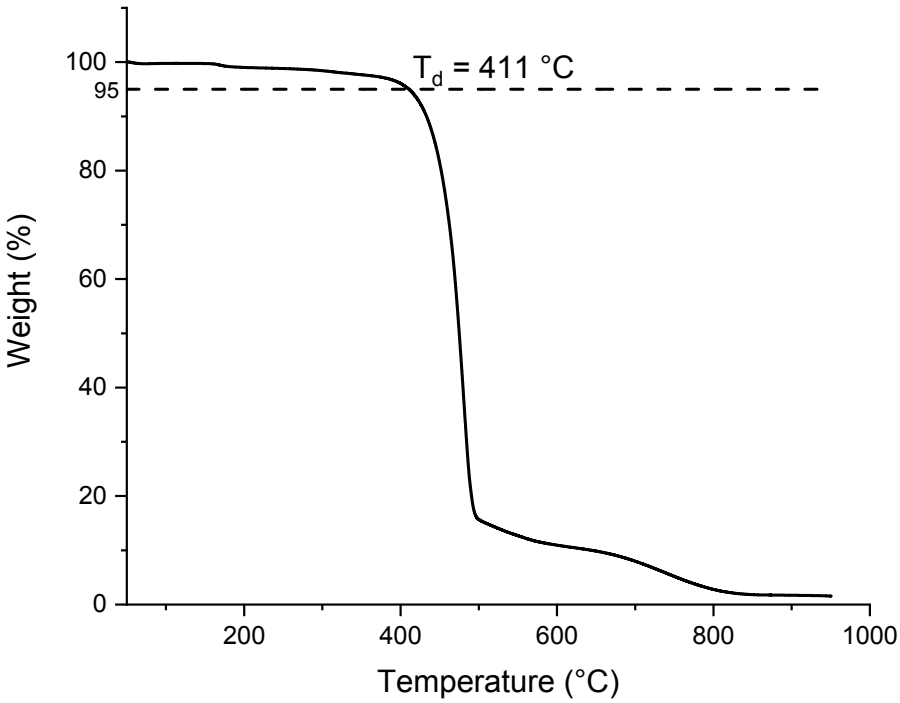

Figure S 3 TGA trace of ***SPA-3,6-F(POPh$_2$)$_2$***

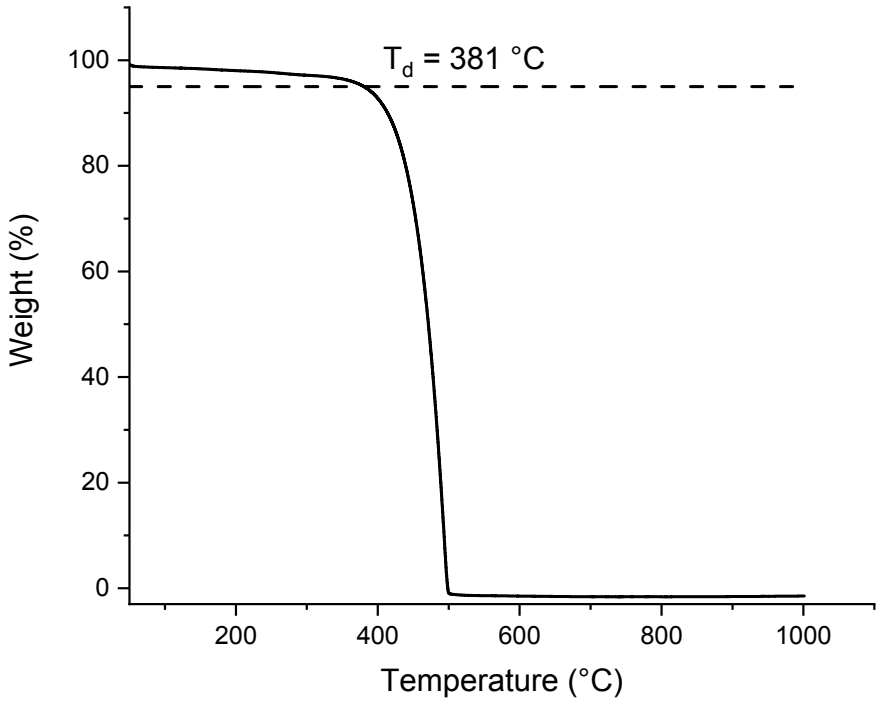

Figure S 4 TGA trace of ***SPA-2-FPOPh$_2$***

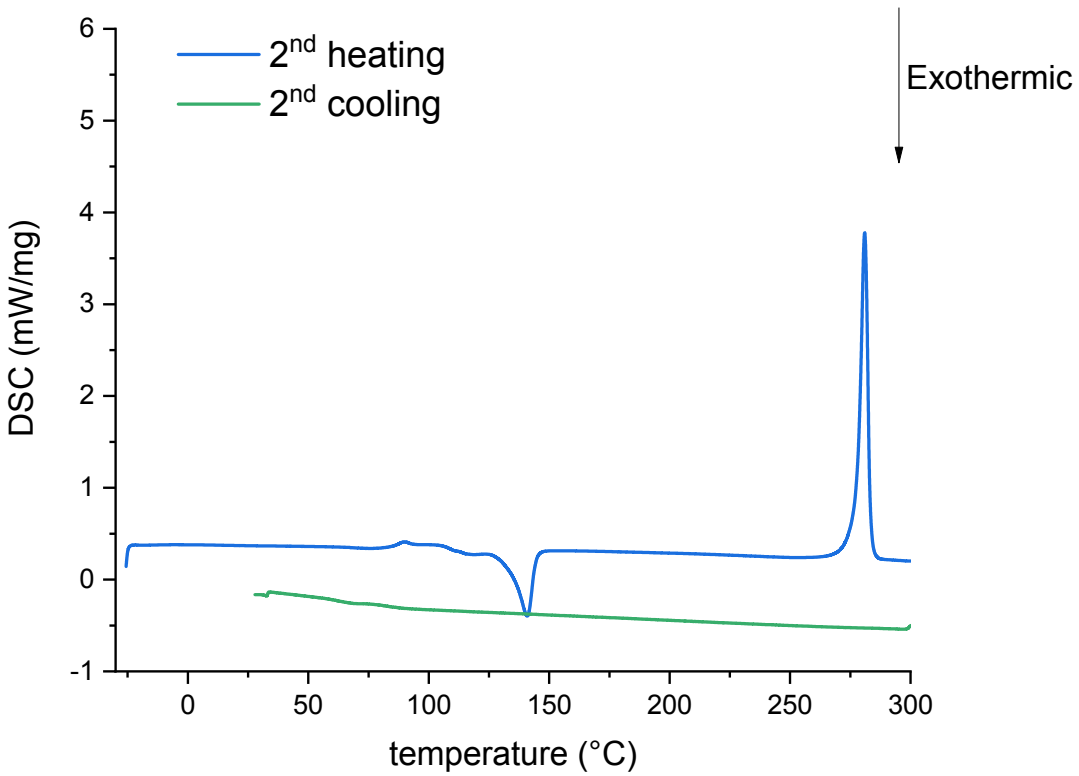

Figure S 5 DSC curves of ***SPA-F***

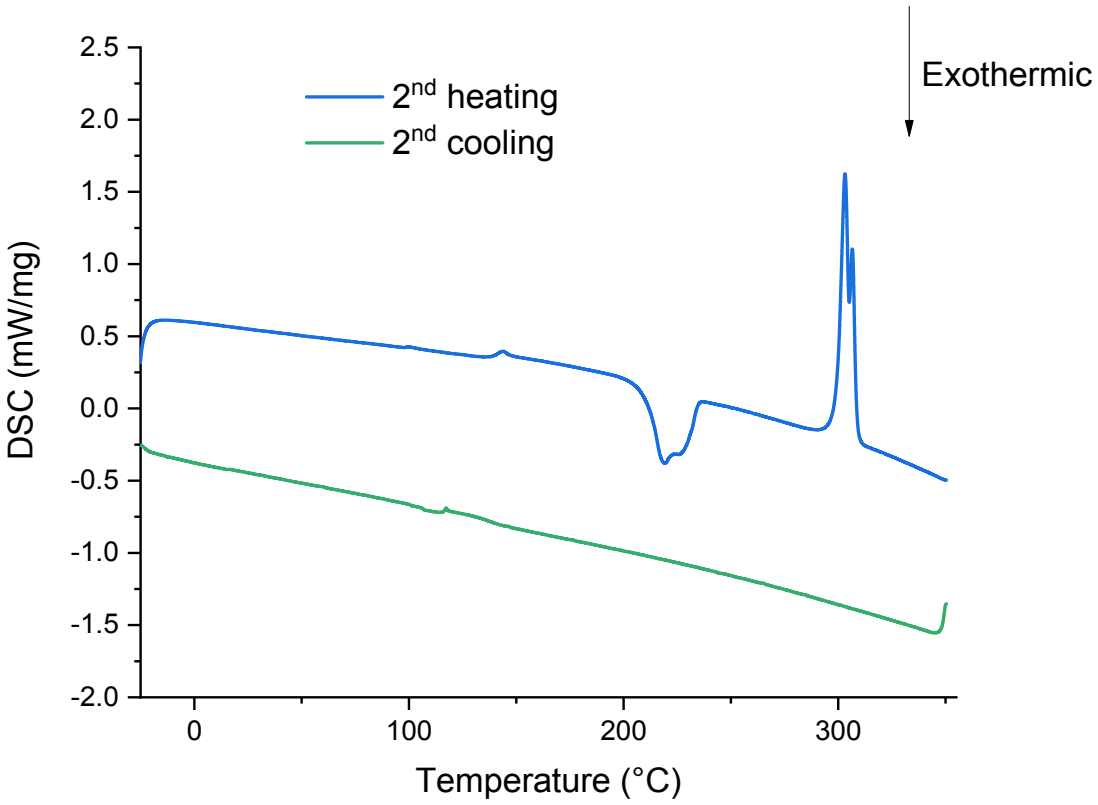

Figure S 6 DSC curves of ***SPA-2,7-F(POPh$_2$)$_2$***

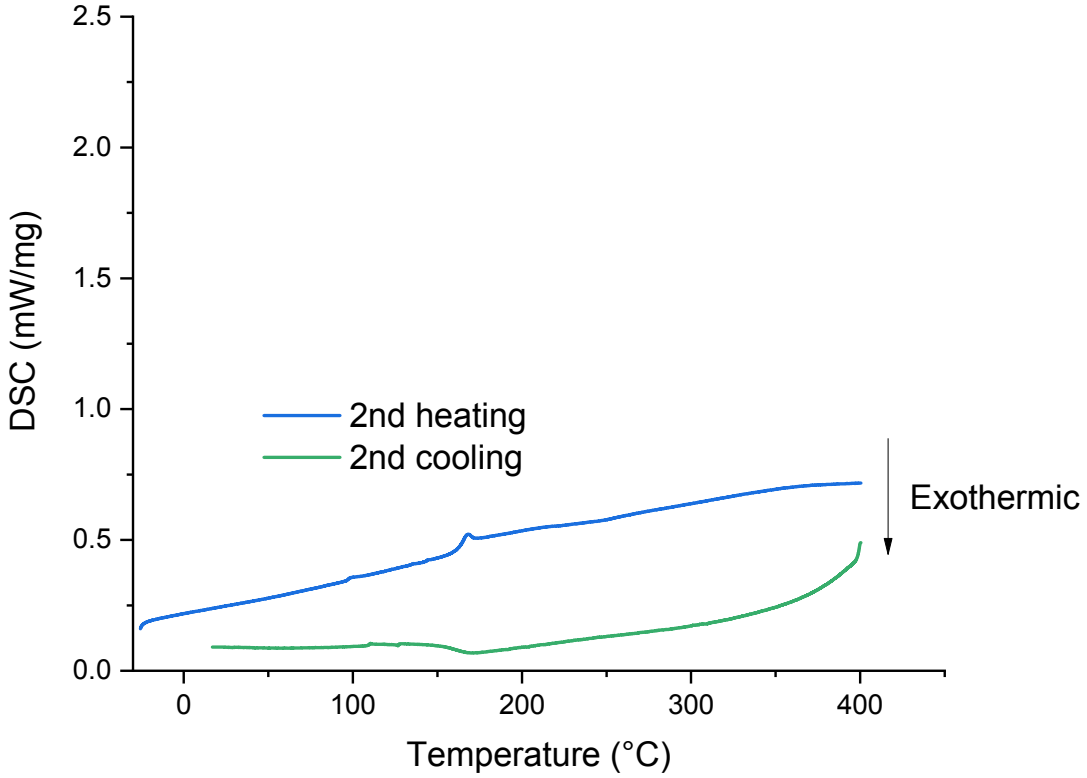

Figure S 7 DSC curves of ***SPA-3,6-F(POPh$_2$)$_2$***

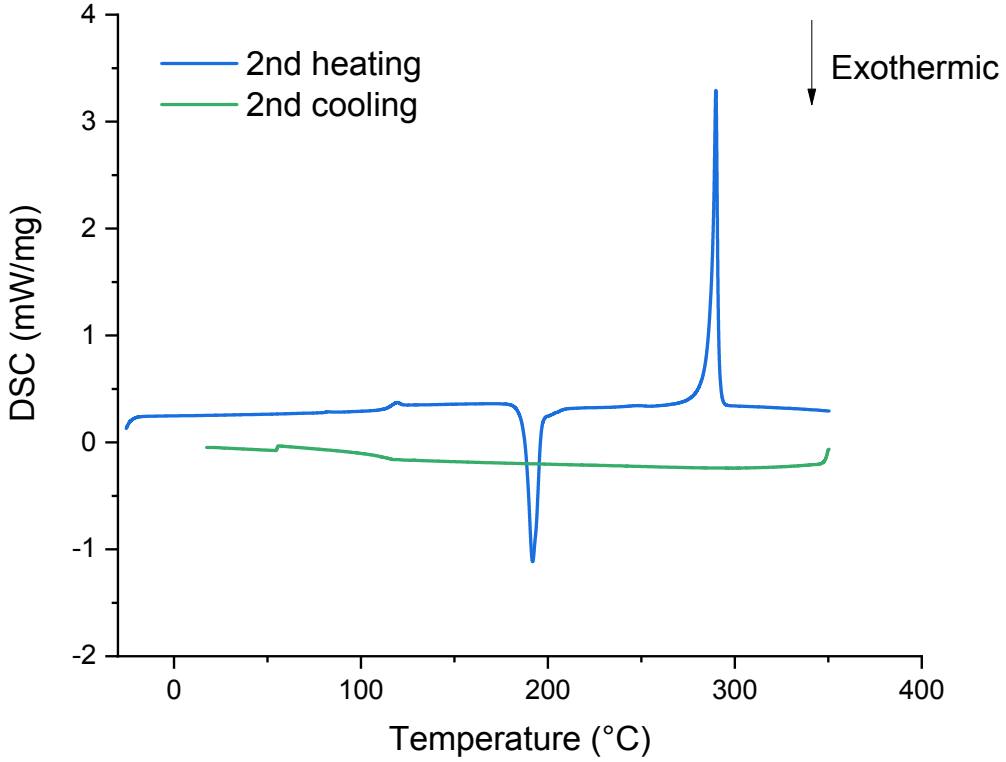

Figure S 8 DSC curves of ***SPA-2-FPOPh$_2$***

Table S 1 Thermal properties of ***SPA-F***, ***SPA-2,7-F(POPh$_2$)$_2$***, ***SPA-3,6-F(POPh$_2$)$_2$*** *and* ***SPA-2-FPOPh$_2$***

compound	**m.p. (°C)**	**T_d (°C)[b]**	**T_g (°C)[a]**	**T_c (°C)[a]**
SPA-F	281	286	90	141
SPA-2,7-F(POPh$_2$)$_2$	303	474	143	218
SPA-3,6-F(POPh$_2$)$_2$	320	411	165	-
SPA-2-FPOPh$_2$	290	381	118	191

[a]From 2nd heating DSC curves, [b]From TGA traces

4 Photophysical properties

4.1 Host matrices

*Table S 2 Summary of the photophysical data of **SPA-F**, **SPA-2,7-F(POPh$_2$)$_2$**, **SPA-3,6-F(POPh$_2$)$_2$** and **SPA-2-FPOPh$_2$***

	SPA-F	**SPA-2,7-F(POPh$_2$)$_2$**	**SPA-3,6-F(POPh$_2$)$_2$**	**SPA-2-FPOPh$_2$**
λ_{abs} [nm][a] (ε) [×10^4 L.mol^{-1}cm^{-1}]	309 (2.4) 297 (2.7) 270 (4.2)	323 (2.0) 309 (1.3) 294 (2.4) 282 (2.1) 259 (1.6)	316 (1.2) 304 (1.2) 273 (2.2) 252 (6.6)	315 (2.5) 310 (1.3) 295 (2.4) 283 (2.1) 274 (1.7) 259 (1.6)
QY[a]	N.D.	<0.01	<0.01	0.02
τ_p[b] [s] (λ_{em} [nm])	5.6 (428)	3.1 (450)	4.7 (428)	3.9 (439)
E_T[b] [eV]	2.90	2.76	2.90	2.82

[a]in cyclohexane at room temperature, [b]in 2-MeTHF at 77 K, λ_{exc}= 310 nm, N.D.: Not Determined

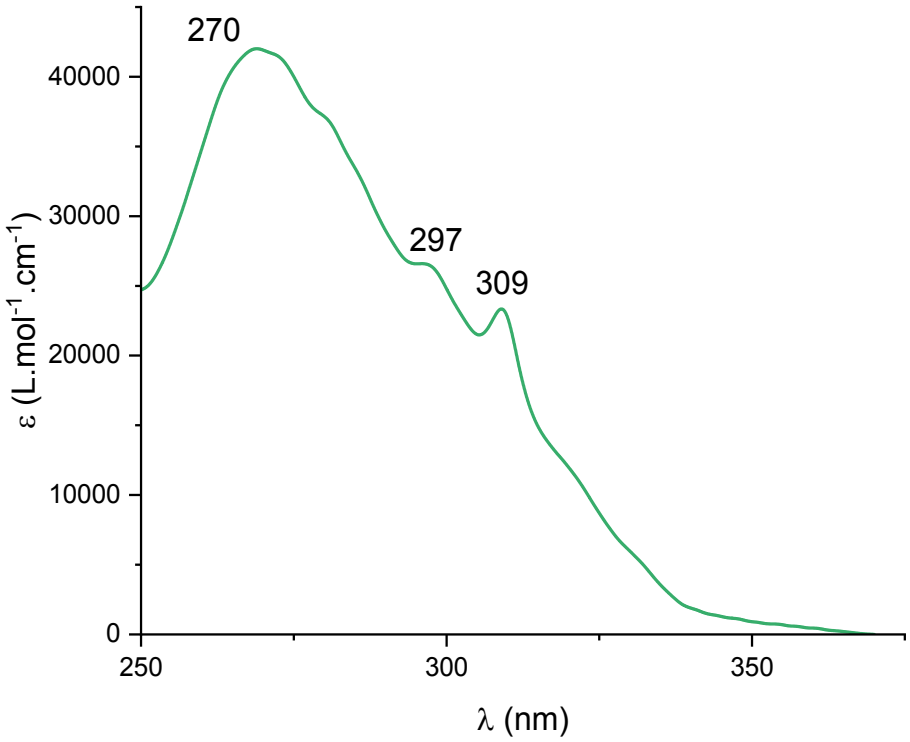

*Figure S 9 Absorption spectrum of **SPA-F** in cyclohexane*

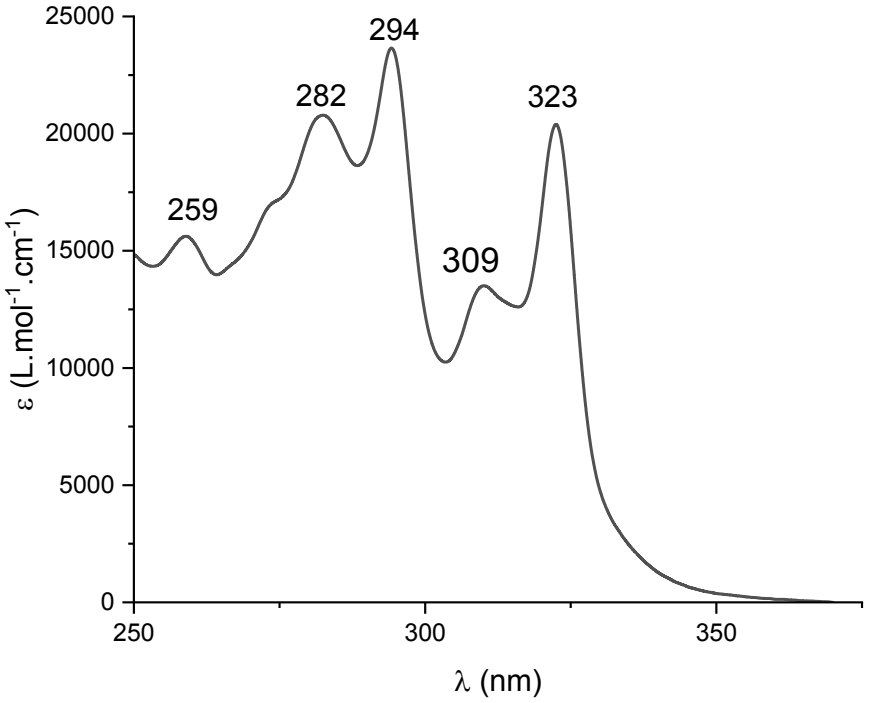

Figure S 10 Absorption spectrum of ***SPA-2,7-F(POPh$_2$)$_2$*** *in cyclohexane*

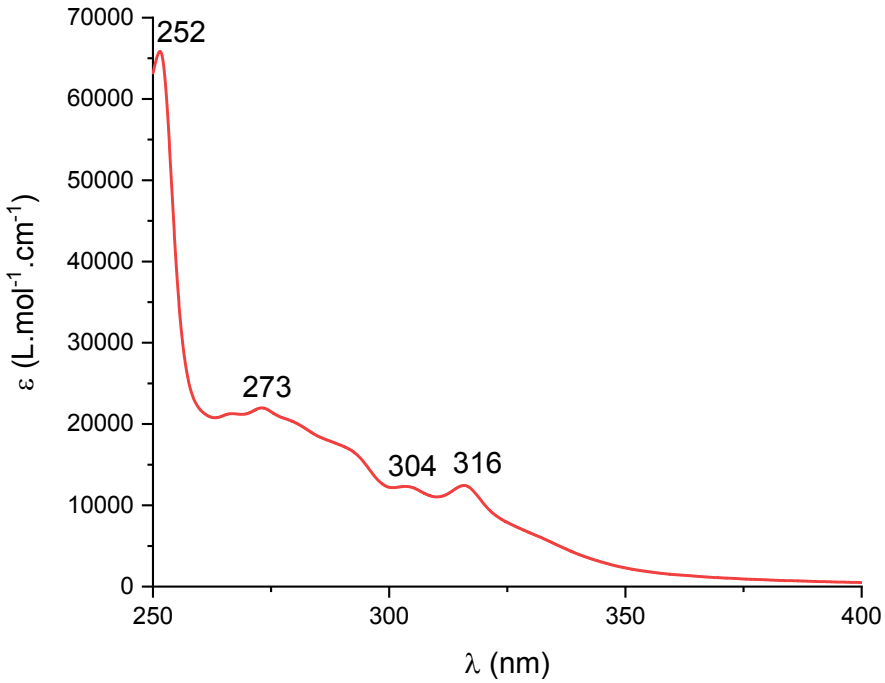

Figure S 11 Absorption spectrum of ***SPA-3,6-F(POPh$_2$)$_2$*** *in cyclohexane*

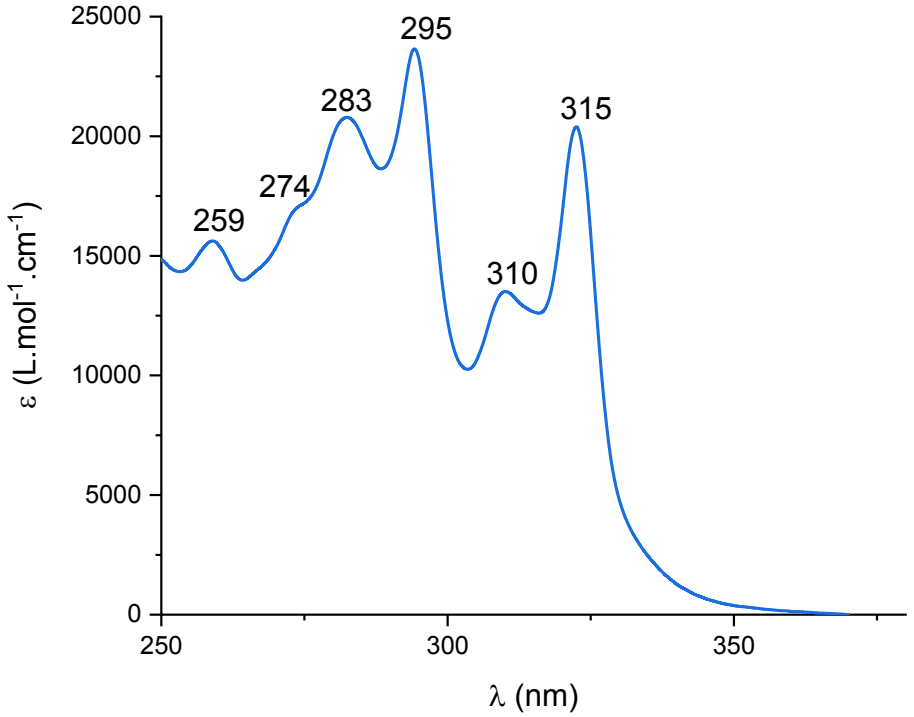

Figure S 12 Absorption spectrum of ***SPA-2-FPOPh₂*** *in cyclohexane*

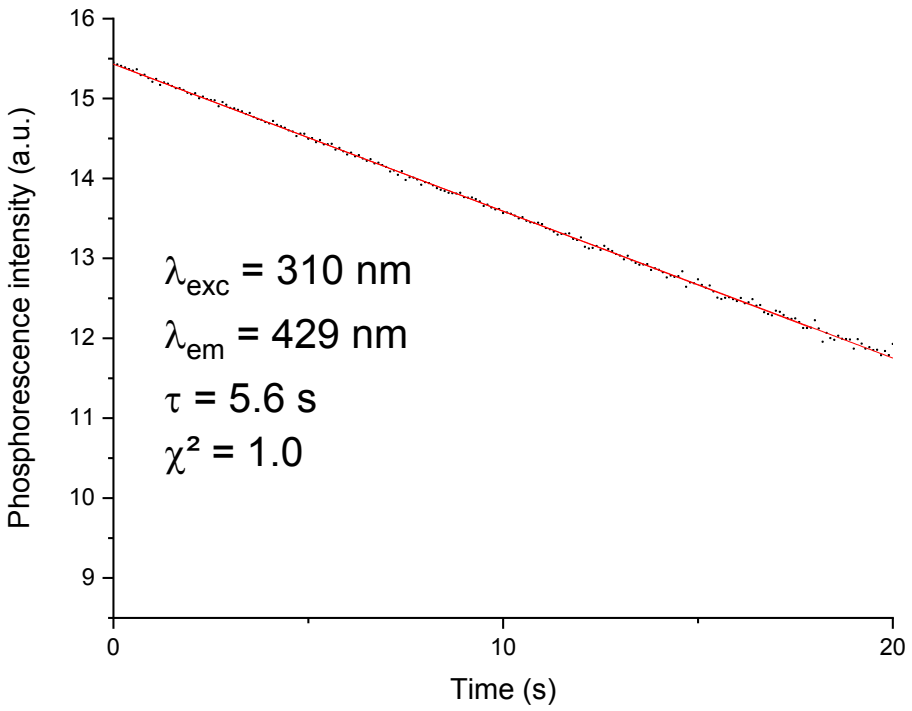

Figure S 13 Phosphorescence decay of ***SPA-F*** *in a frozen matrix of 2-MeTHF at 77K*

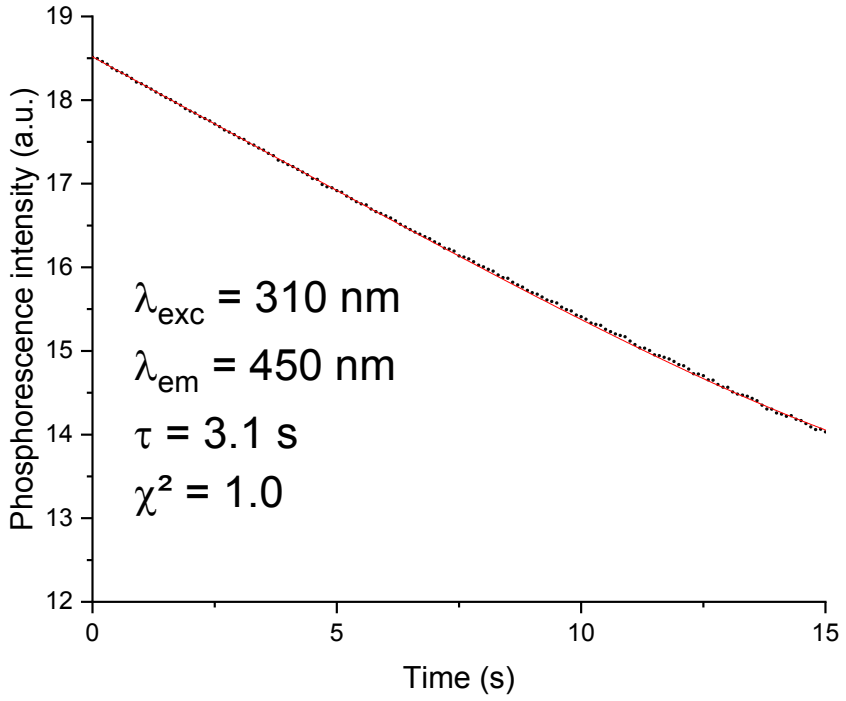

Figure S 14 Phosphorescence decay of ***SPA-2,7-F(POPh$_2$)$_2$*** *in a frozen matrix of 2-MeTHF at 77K*

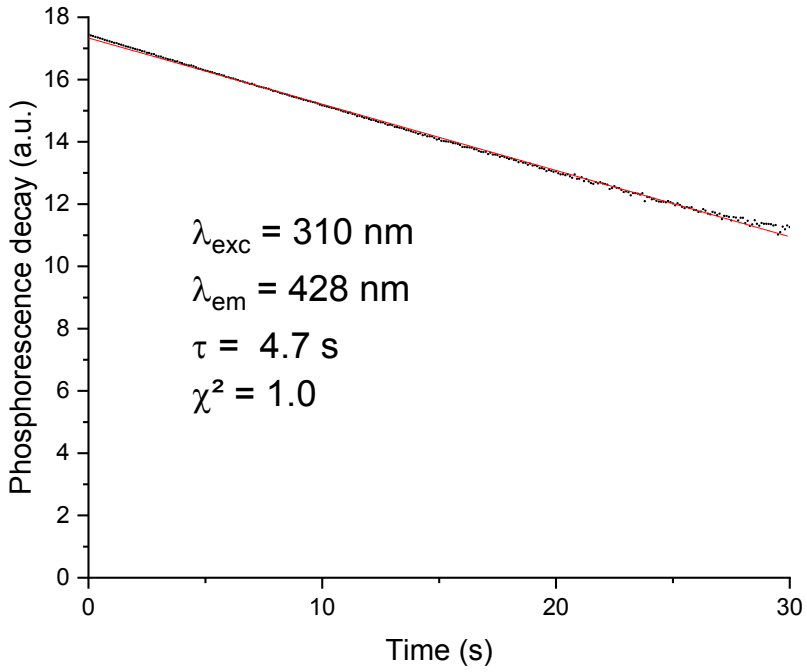

Figure S 15 Phosphorescence decay of ***SPA-3,6-F(POPh$_2$)$_2$*** *in a frozen matrix of 2-MeTHF at 77K*

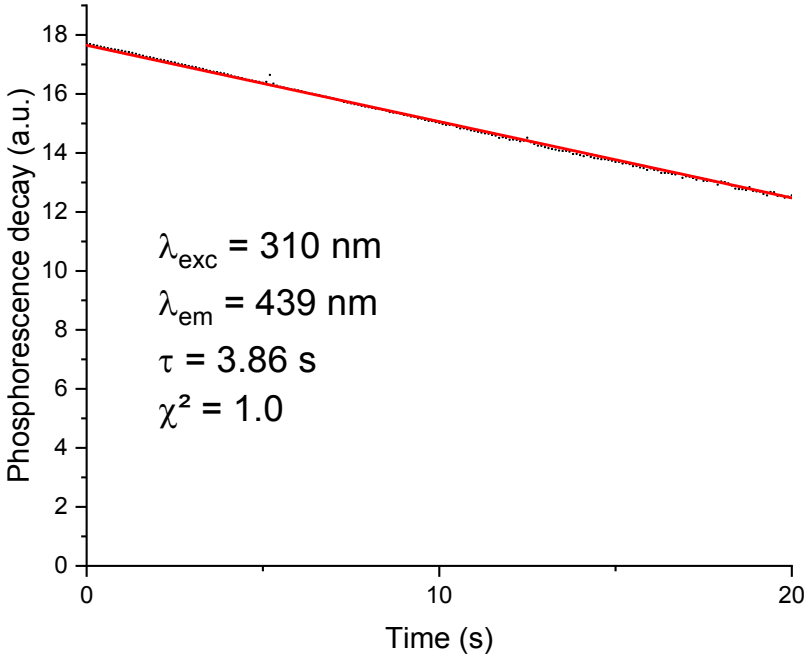

*Figure S 16 Phosphorescence decay of **SPA-2-FPOPh$_2$** in a frozen matrix of 2-MeTHF at 77K*

4.2 Phosphorescent guests

Table S 3 Summary of photophysical properties of Ir(MDQ)$_2$acac, Ir(ppy)$_3$, FIrpic and Fir$_6$ in 2-MeTHF

	Ir(MDQ)$_2$acac	**Ir(ppy)$_3$**	**FIrpic**	**Fir$_6$**
λ_{abs} [nm]	252 430 375 300	457 380 283	460 380 256	370
τ_p [µs] (λ_{em} [nm]) at RT	0.23 (660)	0.03 (61 %), 0.34 (39 %) (590)	0.06 (475)	0.31 (455)
τ_p [µs] (λ_{em} [nm]) at 77K	13.9 (590)	4.28 (491)	2.98 (455)	4.35 (455)
E_T [eV] RT/77K	2.02/2.08	2.43/2.51	2.67/2.72	2.72/2.76

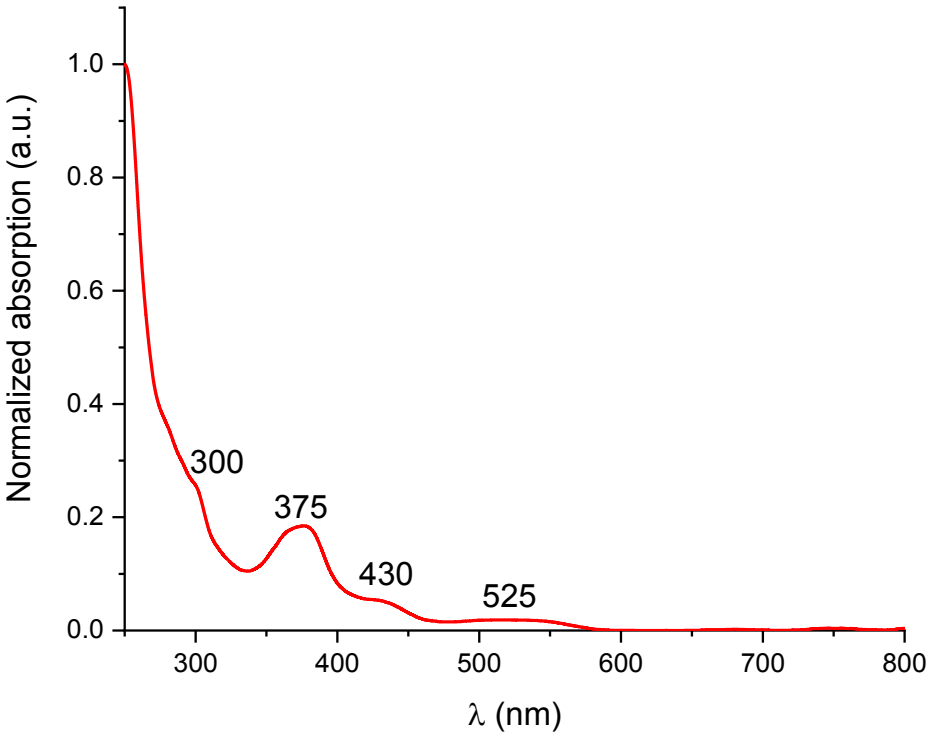

Figure S 17 Normalized absorption spectrum of Ir(MDQ)$_2$acac in 2-MeTHF at RT

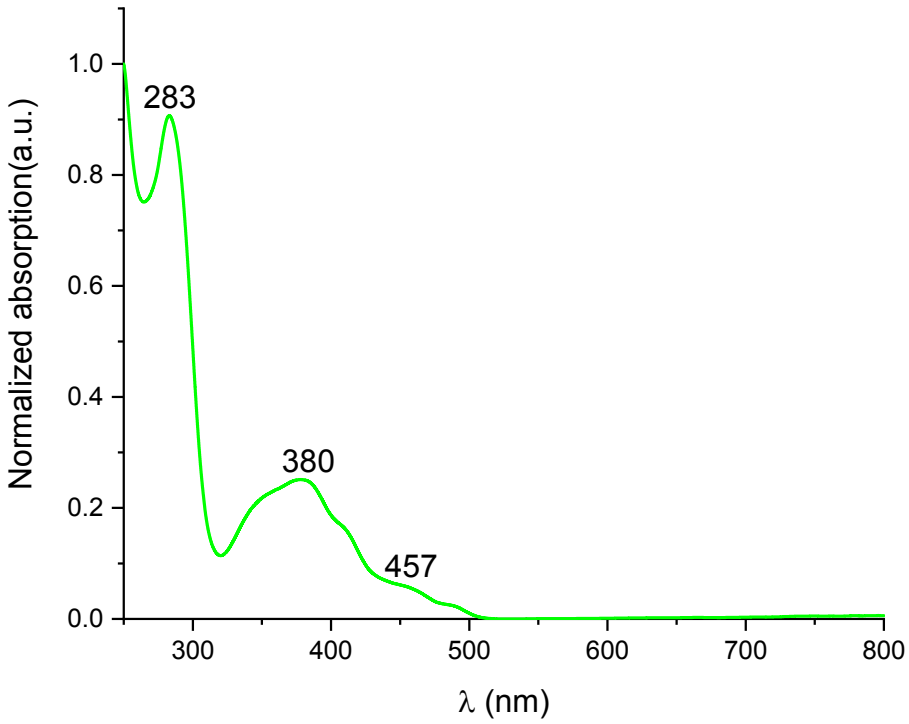

Figure S 18 Normalized absorption spectrum of Ir(ppy)$_3$ in 2-MeTHF at RT

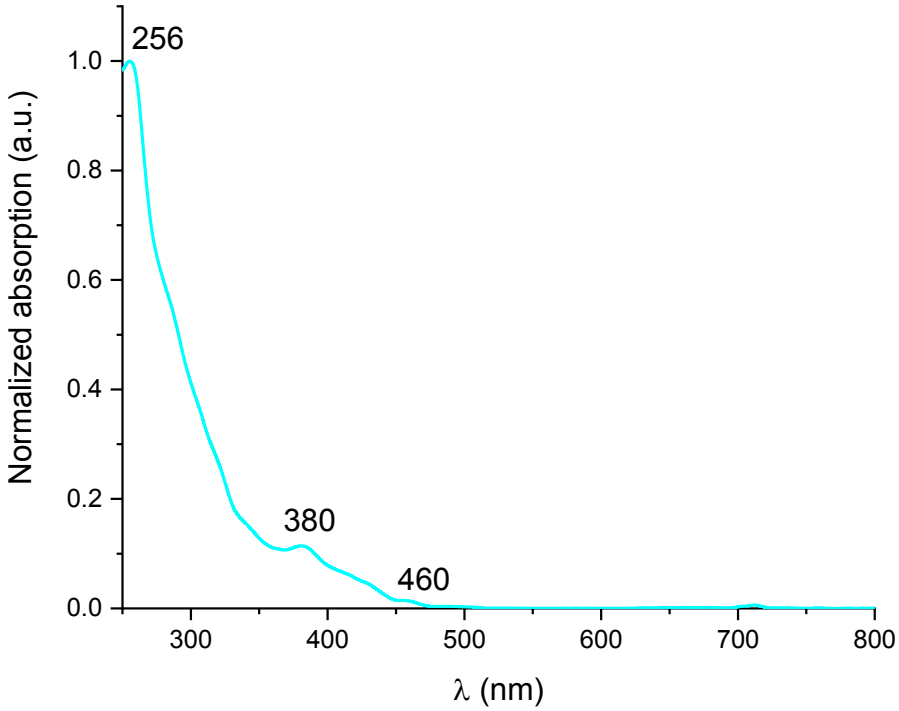

Figure S 19 Normalized absorption spectrum of FIrpic in 2-MeTHF at RT

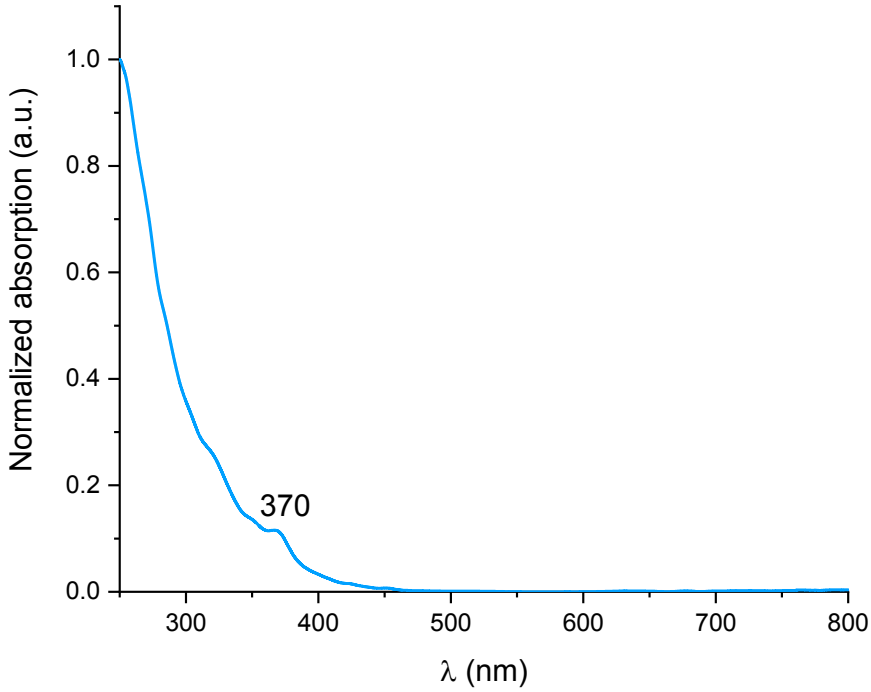

Figure S 20 Normalized absorption spectrum of Fir_6 in 2-MeTHF at RT

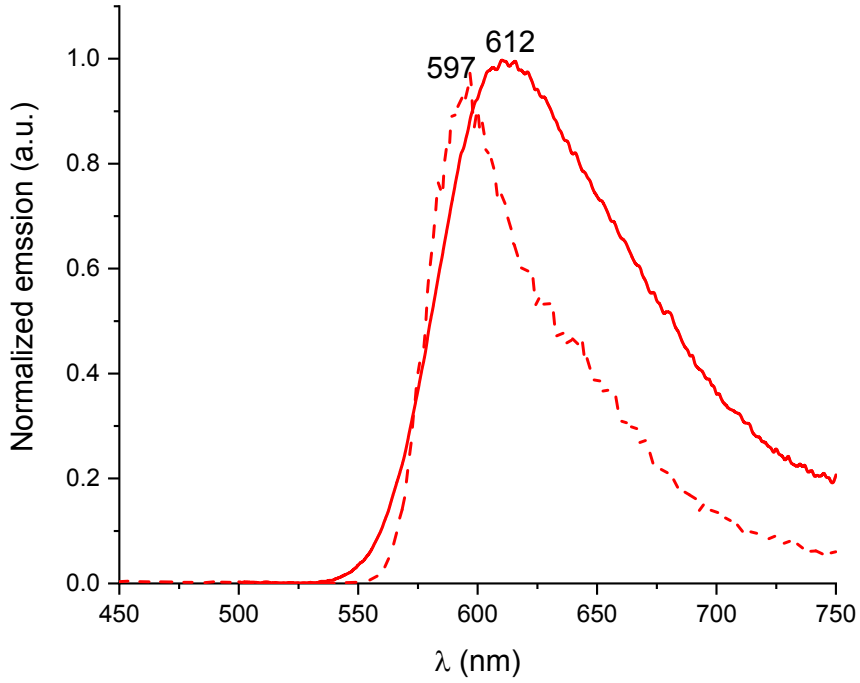

Figure S 21 Normalized emission spectra of Ir(MDQ)$_2$acac in 2-MeTHF at RT (solid line) and at 77 K (dashed line), λ_{exc} = 415 nm.

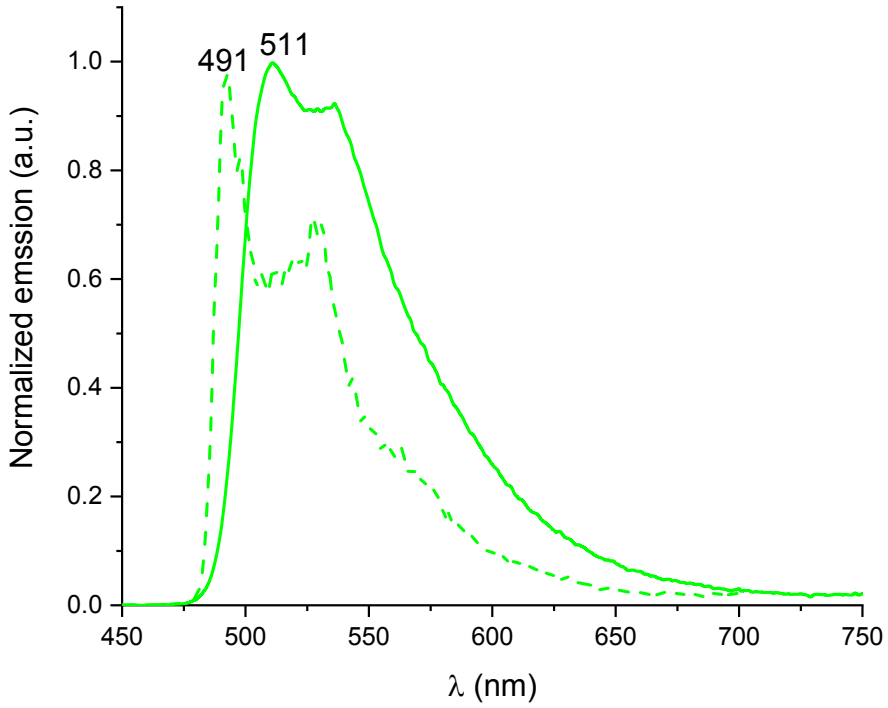

Figure S 22 Normalized emission spectra of Ir(ppy)$_3$ in 2-MeTHF at RT (solid line) and at 77 K (dashed line), λ_{exc} = 415 nm.

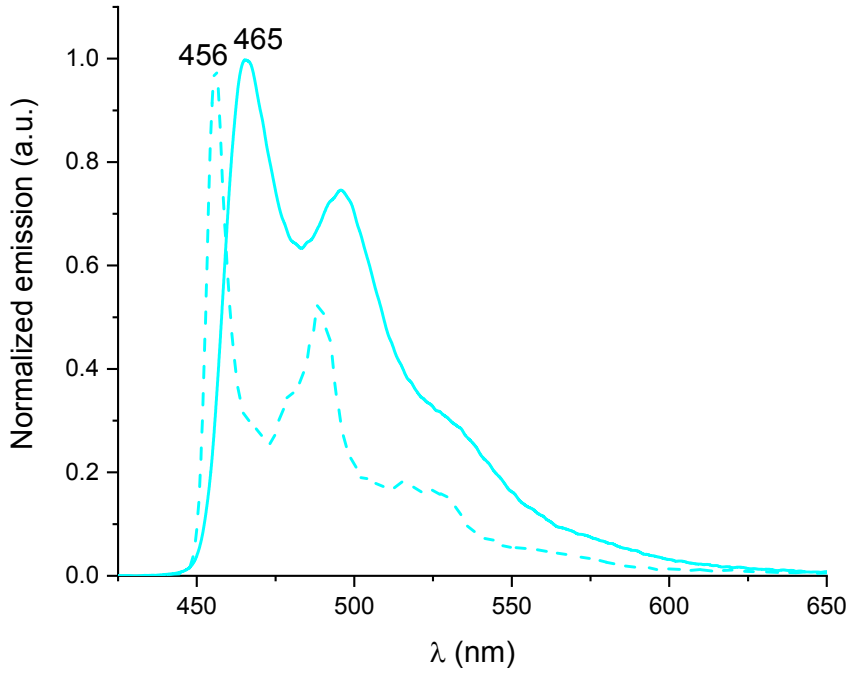

Figure S 23 Normalized emission spectra of FIrpic in 2-MeTHF at RT (solid line) and at 77 K (dashed line), λ_{exc} = 415 nm.

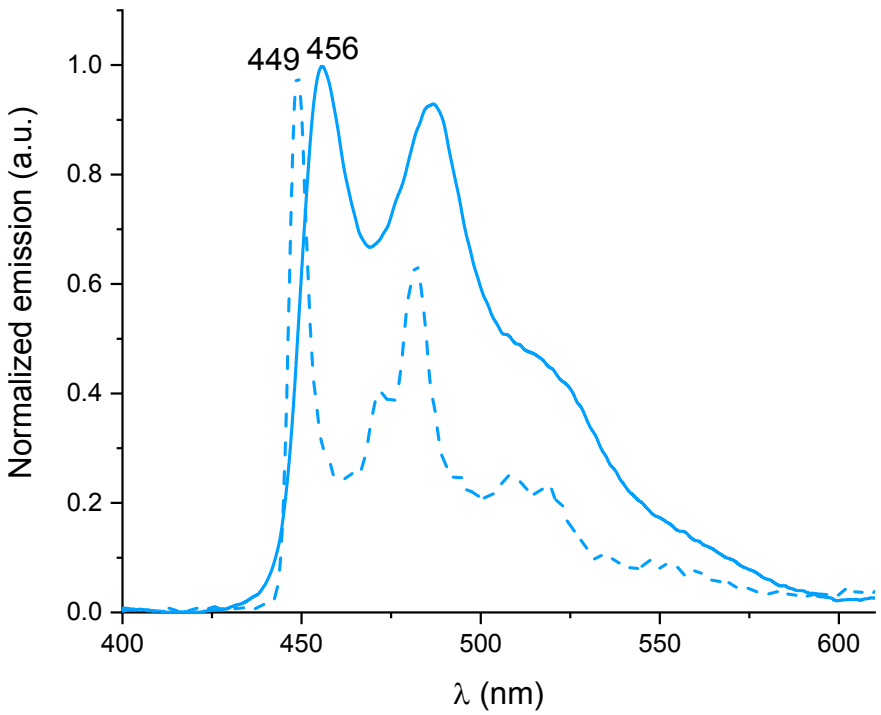

Figure S 24 Normalized emission spectra of FIr_6 in 2-MeTHF at RT (solid line) and at 77 K (dashed line), λ_{exc} = 310 nm.

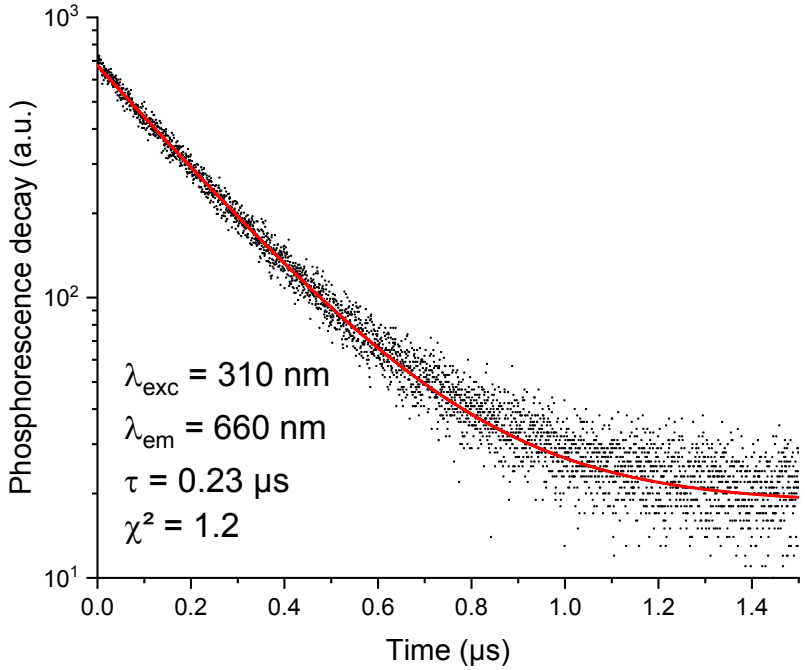

Figure S 25 Phosphorescence decay of Ir(MDQ)$_2$acac in 2-MeTHF at RT

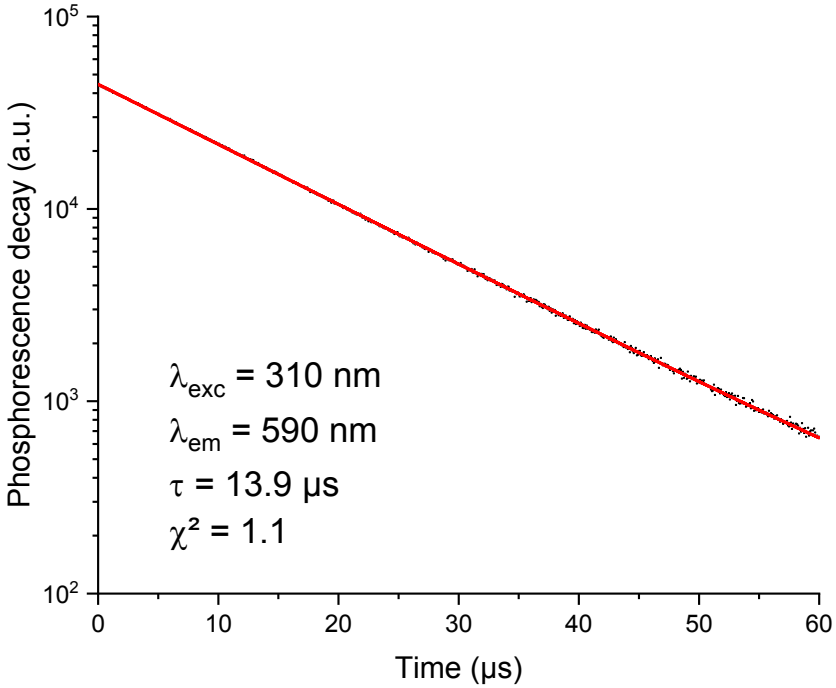

Figure S 26 Phosphorescence decay of Ir(MDQ)$_2$acac in a frozen matrix of 2-MeTHF at 77 K

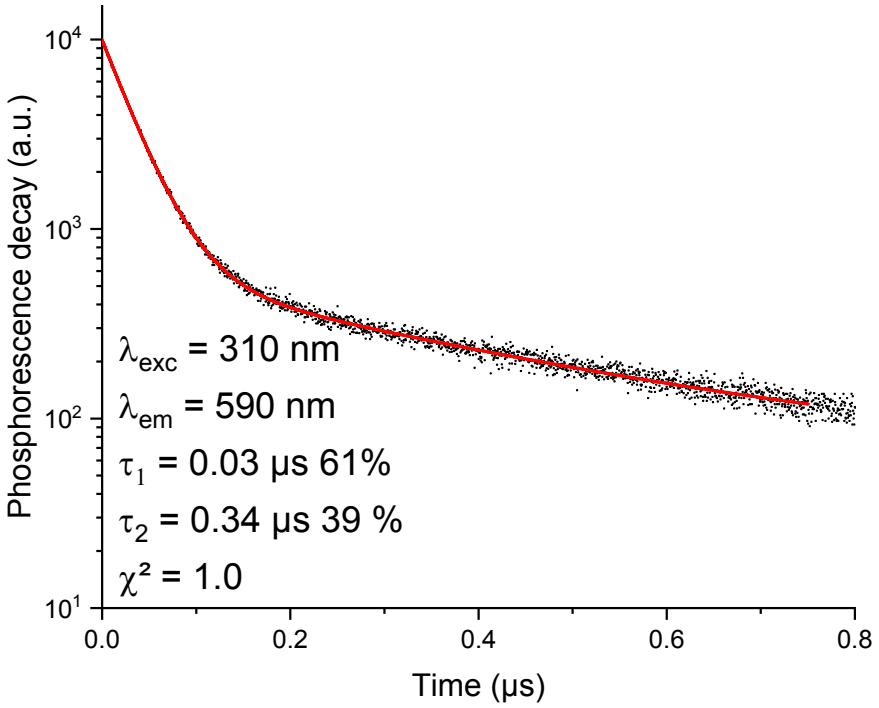

Figure S 27 Phosphorescence decay of Ir(ppy)$_3$ in 2-MeTHF at RT

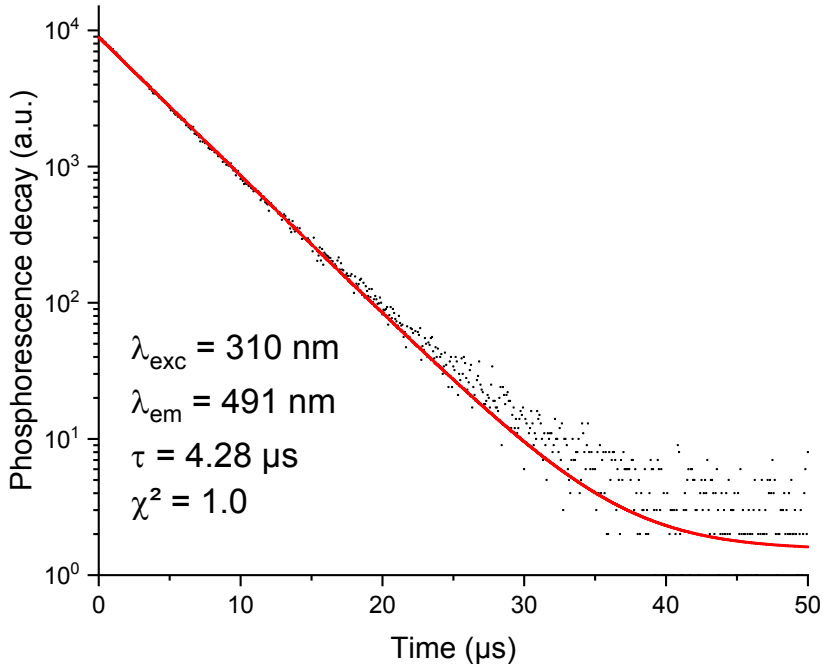

Figure S 28 Phosphorescence decay of Ir(ppy)$_3$ in a frozen matrix of 2-MeTHF at 77 K

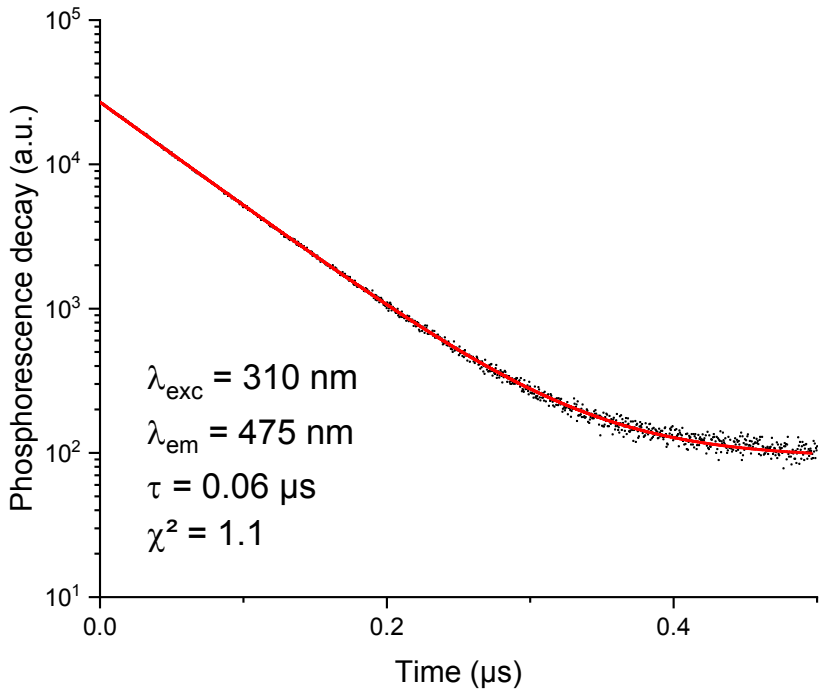

Figure S 29 Phosphorescence decay of FIrpic in 2-MeTHF at RT

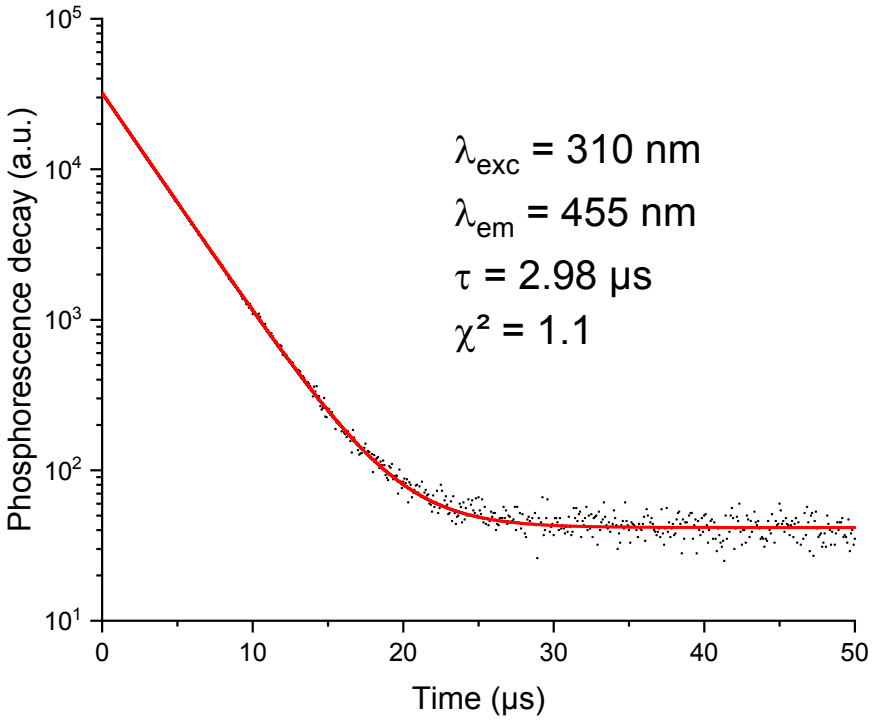

Figure S 30 Phosphorescence decay of FIrpic in a frozen matrix of 2-MeTHF at 77 K

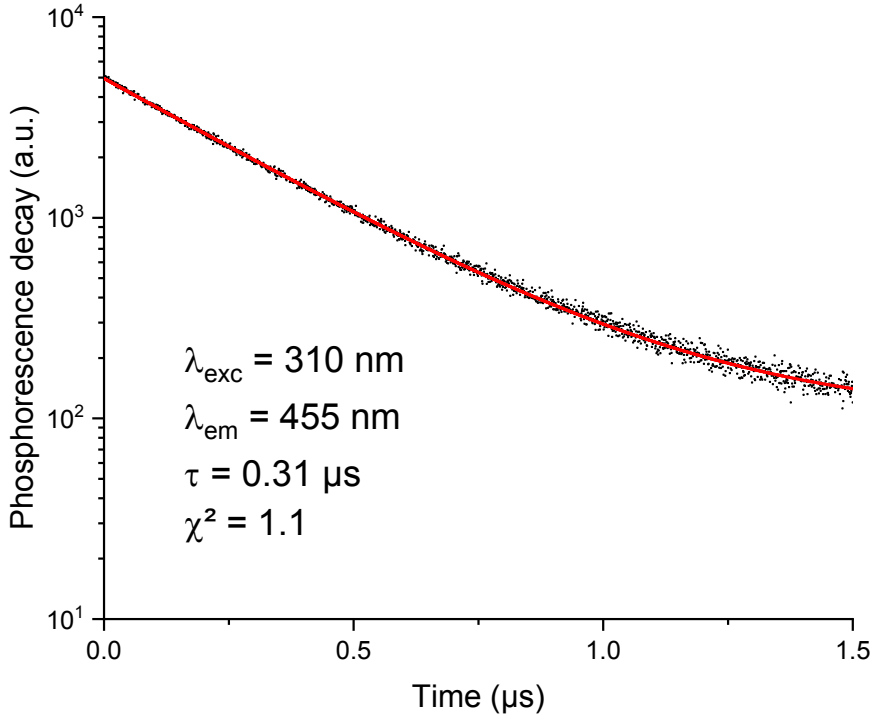

Figure S 31 Phosphorescence decay of FIr_6 in 2-MeTHF at RT

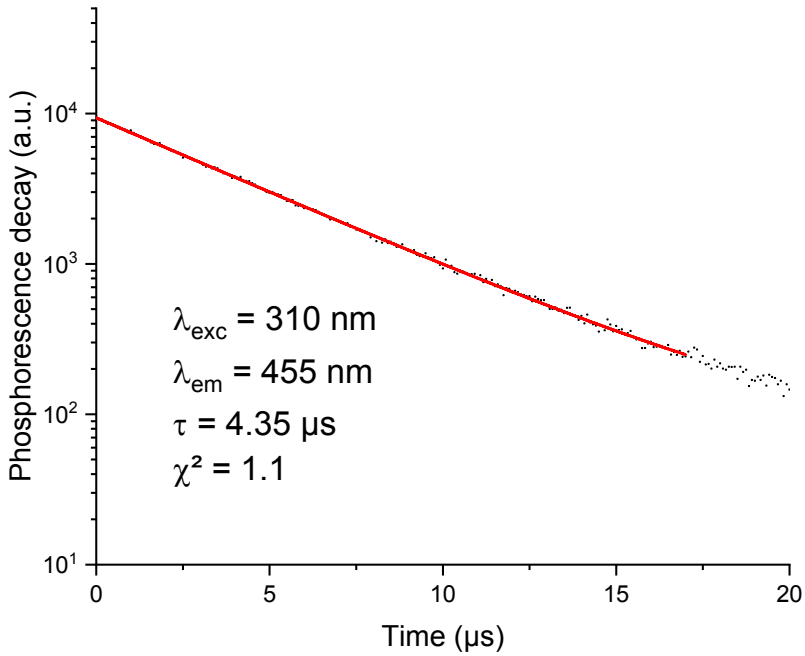

Figure S 32 Phosphorescence decay of FIr_6 in a frozen matrix of 2-MeTHF at 77 K

4.3 Combine solid state absorption of phosphorescent guest and emission host matrices spectra

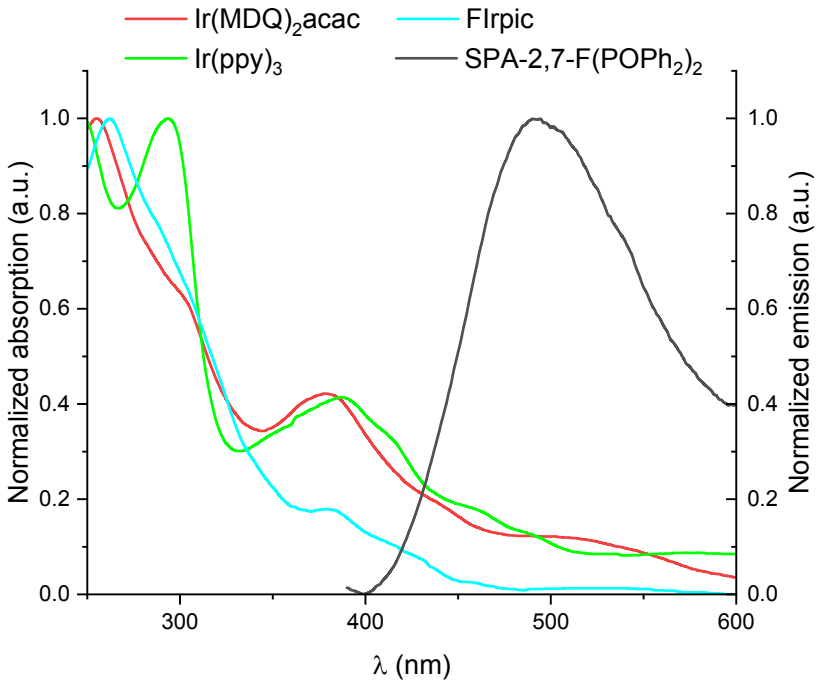

Figure S 33 Combine solid state absorption spectra of Ir(MDQ)$_2$acac (red line), Ir(ppy)$_3$ (green line), Firpic (sky blue line)and solid state emission spectra of ***SPA-2,7-F(POPh$_2$)$_2$****. Absorption spectra of dopants have been obtained from thermal evaporated film while emission spectrum of the matrix from a spin-coated film.*

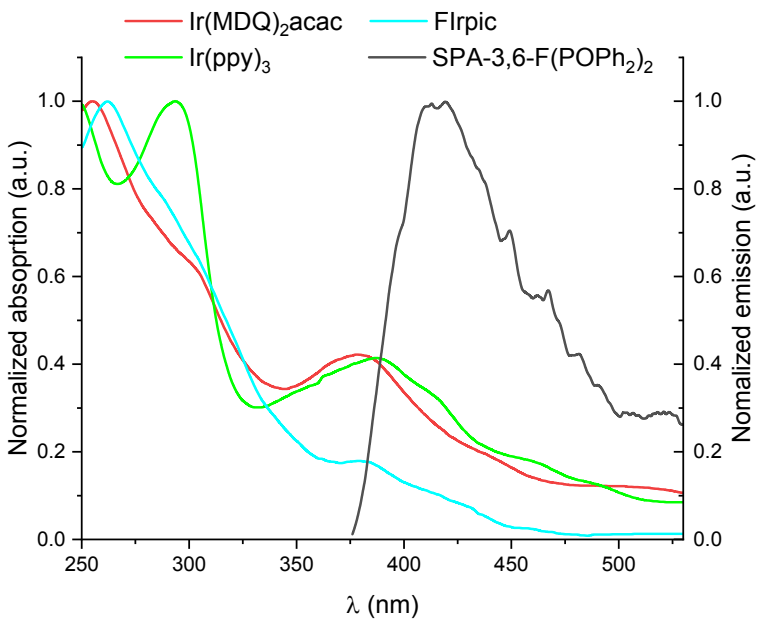

Figure S 34 Combine solid state absorption spectra of Ir(MDQ)$_2$acac (red line), Ir(ppy)$_3$ (green line), Firpic (sky blue line) and solid state emission spectra of ***SPA-3,6-F(POPh$_2$)$_2$****. Absorption spectra of dopants have been obtained from thermal evaporated film while emission spectrum of the matrix from a spin-coated film.*

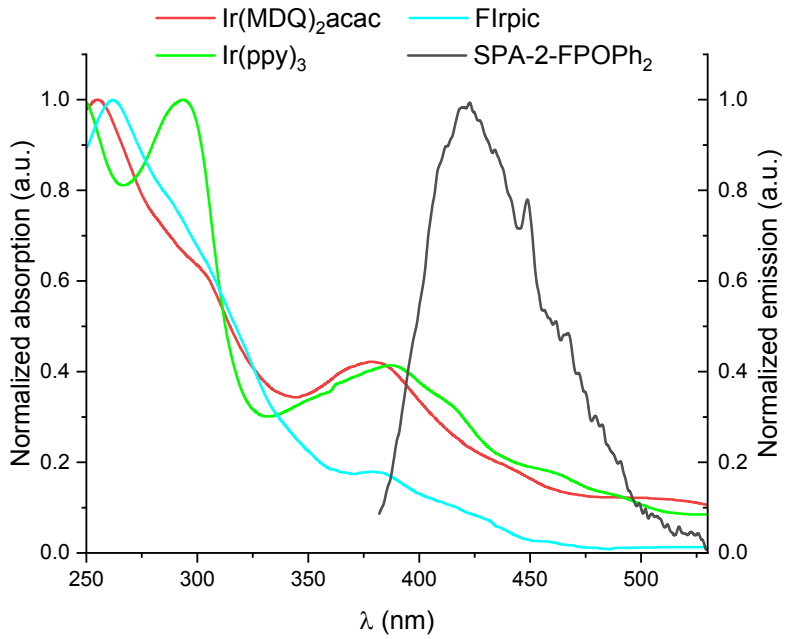

Figure S 35 Combine solid state absorption spectra of Ir(MDQ)$_2$acac (red line), Ir(ppy)$_3$ (green line), Firpic (sky blue line) and solid state emission spectra of ***SPA-2-FPOPh$_2$****. Absorption spectra of dopants have been obtained from thermal evaporated film while emission spectrum of the matrix from a spin-coated film.*

4.4 Co-evaporated films

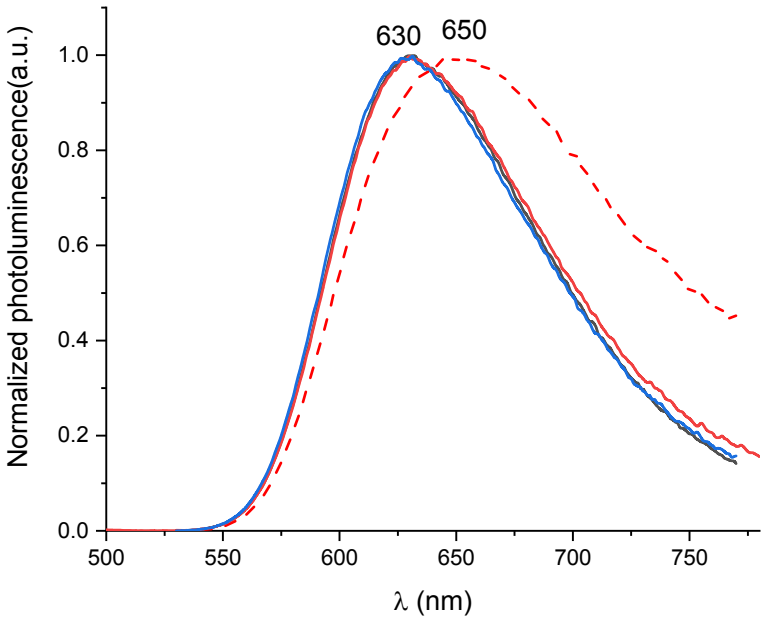

Figure S 36 Normalized photoluminescence spectra of ***SPA-2,7-F(POPh$_2$)$_2$****:Ir(MDQ)$_2$acac 10% (black solid line),* ***SPA-3,6-F(POPh$_2$)$_2$****:Ir(MDQ)$_2$acac 10% (red solid line),* ***SPA-2-FPOPh$_2$****:Ir(MDQ)$_2$acac 10% (blue solid line) and neat Ir(MDQ)$_2$acac (red dashed line), λ_{exc} = 450 nm. All the data have been obtained from thermal evaporated thin film*

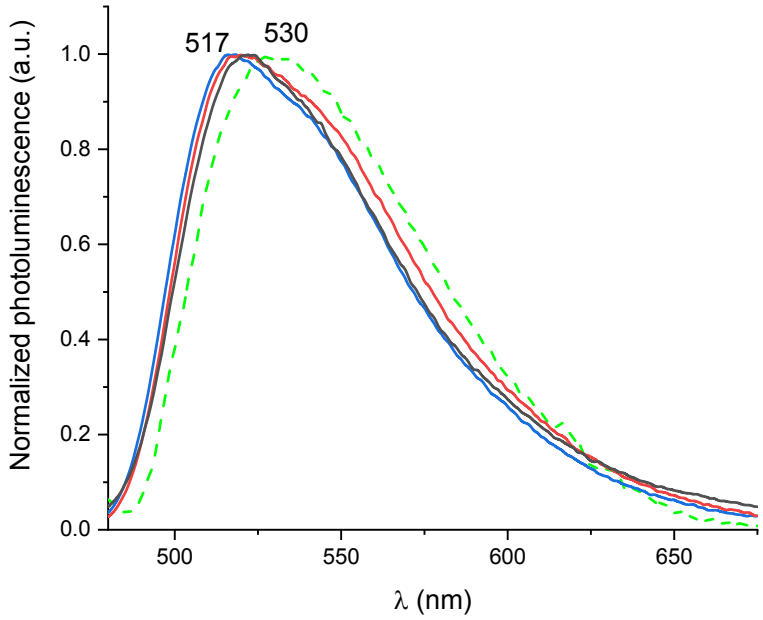

Figure S 37 Normalized photoluminescence spectra of ***SPA-2,7-F(POPh$_2$)$_2$****:Ir(ppy)$_3$ 10% (black solid line),* ***SPA-3,6-F(POPh$_2$)$_2$****: Ir(ppy)$_3$ 10% (red solid line),* ***SPA-2-FPOPh$_2$****: Ir(ppy)$_3$ 10% (blue solid line) and neat Ir(ppy)$_3$ (green dashed line), λ_{exc} = 455 nm. All the data have been obtained from thermal evaporated thin film*

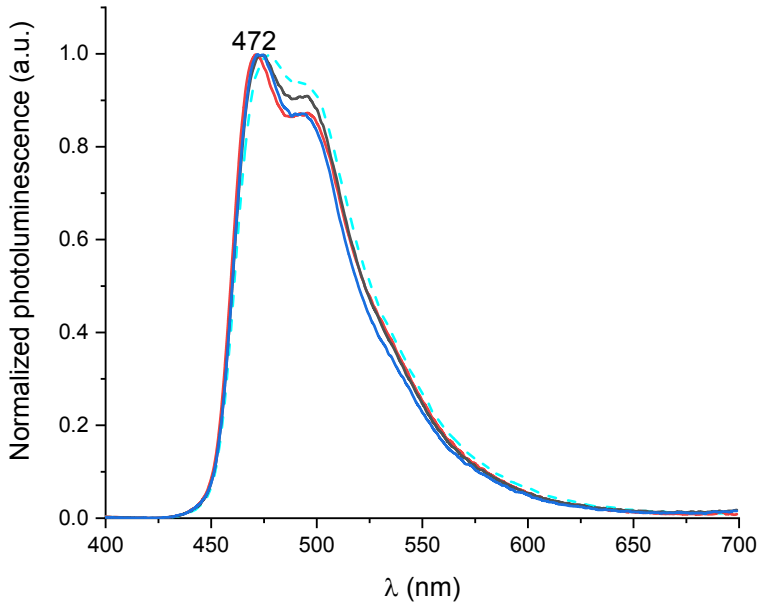

Figure S 38 Normalized photoluminescence spectra of ***SPA-2,7-F(POPh$_2$)$_2$****:FIrpic 10% (black solid line),* ***SPA-3,6-F(POPh$_2$)$_2$****: FIrpic 10% (red solid line),* ***SPA-2-FPOPh$_2$****: FIrpic 10% (blue solid line) and neat FIrpic (sky blue dashed line), λ_{exc} = 380 nm. All the data have been obtained from thermal evaporated thin film*

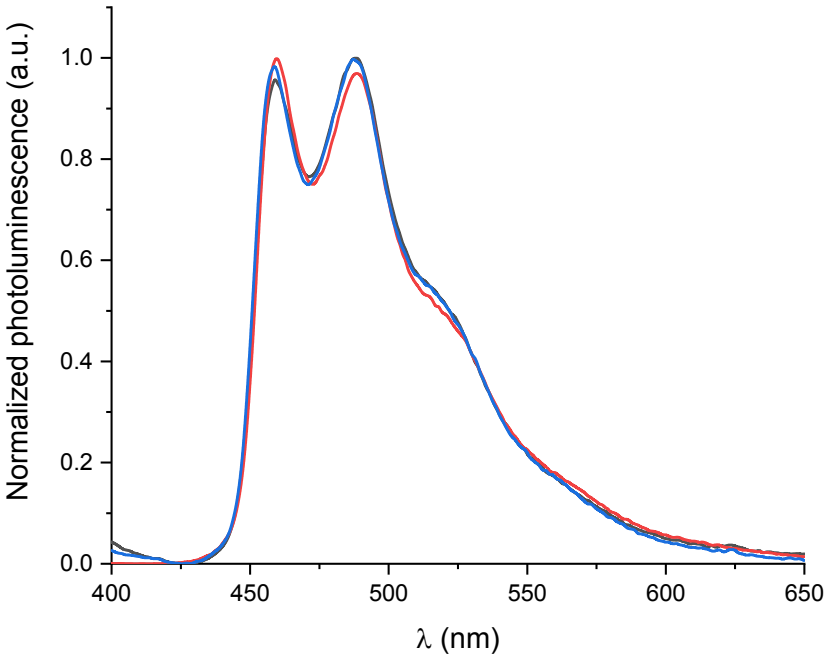

Figure S 39 Normalized photoluminescence spectra of ***SPA-2,7-F(POPh$_2$)$_2$****:Fir$_6$ 10% (black solid line),* ***SPA-3,6-F(POPh$_2$)$_2$****: Fir$_6$ 10% (red solid line),* ***SPA-2-FPOPh$_2$****: Fir$_6$ 10% (blue solid line), λ_{exc} = 380 nm. All the data have been obtained from thermal evaporated thin film*

5 Electrochemical studies

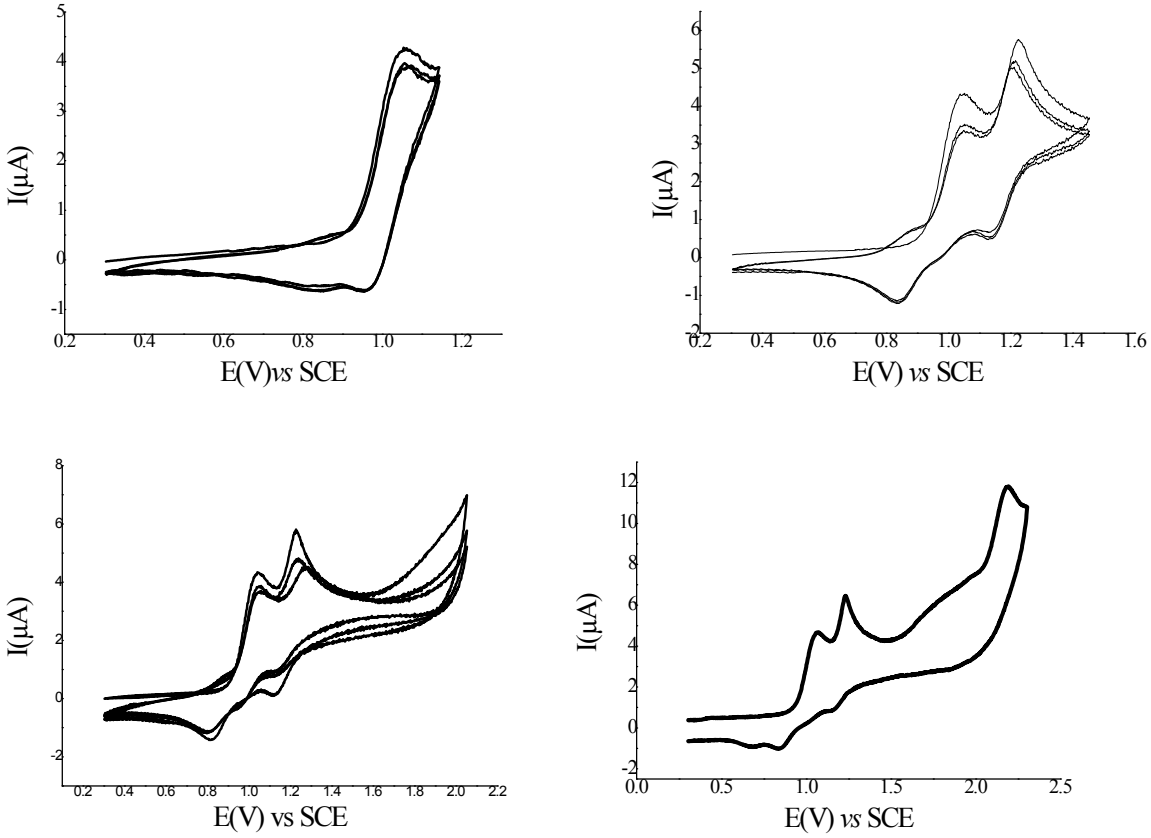

Figure S 40 Cyclic voltammograms of ***SPA-2,7-F(POPh2)2*** *recorded in the anodic range in CH_2Cl_2 + BuN_4PF_6 0.2 M. The CVs are recorded between 0.3 and 1.14 V, three cycles (A), between 0.3 and 1.45V, three cycles (B), between 0.3 and 2.05 V, three cycles (C) and between 0.3 and 2.3 V, one cycle (D) showing the successive first, second and third irreversible oxidation processes. Sweep-rate: 100 mV/s.*

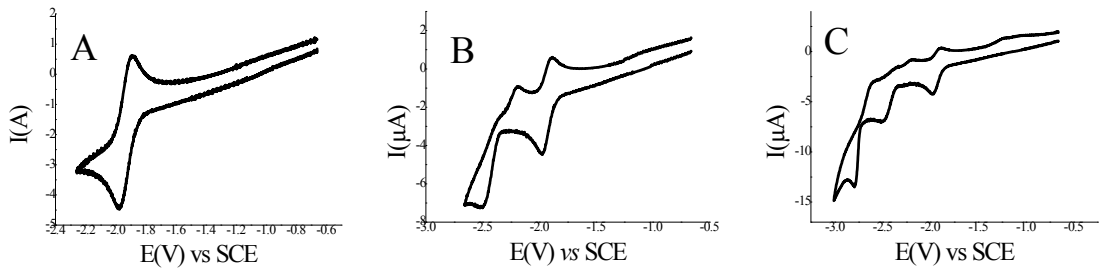

Figure S X Cyclic voltammograms of ***SPA-2,7-F(POPh2)2*** *recorded in the cathodic range in DMF+ BuN_4PF_6 0.1 M. The CVs are recorded between -0.62 and -2.26 (A), -0.62 and -2.66 V (B) and -0.62 and -3.02 V (C) showing the successive one reversible, second and third irreversible reduction processes. Sweep-rate: 100 mV/s.*

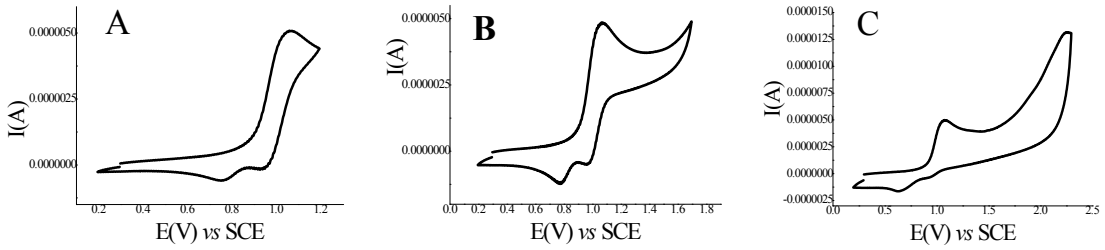

Figure S 41 Cyclic voltammograms of ***SPA-3,6-F(POPh2)2*** *recorded in the anodic range in CH_2Cl_2+ BuN_4PF_6 0.2 M. The CVs are recorded between 0.2 and 1.2 V (A), 0.2 and 1.7 V (B) and between 0.2 and 2.3V (C) showing the successive two irreversible oxidation processes. Sweep-rate: 100 mV/s.*

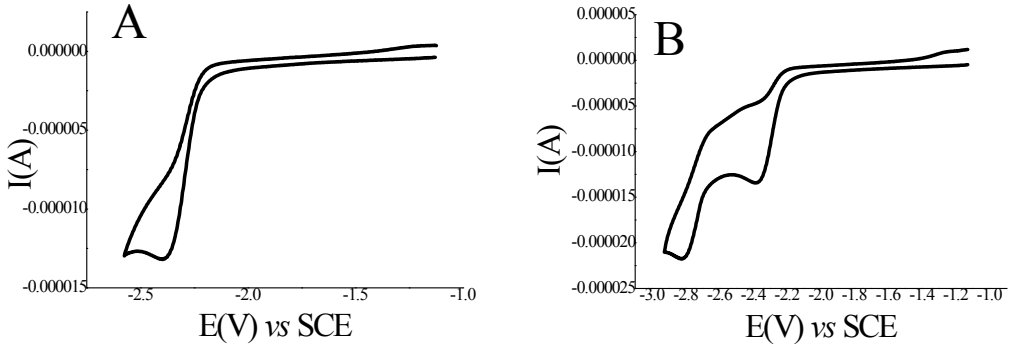

Figure S 42 Cyclic voltammograms of ***SPA-3,6-F(POPh2)2*** *recorded in the cathodic range in DMF + BuN_4PF_6 0.1 M. The CVs are recorded between -1.1 and -2.58 V (A) and between -1.1 and 1.45V(D)) showing the two successive irreversible reduction processes. Sweep-rate: 100 mV/s.*

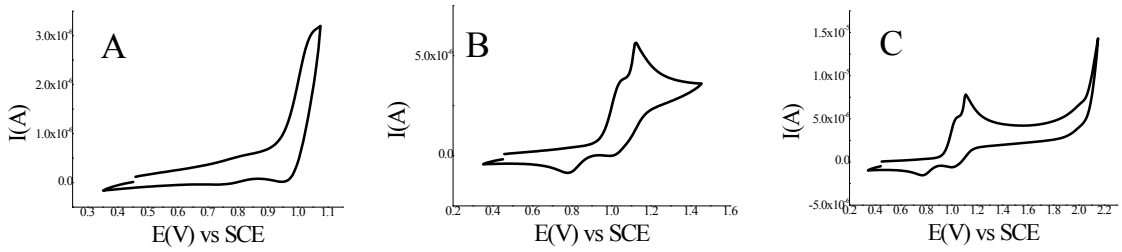

Figure S 43 Cyclic voltammograms of ***SPA-2-F(POPh2)2*** *recorded in the anodic range in CH_2Cl_2 + BuN_4PF_6 0.2 M. The CVs are recorded between 0.35 and 1.07 V(A), between 0.35 and 1.46V (B) and between 0.35 and 2.15 V(C)) showing the successive irreversible oxidation processes. Sweep-rate: 100 mV/s.*

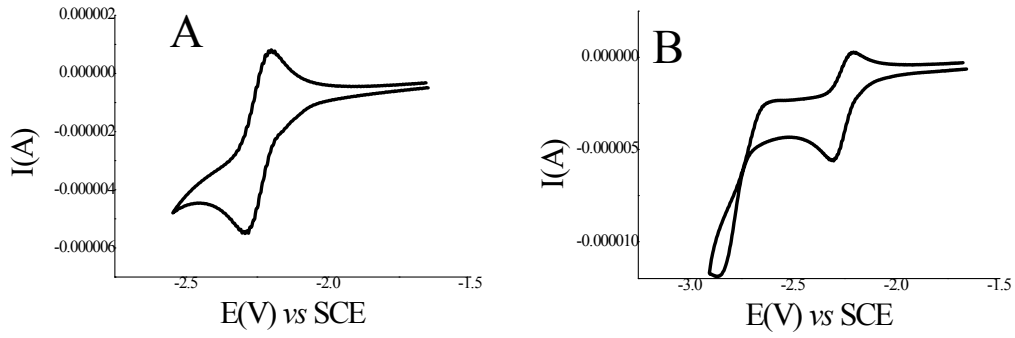

Figure S 44 Cyclic voltammograms of ***SPA-2-F(POPh2)*** *recorded in the cathodic range in DMF + BuN_4PF_6 0.1 M. The CVs are recorded between -1.65 and -2.53 V (A) and between -1.65 and -2.91V (B) showing the successive first reversible and second irreversible reduction processes. Sweep-rate: 100 mV/s.*

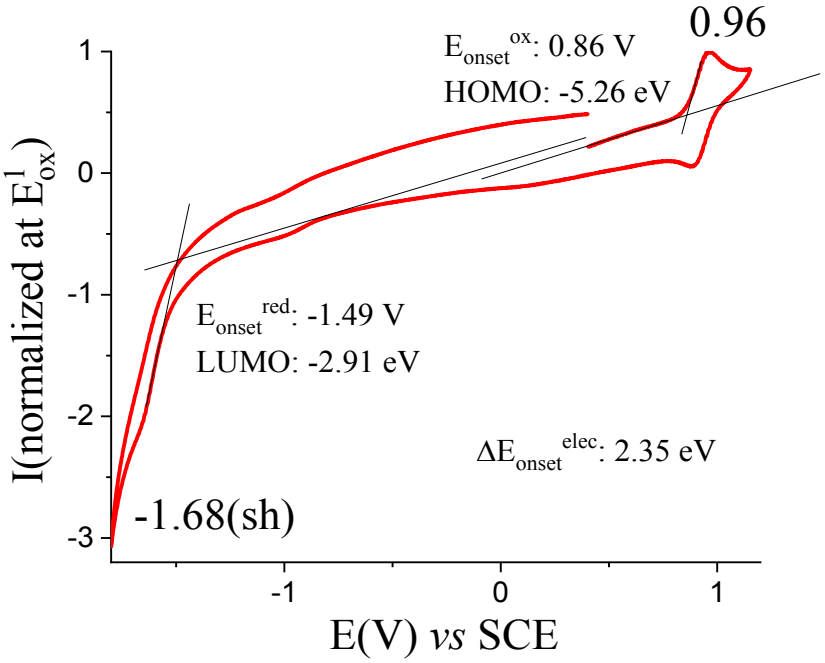

Figure S 45 Normalized cyclic voltammogramms of ***Ir(MDQ)$_2$acac*** *recorded in CH_2Cl_2. Sweep-rate 100 mV/s, platinum disk working electrode.*

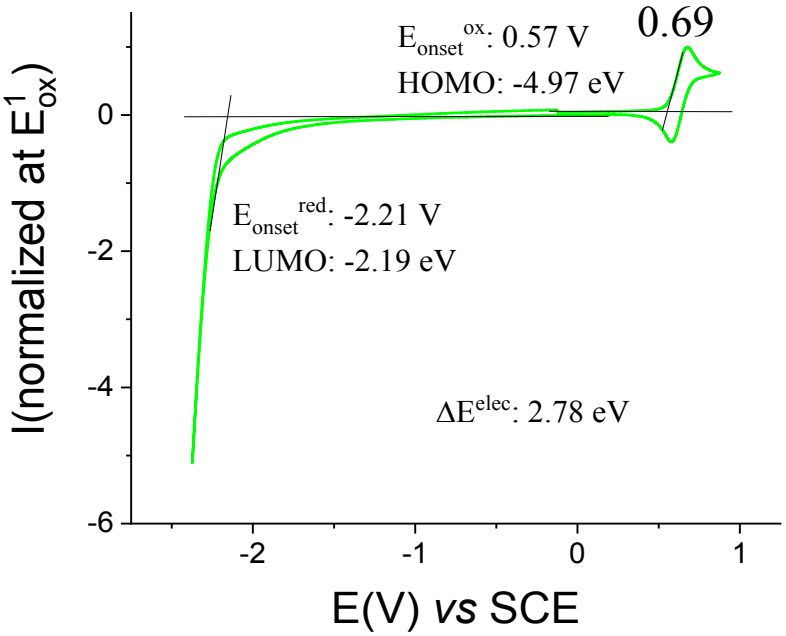

Figure S 46 Normalized cyclic voltammogramms of ***Ir(ppy)$_3$*** *recorded in CH_2Cl_2. Sweep-rate 100 mV/s, platinum disk working electrode.*

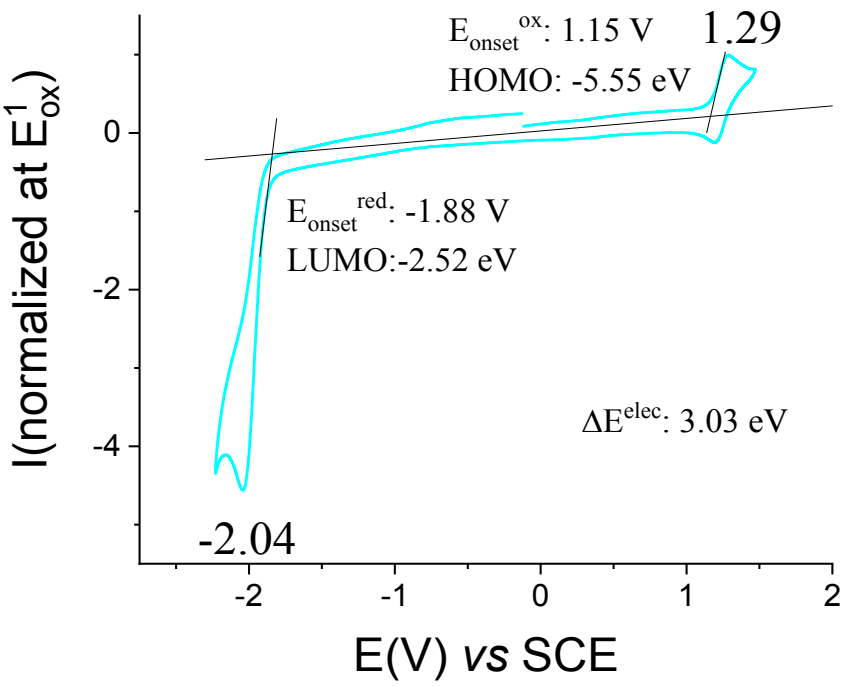

*Figure S 47 Normalized cyclic voltammogramms of **FIrpic** recorded in CH_2Cl_2. Sweep-rate 100 mV/s, platinum disk working electrode.*

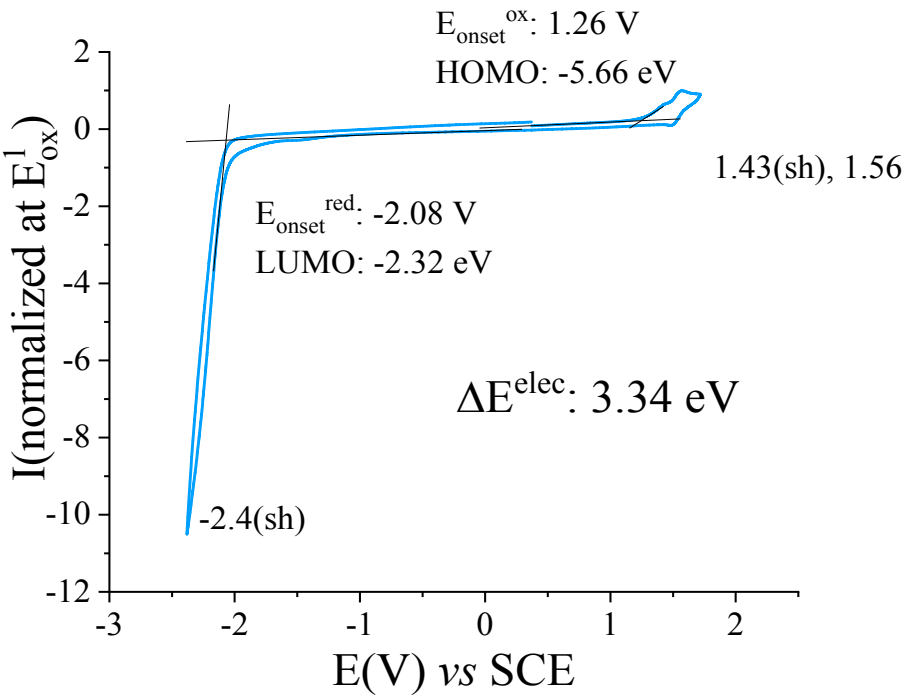

Figure S 48 Normalized cyclic voltammogramms of **FIr_6** recorded in CH_2Cl_2. Sweep-rate 100 mV/s, platinum disk working electrode.

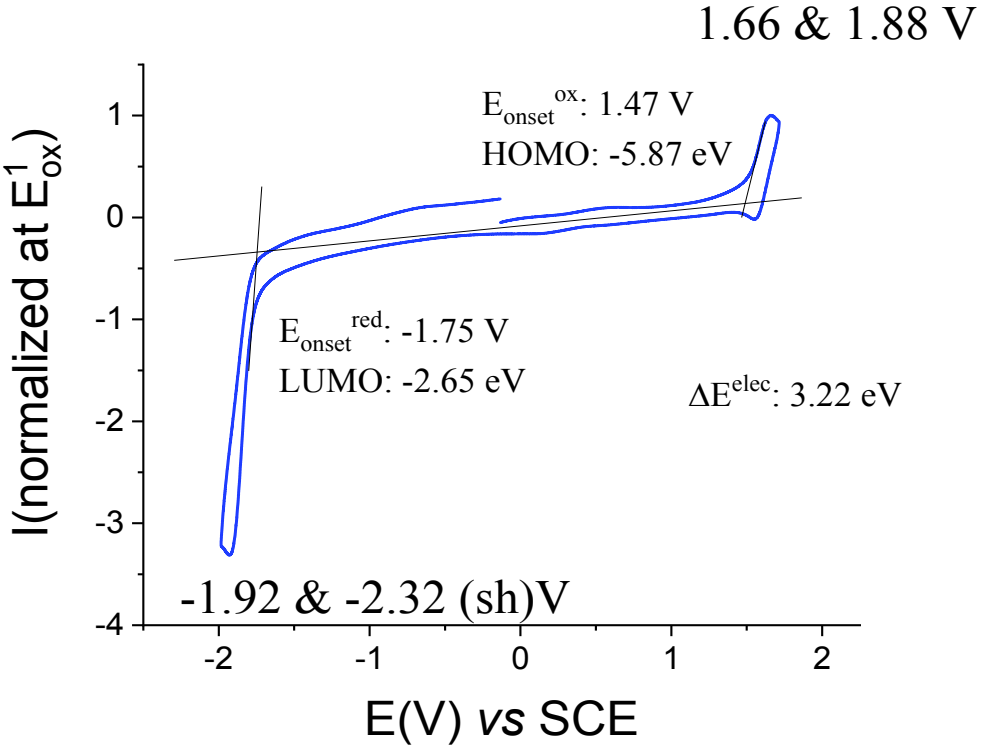

Figure S 49 Normalized cyclic voltammogramms of **FCNIrpic** recorded in CH_2Cl_2. Sweep-rate 100 mV/s, platinum disk working electrode.

6 Molecular modelling

*Table S 4 Results of TD-DFT calculations for **SPA-F***

Wavelength (nm)	Oscillator Strength	Major contributions
354	0	HOMO→LUMO (98%)
348	0	HOMO→L+2 (98%)
340	0.003	HOMO→L+1 (99%)
319	0	HOMO→L+3 (99%)
313	0.043	HOMO→L+4 (94%)
305	0.118	HOMO→L+5 (97%)
292	0.134	H-1→LUMO (77%)
276	0.044	H-1→LUMO (14%), H-1→L+3 (76%)
274	0.062	HOMO→L+7 (88%)
272	0.003	HOMO→L+6 (95%)
271	0.013	H-1→L+1 (88%)
268	0	H-1→L+2 (98%)

*Table S 5 Results of TD-DFT calculations for **SPA-2,7-F(POPh$_2$)$_2$***

Wavelength (nm)	Oscillator Strength	Major contributions
400	0	HOMO→LUMO (99%)
342	0	HOMO→L+3 (43%), HOMO→L+4 (52%)
337	0.009	HOMO→L+1 (55%), HOMO→L+3 (30%), HOMO→L+4 (11%)

332	0.001	HOMO→L+1 (22%), HOMO→L+2 (22%), HOMO→L+5 (35%)
318	0.001	HOMO→L+2 (58%), HOMO→L+3 (12%), HOMO→L+4 (15%)
315	0.374	H-1→LUMO (83%)
315	0.051	HOMO→L+5 (32%), HOMO→L+8 (10%), HOMO→L+9 (16%)
312	0.027	HOMO→L+5 (22%), HOMO→L+7 (26%), HOMO→L+8 (29%)
303	0.046	HOMO→L+6 (10%), HOMO→L+8 (16%), HOMO→L+9 (53%)
301	0.003	HOMO→L+6 (81%)
296	0.001	HOMO→L+7 (61%), HOMO→L+8 (25%)
288	0.015	HOMO→L+10 (84%)

Table S 6 Results of TD-DFT calculations for ***SPA-3,6-F(POPh$_2$)$_2$***

Wavelength (nm)	Osc. Strength	Major contribs
370	0	HOMO→LUMO (92%)
358	0	HOMO→L+1 (91%)
343	0	HOMO→L+5 (35%), HOMO→L+6 (64%)
339	0.013	HOMO→L+2 (32%), HOMO→L+3 (26%), HOMO→L+5 (23%), HOMO→L+6 (18%)
327	0.021	HOMO→L+2 (30%), HOMO→L+5 (33%), HOMO→L+6 (14%)
317	0.017	HOMO→L+2 (26%), HOMO→L+3 (51%), HOMO→L+8 (12%)
314	0.046	HOMO→L+3 (12%), HOMO→L+8 (51%), HOMO→L+9 (16%)
307	0.002	HOMO→L+4 (94%)
299	0.126	H-1→LUMO (34%), H-1→L+1 (48%)
299	0.012	HOMO→L+7 (79%)
292	0.028	HOMO→L+7 (10%), HOMO→L+9 (37%), HOMO→L+10 (31%)
290	0.050	H-1→LUMO (55%), H-1→L+1 (40%)

Table S 7 Results of TD-DFT calculations for ***SPA-2-FPOPh$_2$***

Wavelength (nm)	Osc. Strength	Major contribs
381	0	HOMO→LUMO (99%)

345	0	HOMO→L+2 (43%), HOMO→L+3 (50%)
338	0.009	HOMO→L+1 (41%), HOMO→L+2 (38%), HOMO→L+3 (17%)
330	0.005	HOMO→L+1 (28%), HOMO→L+4 (56%)
319	0.005	HOMO→L+1 (27%), HOMO→L+2 (12%), HOMO→L+3 (19%), HOMO→L+4 (39%)
313	0.036	HOMO→L+5 (13%), HOMO→L+6 (79%)
304	0.152	H-1→LUMO (55%), HOMO→L+5 (24%)
304	0.132	H-1→LUMO (31%), HOMO→L+5 (28%), HOMO→L+7 (11%), HOMO→L+8 (13%)
302	0.043	HOMO→L+5 (28%), HOMO→L+7 (51%), HOMO→L+8 (14%)
291	0.015	HOMO→L+7 (29%), HOMO→L+8 (61%)
283	0.058	H-2→LUMO (13%), H-1→L+1 (43%), H-1→L+4 (25%)
280	0.001	HOMO→L+9 (95%)

*Table S 8 Atomic coordinates of **SPA-F** at the fundamental state after geometry optimization*

Atom	X (Å)	Y (Å)	Z (Å)
C	-1.0443	0.00002	0.00007
C	-2.02838	-0.00002	1.18453
C	-1.7404	-0.00005	2.54382
H	-0.71027	-0.00003	2.89058
C	-2.79715	-0.00009	3.46047
H	-2.58578	-0.00011	4.52649
C	-4.12434	-0.00012	3.01619
H	-4.93475	-0.00016	3.74038
C	-4.4169	-0.0001	1.65072
H	-5.44954	-0.00012	1.3107
C	-3.36201	-0.00005	0.7349
C	-3.36184	-0.00001	-0.7353
C	-4.41651	0	-1.65136
H	-5.44923	-0.00004	-1.31159
C	-4.12364	0.00005	-3.01676
H	-4.93388	0.00006	-3.74115
C	-2.79635	0.0001	-3.46074
H	-2.58473	0.00014	-4.52671
C	-1.73982	0.00009	-2.54385
H	-0.70961	0.00013	-2.89038
C	-2.0281	0.00004	-1.18463
C	-0.18399	1.26857	0.00019
C	-0.82016	2.51682	0.00021
H	-1.90621	2.54053	0.0002
C	-0.10973	3.71138	0.00023
H	-0.63508	4.6618	0.00025
C	1.28545	3.6632	0.00022
H	1.86905	4.5801	0.00022
C	1.94437	2.44088	0.0002
C	1.22393	1.22762	0.0002
C	-0.18399	-1.26854	0.00014
C	-0.82013	-2.51681	0.00013

H	-1.90618	-2.54055	0.0001
C	-0.10967	-3.71135	0.00014
H	-0.63501	-4.66178	0.00014
C	1.2855	-3.66315	0.00015
H	1.86912	-4.58004	0.00016
C	1.94441	-2.44082	0.00017
H	3.02713	-2.41971	0.00019
C	1.22393	-1.22758	0.00016
C	3.34853	0.00001	0.00008
C	4.04882	-0.00014	-1.21046
H	3.49254	-0.00025	-2.14317
C	5.44452	-0.00017	-1.20907
H	5.98467	-0.00029	-2.15186
C	6.1438	-0.00003	-0.00018
H	7.23036	-0.00004	-0.00028
C	5.44475	0.00012	1.20885
H	5.98506	0.00022	2.15153
C	4.04904	0.00013	1.21048
N	1.91205	0.00002	0.00021
H	3.0271	2.4198	0.00018
H	3.49292	0.00023	2.1433

No imaginary frequency

*Table S 9 Atomic coordinates of **SPA-F** at the first triplet state after geometry optimization*

Atom	X (Å)	Y (Å)	Z (Å)
C	-1.0443	0.00002	0.00007
C	-2.02838	-0.00002	1.18453
C	-1.7404	-0.00005	2.54382
H	-0.71027	-0.00003	2.89058
C	-2.79715	-0.00009	3.46047
H	-2.58578	-0.00011	4.52649
C	-4.12434	-0.00012	3.01619
H	-4.93475	-0.00016	3.74038
C	-4.4169	-0.0001	1.65072
H	-5.44954	-0.00012	1.3107
C	-3.36201	-0.00005	0.7349
C	-3.36184	-0.00001	-0.7353
C	-4.41651	0	-1.65136
H	-5.44923	-0.00004	-1.31159
C	-4.12364	0.00005	-3.01676
H	-4.93388	0.00006	-3.74115
C	-2.79635	0.0001	-3.46074
H	-2.58473	0.00014	-4.52671
C	-1.73982	0.00009	-2.54385
H	-0.70961	0.00013	-2.89038
C	-2.0281	0.00004	-1.18463
C	-0.18399	1.26857	0.00019

C	-0.82016	2.51682	0.00021
H	-1.90621	2.54053	0.0002
C	-0.10973	3.71138	0.00023
H	-0.63508	4.6618	0.00025
C	1.28545	3.6632	0.00022
H	1.86905	4.5801	0.00022
C	1.94437	2.44088	0.0002
C	1.22393	1.22762	0.0002
C	-0.18399	-1.26854	0.00014
C	-0.82013	-2.51681	0.00013
H	-1.90618	-2.54055	0.0001
C	-0.10967	-3.71135	0.00014
H	-0.63501	-4.66178	0.00014
C	1.2855	-3.66315	0.00015
H	1.86912	-4.58004	0.00016
C	1.94441	-2.44082	0.00017
H	3.02713	-2.41971	0.00019
C	1.22393	-1.22758	0.00016
C	3.34853	0.00001	0.00008
C	4.04882	-0.00014	-1.21046
H	3.49254	-0.00025	-2.14317
C	5.44452	-0.00017	-1.20907
H	5.98467	-0.00029	-2.15186
C	6.1438	-0.00003	-0.00018
H	7.23036	-0.00004	-0.00028
C	5.44475	0.00012	1.20885
H	5.98506	0.00022	2.15153
C	4.04904	0.00013	1.21048
N	1.91205	0.00002	0.00021
H	3.0271	2.4198	0.00018
H	3.49292	0.00023	2.1433

Table S 10 Atomic coordinates of ***SPA-2,7-F(POPh$_2$)$_2$*** *at the fundamental state after geometry optimization*

Atom	X (Å)	Y (Å)	Z (Å)
C	3.21347	-2.19264	-0.70169
C	2.70347	-3.49873	-0.81255
C	1.3393	-3.74786	-0.66861
C	0.47918	-2.67598	-0.41564
C	0.98247	-1.36506	-0.32933
C	2.34061	-1.11646	-0.47308
C	-0.97332	-2.63427	-0.20355
C	-1.35632	-1.29793	0.01529
C	-0.14737	-0.35235	-0.05775

C	-1.92799	-3.65481	-0.1851
C	-3.26426	-3.32478	0.03747
C	-3.65304	-1.98878	0.24187
C	-2.68559	-0.97027	0.2451
P	5.02847	-2.00192	-0.84237
P	-5.44395	-1.68271	0.47009
C	-0.29176	0.63397	-1.22312
C	0.02375	2.00006	-1.08784
N	0.44602	2.52425	0.14793
C	0.41607	1.74617	1.32033
C	0.09409	0.37528	1.2688
C	0.71208	2.33274	2.5685
C	0.67766	1.58198	3.73657
C	0.34638	0.22663	3.69443
C	0.06206	-0.35502	2.46399
C	-0.70913	0.16037	-2.47421
C	-0.82273	0.99391	-3.58133
C	-0.51063	2.34703	-3.43892
C	-0.09491	2.84499	-2.21109
C	0.83261	3.90604	0.22851
C	2.15917	4.27075	-0.02052
C	2.53796	5.61204	0.05714
C	1.59617	6.58953	0.38498
C	0.27084	6.22469	0.63226
C	-0.11253	4.88522	0.55252
C	5.32193	-0.29004	-1.42972
C	5.67394	-2.07659	0.87027
C	-5.58615	-0.22899	1.57528
C	-6.08198	-1.15133	-1.16335
C	4.96881	-1.60922	1.98935
C	5.53914	-1.68881	3.26078
C	6.81015	-2.24367	3.4245
C	7.50986	-2.72529	2.31605
C	6.94488	-2.6441	1.04317
C	5.40016	0.82548	-0.58365
C	5.62661	2.0966	-1.11596
C	5.77941	2.26187	-2.49432
C	5.71509	1.15289	-3.34049
C	5.49161	-0.11824	-2.81175
C	-5.32146	-0.4536	-2.11322
C	-5.89491	-0.07008	-3.32677
C	-7.22585	-0.38792	-3.60425
C	-7.9833	-1.09646	-2.66912
C	-7.41484	-1.47885	-1.4542
C	-5.81825	-0.4896	2.93393

C	-5.92984	0.5634	3.84175
C	-5.81464	1.88336	3.40058
C	-5.59627	2.15016	2.04763
C	-5.48683	1.09904	1.13597
O	5.6552	-3.03227	-1.74014
O	-6.16853	-2.88542	1.00809
H	3.38879	-4.3139	-1.02476
H	0.95825	-4.76225	-0.75299
H	2.71987	-0.09995	-0.41625
H	-1.64058	-4.69145	-0.33985
H	-4.02353	-4.10035	0.06954
H	-2.96547	0.0624	0.43507
H	0.9677	3.38379	2.61832
H	0.9081	2.06385	4.68308
H	0.31124	-0.36769	4.60255
H	-0.18909	-1.41084	2.41778
H	-0.94363	-0.89531	-2.57559
H	-1.1427	0.59273	-4.53836
H	-0.59057	3.02342	-4.2858
H	0.1399	3.89774	-2.11493
H	2.88133	3.50141	-0.27882
H	3.56923	5.89324	-0.13805
H	1.89354	7.63275	0.44633
H	-0.46548	6.98235	0.88584
H	-1.13977	4.58791	0.74218
H	3.96857	-1.19955	1.8767
H	4.98624	-1.3266	4.12338
H	7.2503	-2.30904	4.41613
H	8.49362	-3.16918	2.44334
H	7.47138	-3.03298	0.17657
H	5.30566	0.70387	0.49164
H	5.70093	2.95385	-0.45144
H	5.95983	3.25112	-2.90677
H	5.84618	1.27706	-4.41203
H	5.46503	-0.98931	-3.45981
H	-4.27729	-0.22251	-1.92091
H	-5.29819	0.46889	-4.05785
H	-7.66883	-0.09196	-4.55161
H	-9.01553	-1.35638	-2.88814
H	-7.98939	-2.04761	-0.72905
H	-5.92763	-1.51871	3.2631
H	-6.11239	0.354	4.89237
H	-5.90403	2.70335	4.10834
H	-5.52151	3.17693	1.69926
H	-5.34349	1.31709	0.08127

No imaginary frequency

Table S 11 Atomic coordinates of ***SPA-2,7-F(POPh$_2$)$_2$*** *at the first triplet state after geometry optimization*

Atom	X (Å)	Y (Å)	Z (Å)
C	3.22979	-2.14172	-0.71182
C	2.70576	-3.48202	-0.79842
C	1.37545	-3.74369	-0.63246
C	0.47036	-2.64936	-0.37316
C	1.00608	-1.28939	-0.32156
C	2.34127	-1.04981	-0.48681
C	-0.89862	-2.61921	-0.14744
C	-1.33125	-1.23929	0.05601
C	-0.13103	-0.2814	-0.05642
C	-1.88087	-3.67448	-0.07545
C	-3.18743	-3.35296	0.16678
C	-3.60792	-1.98849	0.34451
C	-2.64205	-0.93991	0.29992
P	5.03114	-1.95887	-0.88706
P	-5.38819	-1.71098	0.60368
C	-0.29148	0.67213	-1.2413
C	-0.00123	2.04524	-1.13858
N	0.40629	2.60613	0.08451
C	0.40503	1.8514	1.27078
C	0.11505	0.47449	1.24899
C	0.69736	2.46703	2.50333
C	0.68891	1.73917	3.68476
C	0.38669	0.37889	3.67197
C	0.10712	-0.23211	2.45644
C	-0.69291	0.15908	-2.47964
C	-0.81256	0.96022	-3.60789
C	-0.52249	2.31885	-3.49946
C	-0.1243	2.85587	-2.28365
C	0.71642	4.00934	0.14393
C	2.02298	4.44026	-0.08517
C	2.32613	5.79995	-0.02955
C	1.32645	6.72897	0.25516
C	0.02032	6.29665	0.48339
C	-0.28585	4.93837	0.42735
C	5.33396	-0.20842	-1.34859
C	5.73672	-2.18453	0.79105
C	-5.53343	-0.15091	1.55823
C	-6.11341	-1.38089	-1.04891
C	5.05941	-1.82681	1.96288
C	5.65894	-2.02387	3.20579

C	6.93241	-2.58578	3.28563
C	7.60496	-2.95678	2.1217
C	7.00983	-2.76038	0.87757
C	5.53522	0.81771	-0.41917
C	5.7721	2.12136	-0.85451
C	5.81193	2.40693	-2.21821
C	5.62112	1.38585	-3.14889
C	5.38752	0.08253	-2.71779
C	-5.41369	-0.75569	-2.08787
C	-6.03416	-0.53487	-3.31645
C	-7.35174	-0.94404	-3.51716
C	-8.04789	-1.58024	-2.48997
C	-7.432	-1.80132	-1.26017
C	-5.57587	-0.26852	2.95337
C	-5.68224	0.86912	3.74918
C	-5.75283	2.13119	3.15995
C	-5.72398	2.25343	1.77205
C	-5.6173	1.11656	0.97175
O	5.61515	-2.92328	-1.88151
O	-6.05138	-2.87108	1.29227
H	3.39792	-4.28749	-1.01562
H	1.0004	-4.75814	-0.70293
H	2.72708	-0.03704	-0.45239
H	-1.58234	-4.70869	-0.20181
H	-3.93811	-4.1308	0.24683
H	-2.94718	0.08709	0.46821
H	0.92854	3.5225	2.5327
H	0.9156	2.24267	4.61794
H	0.37008	-0.1956	4.59031
H	-0.12237	-1.29146	2.43616
H	-0.90719	-0.90072	-2.55777
H	-1.11801	0.53086	-4.55451
H	-0.60435	2.96871	-4.36355
H	0.09529	3.91214	-2.21735
H	2.79095	3.70886	-0.30918
H	3.34217	6.1328	-0.20889
H	1.56363	7.78586	0.29849
H	-0.75997	7.01609	0.7043
H	-1.29726	4.59056	0.60321
H	4.06013	-1.40836	1.91265
H	5.12803	-1.74716	4.10976
H	7.39562	-2.74263	4.25347
H	8.59013	-3.40557	2.18274
H	7.51548	-3.0643	-0.03189
H	5.52594	0.60334	0.64311

H	5.93933	2.90871	-0.12759
H	6.00218	3.41982	-2.55577
H	5.66301	1.60265	-4.21035
H	5.2638	-0.71971	-3.43629
H	-4.38166	-0.45239	-1.95071
H	-5.48575	-0.05185	-4.11742
H	-7.83156	-0.77549	-4.47487
H	-9.06846	-1.91053	-2.64823
H	-7.95786	-2.31314	-0.46229
H	-5.54379	-1.25389	3.4041
H	-5.71715	0.77012	4.82833
H	-5.83949	3.01597	3.78084
H	-5.79441	3.23198	1.31016
H	-5.61756	1.2217	-0.10699

Table S 12 Atomic coordinates of ***SPA-3,6-F(POPh$_2$)$_2$*** *at the fundamental state after geometry optimization*

Atom	X (Å)	Y (Å)	Z (Å)
C	0	0	0
C	0	0	1.39542176
C	1.21153333	0	2.09345391
C	2.42125982	-0.0001871	1.39215476
C	2.4176778	-0.0002453	-0.0032647
C	1.20788244	-9.673E-05	-0.70044
N	1.21254184	0.00036181	3.53056656
C	1.21235412	1.22701424	4.21787087
C	1.1970871	1.26949382	5.62576844
C	1.17040855	0.00048898	6.485195
C	1.19854362	-1.2684963	5.62658928
C	1.2138035	-1.2267698	4.21893354
C	1.20130274	-2.5160841	6.26398773
C	1.21864897	-3.7100995	5.55354511
C	1.23331229	-3.6615639	4.15869692
C	1.23116054	-2.4398923	3.49918722
C	1.22841376	2.4403128	3.49783793
C	1.22939519	3.66232666	4.15650989
C	1.21510498	3.71159362	5.5514092
C	1.19904914	2.517576	6.26204422
C	-0.0450954	0.00068589	7.430464
C	0.3619947	0.00735852	8.77869069
C	1.83166449	0.01224401	8.8250746
C	2.32194649	0.00378991	7.50605008
C	2.70991068	0.0161684	9.90851267

C	4.09108666	0.01561181	9.66563551
C	4.57277152	-0.0111527	8.34571031
C	3.68954288	-0.0121401	7.26221435
C	-1.3939704	-0.0071805	7.10187084
C	-2.3424752	-0.0088203	8.12931191
C	-1.9450418	-0.0004999	9.47606267
C	-0.5812439	0.00648861	9.80501577
P	5.17065469	0.04528426	11.14425
P	-3.2888128	-0.0351611	10.7240635
C	6.67015429	-0.9128045	10.7104536
C	5.71252569	1.78220908	11.3582566
O	4.47839706	-0.4933854	12.3660512
C	-2.9630068	-1.4834515	11.7973185
C	-3.0345596	1.43303697	11.7879524
O	-4.6404427	-0.1180202	10.0676827
C	5.95952443	2.2058915	12.6724768
C	6.38942182	3.50900268	12.9208231
C	6.57234691	4.3997851	11.8612414
C	6.31530472	3.98889181	10.5520949
C	5.88234957	2.68625834	10.299982
C	6.70713545	-2.2497178	11.1330326
C	7.80688398	-3.0515417	10.8292005
C	8.8786764	-2.525005	10.1056481
C	8.85447389	-1.1913191	9.69390374
C	7.75685806	-0.3851174	9.99859595
C	-3.7803235	-2.6057733	11.6039315
C	-3.5704339	-3.7647499	12.3517761
C	-2.5446272	-3.8111493	13.2971257
C	-1.7317917	-2.6938661	13.501404
C	-1.9409376	-1.5330083	12.7571431
C	-3.5920888	1.45460822	13.0766858
C	-3.5064511	2.6010351	13.8646805
C	-2.8667024	3.74107774	13.3736255
C	-2.3170128	3.73271113	12.0912775
C	-2.401987	2.58608053	11.3008782
H	-0.9427377	-5.566E-05	-0.5387741
H	-0.9315506	-8.553E-05	1.95247633
H	3.35425646	-0.0005039	1.9468489
H	3.35892934	-0.0005347	-0.5447176
H	1.2064009	-0.0001979	-1.7862999
H	1.18757901	-2.5409453	7.34944639
H	1.21915985	-4.659831	6.07836767
H	1.24616648	-4.5780589	3.57600835
H	1.24242629	-2.4181914	2.41713019
H	1.23944246	2.41814601	2.41579324

H	1.24089773	4.57847185	3.57321498
H	1.21461595	4.66183301	6.07552568
H	1.18606923	2.54218151	7.34760404
H	2.35274468	0.00089621	10.9338429
H	5.64157494	-0.0532732	8.15943803
H	4.07006697	-0.0365841	6.24524166
H	-1.7119666	-0.0142496	6.06336548
H	-3.4046002	-0.020575	7.90630788
H	-0.2586815	0.00913882	10.8419129
H	5.79392289	1.51120414	13.4900101
H	6.57643819	3.83083951	13.9411379
H	6.90555171	5.41517017	12.0557275
H	6.44228879	4.68445704	9.72761221
H	5.65907825	2.38360365	9.28130191
H	5.87753304	-2.6422093	11.7127357
H	7.82987855	-4.0852535	11.16158
H	9.73566146	-3.1497867	9.87103194
H	9.69384208	-0.7753636	9.14423292
H	7.75875548	0.65841302	9.69796775
H	-4.5814712	-2.549233	10.8736061
H	-4.2094764	-4.6295193	12.198493
H	-2.3812422	-4.7137773	13.8789206
H	-0.9387322	-2.7240845	14.2427086
H	-1.3183432	-0.662527	12.9420109
H	-4.0912091	0.57195527	13.4648546
H	-3.9379444	2.60467668	14.8612916
H	-2.7980422	4.63343835	13.9890446
H	-1.8209418	4.61828882	11.7050823
H	-1.97313	2.58817304	10.3040667

No imaginary frequency

Table S 13 Atomic coordinates of ***SPA-3,6-F(POPh$_2$)$_2$*** *at the first triplet state after geometry optimization*

Atom	X (Å)	Y (Å)	Z (Å)
C	7.63678	-3.6026	-0.21376
C	6.42302	-2.9168	-0.22993
C	5.22634	-3.61379	-0.0666
C	5.24492	-4.99808	0.1127
C	6.45901	-5.68155	0.1287
C	7.65621	-4.9848	-0.03442
N	3.97742	-2.90058	-0.08429

C	3.40905	-2.48187	1.13247
C	2.1975	-1.76518	1.15078
C	1.50102	-1.32837	-0.13999
C	2.05366	-2.08003	-1.35302
C	3.26775	-2.78978	-1.29434
C	1.37718	-2.00377	-2.57462
C	1.86829	-2.59898	-3.72975
C	3.07605	-3.29032	-3.66699
C	3.76685	-3.38747	-2.46716
C	4.04789	-2.7744	2.35252
C	3.49367	-2.37716	3.56134
C	2.28648	-1.68237	3.58765
C	1.65898	-1.38537	2.38429
C	1.63844	0.19544	-0.34041
C	0.31641	0.82586	-0.34746
C	-0.66122	-0.14283	-0.16355
C	-0.02833	-1.45641	-0.03481
C	-2.09615	-0.04131	-0.08578
C	-2.83952	-1.17986	0.10447
C	-2.20081	-2.4646	0.22791
C	-0.79149	-2.57799	0.15429
C	2.76764	0.9521	-0.5027
C	2.65428	2.35239	-0.67516
C	1.36274	2.99222	-0.67524
C	0.21544	2.25408	-0.52572
P	-4.65317	-0.94497	0.22266
P	1.35529	4.80617	-0.93619
C	-5.39399	-1.94442	-1.1224
C	-5.1787	-1.74749	1.78652
O	-5.02466	0.51079	0.1921
C	-0.39512	5.30269	-1.14444
C	1.92969	5.52137	0.65105
O	2.20869	5.23377	-2.09666
C	-5.46118	-0.90154	2.86508
C	-5.83383	-1.43709	4.09635
C	-5.92933	-2.81836	4.25812
C	-5.65834	-3.66589	3.18426
C	-5.28648	-3.13359	1.95163
C	-4.65497	-2.32578	-2.24778
C	-5.27447	-2.99324	-3.30367
C	-6.63647	-3.2795	-3.24618
C	-7.38229	-2.8945	-2.13172
C	-6.76554	-2.23017	-1.07578
C	-0.82846	5.54479	-2.45346
C	-2.15069	5.91122	-2.69557

C	-3.04598	6.0415	-1.63506
C	-2.61595	5.8151	-0.32824
C	-1.29382	5.4509	-0.08139
C	2.6423	6.72469	0.58842
C	3.09475	7.33088	1.75805
C	2.84498	6.73809	2.99539
C	2.14776	5.53274	3.06253
C	1.69319	4.92343	1.8942
H	8.56483	-3.05712	-0.34136
H	6.39537	-1.84238	-0.36905
H	4.30864	-5.52955	0.23841
H	6.47001	-6.75659	0.26815
H	8.60024	-5.51752	-0.02199
H	0.44536	-1.45184	-2.61804
H	1.32356	-2.51628	-4.66253
H	3.48713	-3.75951	-4.55383
H	4.70071	-3.93089	-2.43583
H	4.98213	-3.31807	2.35102
H	4.00956	-2.61735	4.4843
H	1.84437	-1.37221	4.52684
H	0.72449	-0.83635	2.39563
H	-2.59817	0.9162	-0.16834
H	-2.79652	-3.3541	0.38544
H	-0.3285	-3.55411	0.25205
H	3.7506	0.49352	-0.50767
H	3.54074	2.95285	-0.83589
H	-0.76005	2.72448	-0.54592
H	-5.39849	0.17109	2.72119
H	-6.05496	-0.77585	4.92674
H	-6.22107	-3.23435	5.21605
H	-5.74341	-4.74014	3.30437
H	-5.10187	-3.80126	1.11751
H	-3.59623	-2.10243	-2.30392
H	-4.69253	-3.2867	-4.17009
H	-7.11756	-3.7977	-4.0682
H	-8.44393	-3.10981	-2.08665
H	-7.35309	-1.92891	-0.21565
H	-0.11965	5.45576	-3.26869
H	-2.48047	6.09698	-3.71158
H	-4.07576	6.32266	-1.82471
H	-3.30871	5.92354	0.49851
H	-0.96628	5.29362	0.93985
H	2.84938	7.16683	-0.37949
H	3.64736	8.26215	1.70315
H	3.20059	7.20964	3.90481

H	1.96532	5.06222	4.02223
H	1.17013	3.97522	1.95291

*Table S 14 Atomic coordinates of **SPA-2-FPOPh$_2$** at the fundamental state after geometry optimization*

Atom	X (Å)	Y (Å)	Z (Å)
C	4.45103	-4.38764	1.17046
C	4.13196	-3.04094	0.99115
C	2.84097	-2.67521	0.59516
C	1.87318	-3.65982	0.37439
C	2.19704	-5.00601	0.55201
C	3.48419	-5.37152	0.95137
N	2.50522	-1.29062	0.40825
C	2.10722	-0.52097	1.51649
C	1.72306	0.82592	1.35892
C	1.63171	1.48778	-0.01991
C	2.29137	0.62537	-1.10281
C	2.67079	-0.70989	-0.86419
C	2.47898	1.15896	-2.38437
C	3.02441	0.41402	-3.42372
C	3.39798	-0.90831	-3.17977
C	3.2266	-1.46366	-1.91836
C	2.08632	-1.0919	2.80634
C	1.7047	-0.34385	3.91274
C	1.33491	0.99415	3.76579
C	1.3482	1.55644	2.49401
C	2.20946	2.9117	-0.01212
C	1.22546	3.86206	-0.34326
C	-0.04522	3.16108	-0.57172
C	0.16172	1.7828	-0.37939
C	-1.3096	3.64239	-0.92075
C	-2.36345	2.73934	-1.05451
C	-2.16565	1.36387	-0.83869
C	-0.88665	0.88293	-0.51231
C	3.51227	3.31047	0.26214
C	3.83009	4.67139	0.20412
C	2.85322	5.61832	-0.12628
C	1.54367	5.2214	-0.40262
P	-3.63945	0.29046	-0.97934
C	-3.02698	-1.37838	-1.42827
C	-4.32075	0.14539	0.71548
O	-4.65148	0.81214	-1.96159
C	-5.71065	-0.00636	0.82801
C	-6.30355	-0.13513	2.08406

C	-5.5148	-0.11061	3.23629
C	-4.1319	0.05255	3.13204
C	-3.53532	0.18535	1.87702
C	-2.58367	-2.32631	-0.49494
C	-2.1351	-3.57764	-0.92308
C	-2.12872	-3.89174	-2.28389
C	-2.58083	-2.95635	-3.21693
C	-3.03196	-1.70675	-2.79223
H	5.45447	-4.66765	1.47912
H	4.87486	-2.26609	1.1563
H	0.8771	-3.36314	0.05838
H	1.44346	-5.76933	0.37811
H	3.7339	-6.41985	1.09004
H	2.18223	2.18804	-2.56417
H	3.15289	0.85759	-4.40652
H	3.82841	-1.51493	-3.97216
H	3.52565	-2.48953	-1.74287
H	2.37437	-2.12753	2.93739
H	1.70129	-0.81233	4.89346
H	1.03899	1.58885	4.62493
H	1.05506	2.59442	2.3653
H	-1.47686	4.70344	-1.08735
H	-3.35099	3.08912	-1.34032
H	-0.71515	-0.18103	-0.37366
H	4.27221	2.57664	0.51707
H	4.84486	4.99674	0.41697
H	3.11666	6.67178	-0.16773
H	0.78799	5.95974	-0.65823
H	-6.31645	-0.00383	-0.07337
H	-7.3814	-0.24914	2.16381
H	-5.97775	-0.20913	4.21475
H	-3.51695	0.08639	4.02744
H	-2.46154	0.33797	1.80873
H	-2.60656	-2.09985	0.56722
H	-1.80735	-4.31207	-0.1915
H	-1.783	-4.86745	-2.61523
H	-2.58873	-3.20265	-4.27529
H	-3.40888	-0.98294	-3.50881

No imaginary frequency

Table S 15 Atomic coordinates of ***SPA-2-FPOPh$_2$*** *at the first triplet state after geometry optimization*

Atom	X (Å)	Y (Å)	Z (Å)
C	4.96645	-3.94891	1.15309
C	4.48251	-2.6514	0.9684
C	3.15005	-2.44935	0.59172

C	2.30397	-3.54548	0.39741
C	2.79071	-4.84278	0.58157
C	4.12111	-5.04631	0.96002
N	2.64678	-1.11614	0.3995
C	2.16599	-0.39547	1.50811
C	1.65532	0.91039	1.35367
C	1.51958	1.57303	-0.01955
C	2.26209	0.78265	-1.10066
C	2.76228	-0.51522	-0.86918
C	2.40487	1.34199	-2.37834
C	3.01953	0.6573	-3.42342
C	3.50835	-0.62987	-3.18768
C	3.38432	-1.20898	-1.92863
C	2.18736	-0.974	2.7956
C	1.72442	-0.27174	3.90399
C	1.22989	1.02715	3.76053
C	1.20126	1.59557	2.48933
C	1.96638	3.0474	0.00829
C	0.84904	3.92459	-0.33541
C	-0.28786	3.16093	-0.57683
C	0.0308	1.73959	-0.39489
C	-1.63579	3.52997	-0.95557
C	-2.57932	2.54988	-1.10822
C	-2.26526	1.15268	-0.89177
C	-0.92766	0.77467	-0.55006
C	3.20476	3.56691	0.29189
C	3.39898	4.97466	0.25059
C	2.31819	5.84505	-0.08467
C	1.0649	5.35385	-0.37422
P	-3.64036	-0.02548	-1.04448
C	-2.89015	-1.675	-1.33985
C	-4.43844	-0.10662	0.60653
O	-4.61821	0.36042	-2.12661
C	-5.8204	-0.34867	0.64427
C	-6.48701	-0.42498	1.86937
C	-5.78067	-0.25523	3.06424
C	-4.40613	-0.00219	3.03254
C	-3.73663	0.0755	1.8082
C	-2.5145	-2.55682	-0.31596
C	-1.96292	-3.80341	-0.62681
C	-1.78432	-4.17797	-1.96145
C	-2.16449	-3.30632	-2.98677
C	-2.71942	-2.06268	-2.67869
H	6.00188	-4.10217	1.44606
H	5.12984	-1.79082	1.1142

H	1.2731	-3.37452	0.0992
H	2.13111	-5.69312	0.4286
H	4.49832	-6.05556	1.10306
H	2.01544	2.34101	-2.55419
H	3.11064	1.11817	-4.40279
H	3.99133	-1.19088	-3.98378
H	3.77269	-2.20684	-1.76352
H	2.57171	-1.97842	2.92709
H	1.75619	-0.74497	4.88225
H	0.87129	1.58608	4.62028
H	0.81073	2.60213	2.36538
H	-1.89042	4.5729	-1.12472
H	-3.59053	2.80539	-1.41224
H	-0.67841	-0.27525	-0.41934
H	4.03595	2.91335	0.54628
H	4.37579	5.39271	0.4746
H	2.49551	6.91753	-0.10959
H	0.24767	6.0234	-0.62777
H	-6.36509	-0.45971	-0.28935
H	-7.55812	-0.60995	1.89063
H	-6.30117	-0.31121	4.01716
H	-3.85527	0.14286	3.95851
H	-2.67126	0.29236	1.79409
H	-2.6649	-2.28379	0.72492
H	-1.68648	-4.48472	0.17444
H	-1.36008	-5.14966	-2.20255
H	-2.03716	-3.59818	-4.02611
H	-3.03962	-1.39243	-3.47169

7 Single layer Phosphorescent OLED characteristics

The architecture of the single layer devices is the following: ITO/PEDOT:PSS (40 nm)/Emissive layer (host matrix + red or green or blue phosphorescent guest 10%, 100 nm)/LiF (1.2 nm)/Al (100 nm).

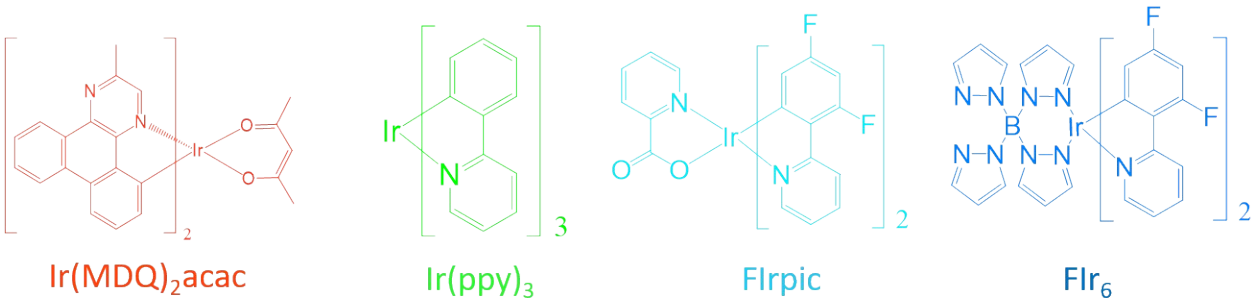

Chart 1 Phosphorescent guest structures

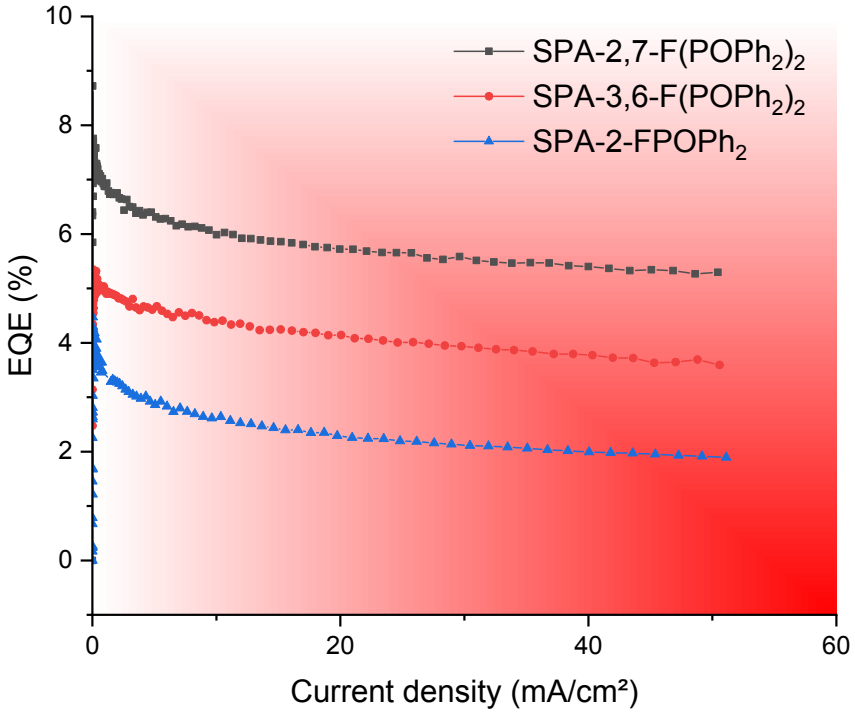

Figure S 50 EQE (%) versus Current density (mA/cm²) for red SL-PhOLED using $Ir(MDQ)_2acac$ (10 %) as phosphorescent guest

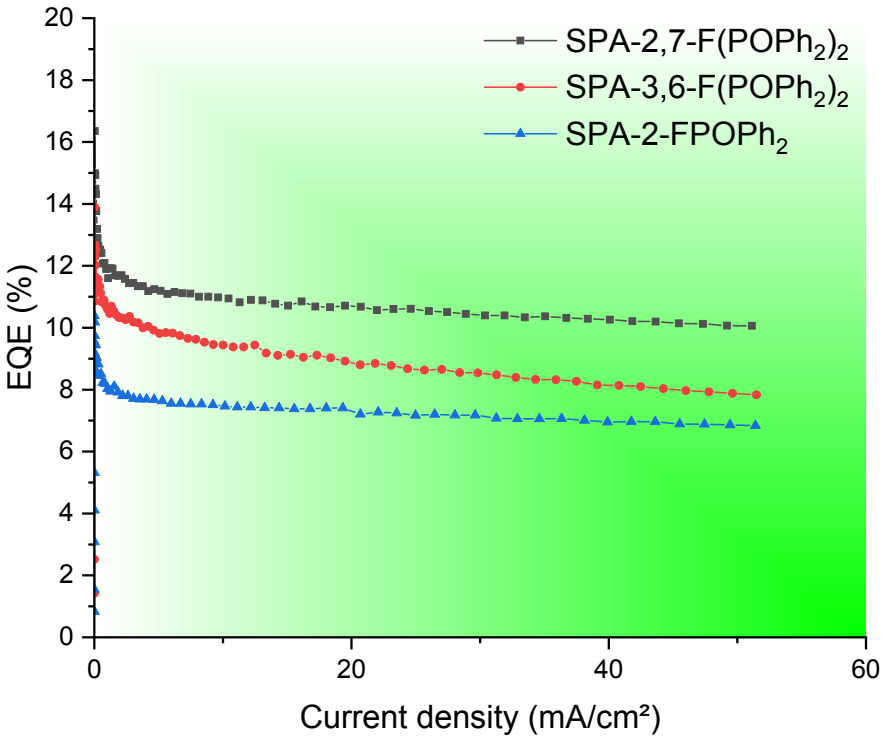

Figure S 51 EQE (%) versus Current density (mA/cm²) for green SL-PhOLED using $Ir(ppy)_3$ (10 %) as phosphorescent guest

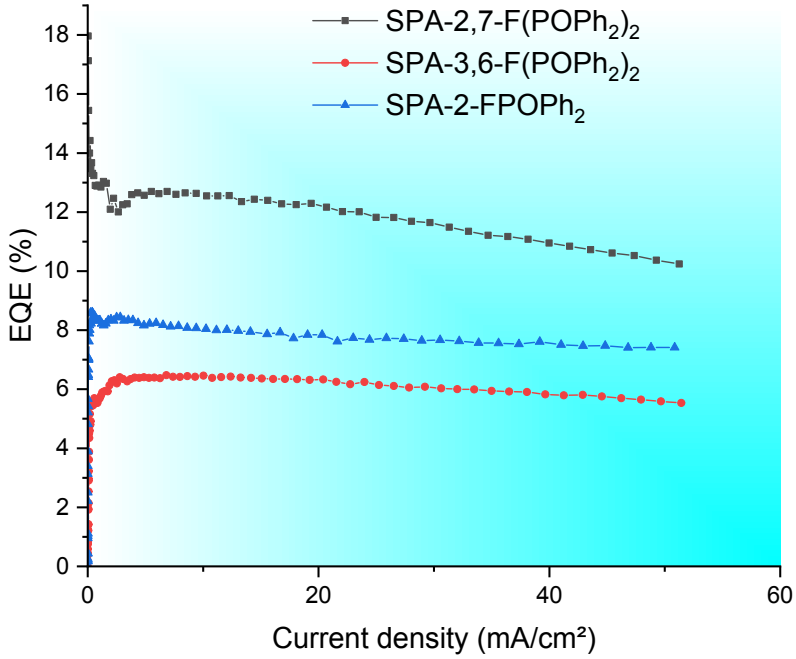

Figure S 52 EQE (%) versus Current density (mA/cm²) for sky blue SL-PhOLED using FIrpic (10 %) as phosphorescent guest

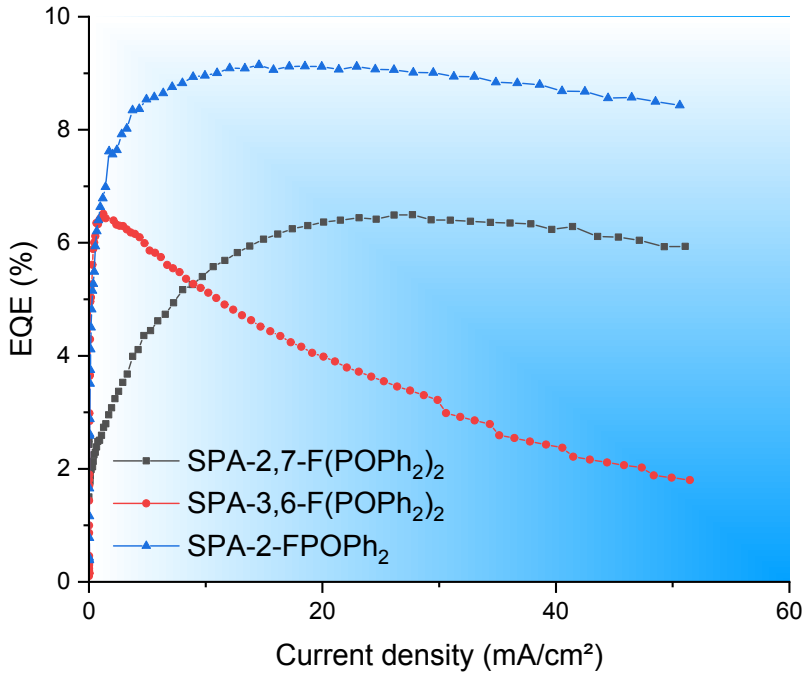

Figure S 53 EQE (%) versus Current density (mA/cm²) for blue SL-PhOLED using Fir_6 (10 %) as phosphorescent guest

8 Copy of NMR spectra

8.1 **SPA-F** – ^{1}H – CD_2Cl_2

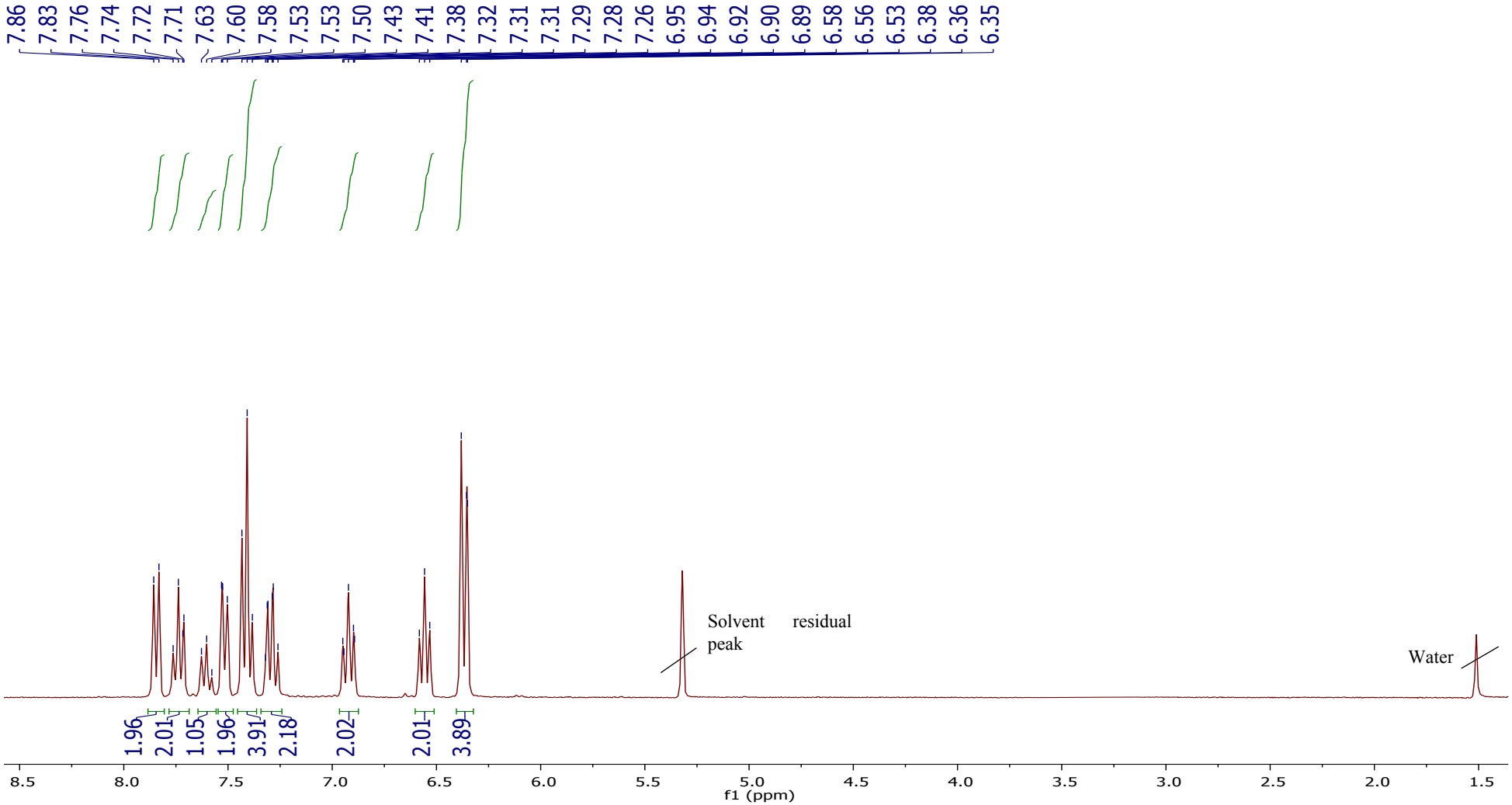

Figure S 54 ***SPA-F*** *– ^{1}H – CD_2Cl_2*

8.2 **SPA-F** – ^{13}C – CD_2Cl_2

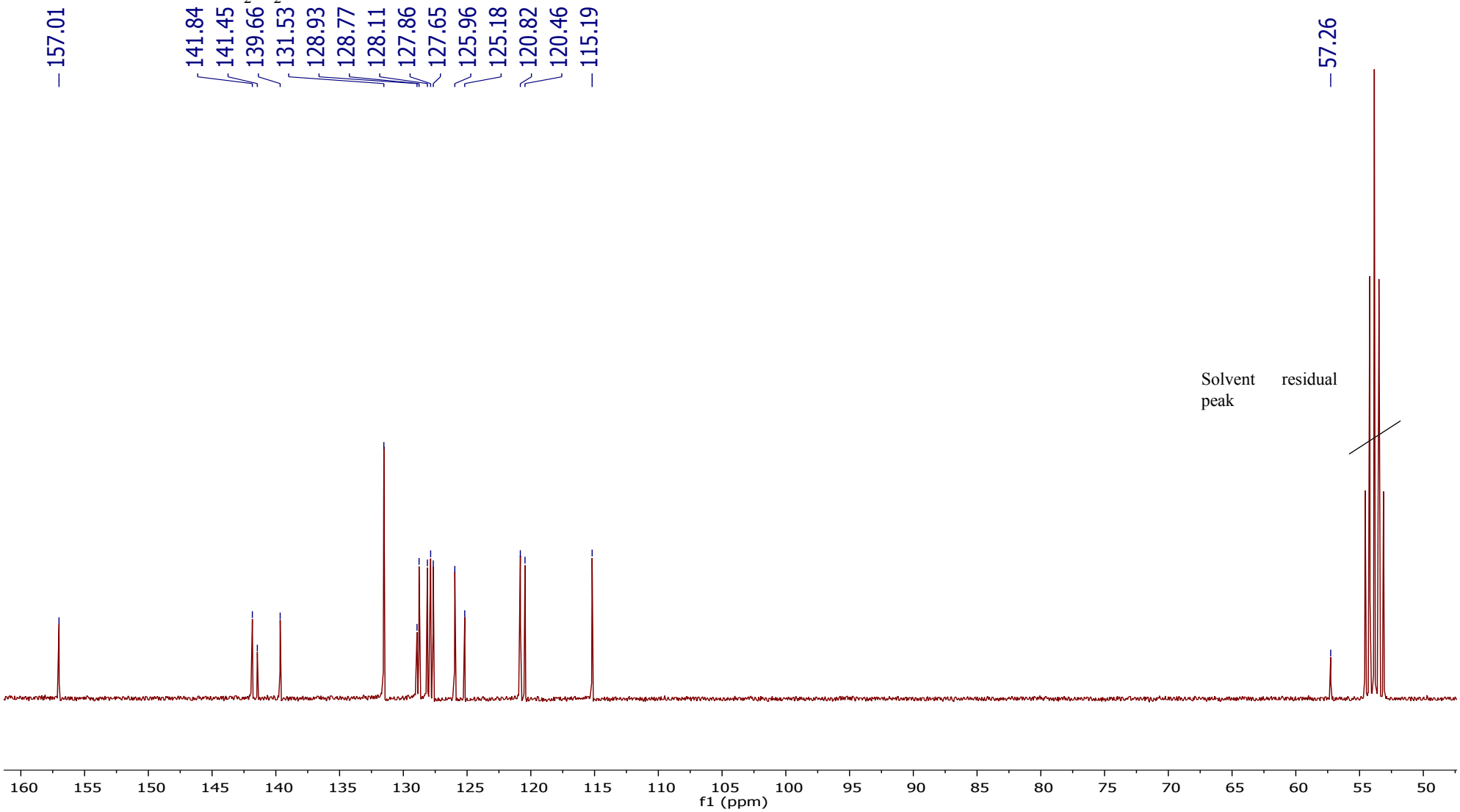

Figure S 55 ***SPA-F*** *– ^{13}C – CD_2Cl_2*

8.3 **SPA-F** – ^{13}C – DEPT135 – CD_2Cl_2

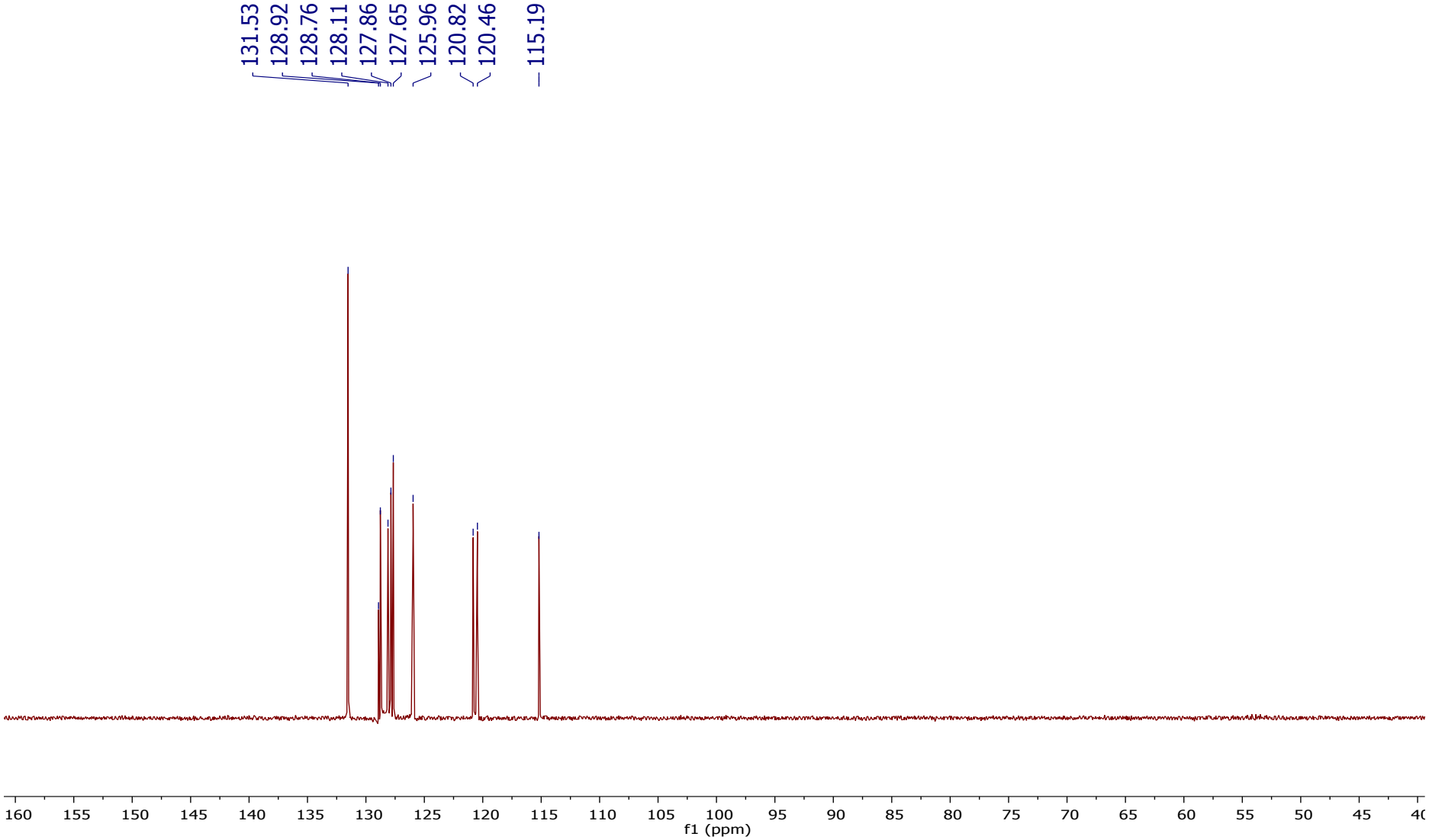

Figure S 56 ***SPA-F*** *– ^{13}C – DEPT135 – CD_2Cl_2*

8.4 **SPA-2-FBr** – ^{1}H – CD_2Cl_2

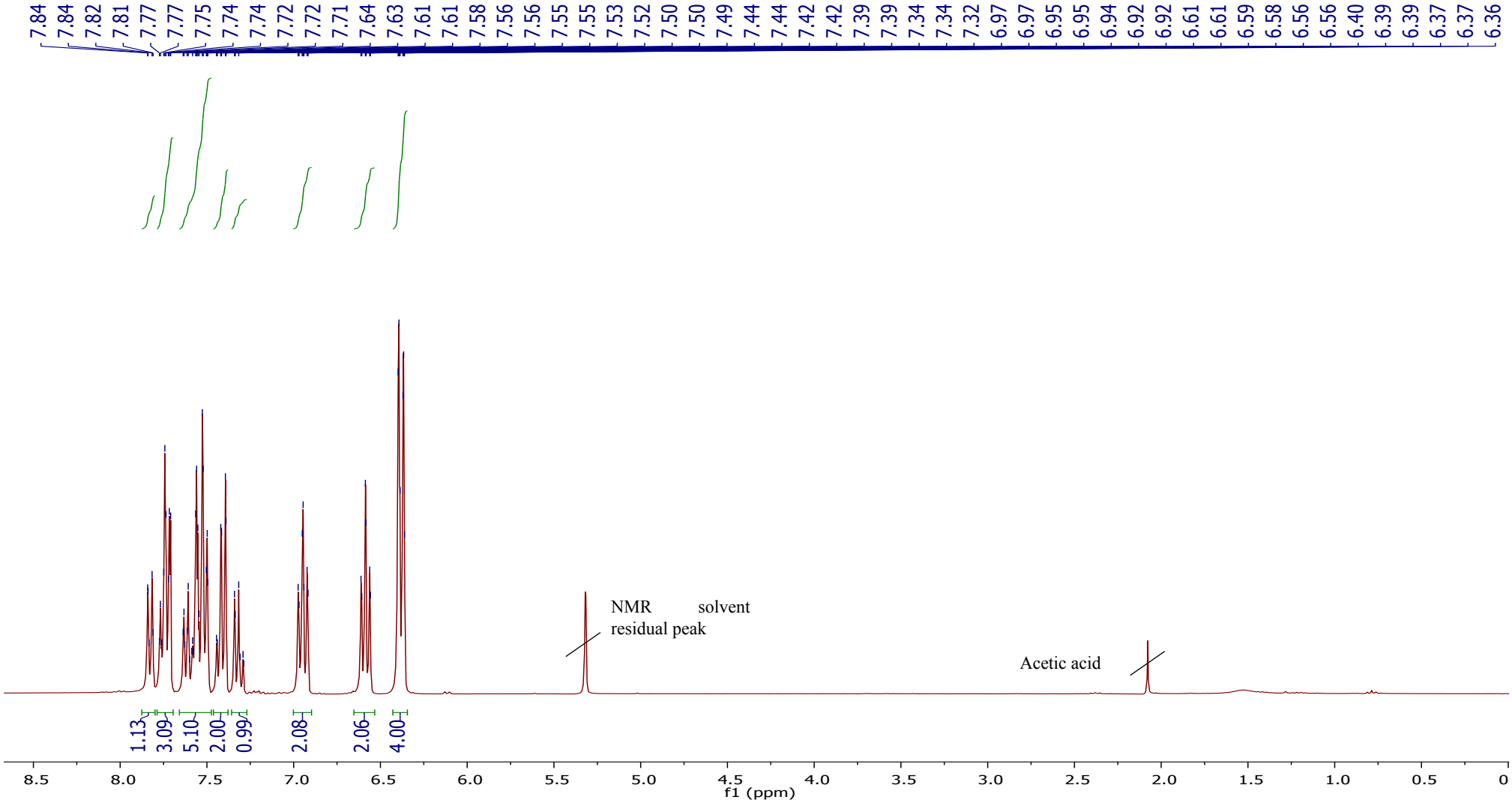

Figure S 57 ***SPA-2-FBr*** *– ^{1}H – CD_2Cl_2*

8.5 **SPA-2-FBr** – ^{13}C – CD_2Cl_2

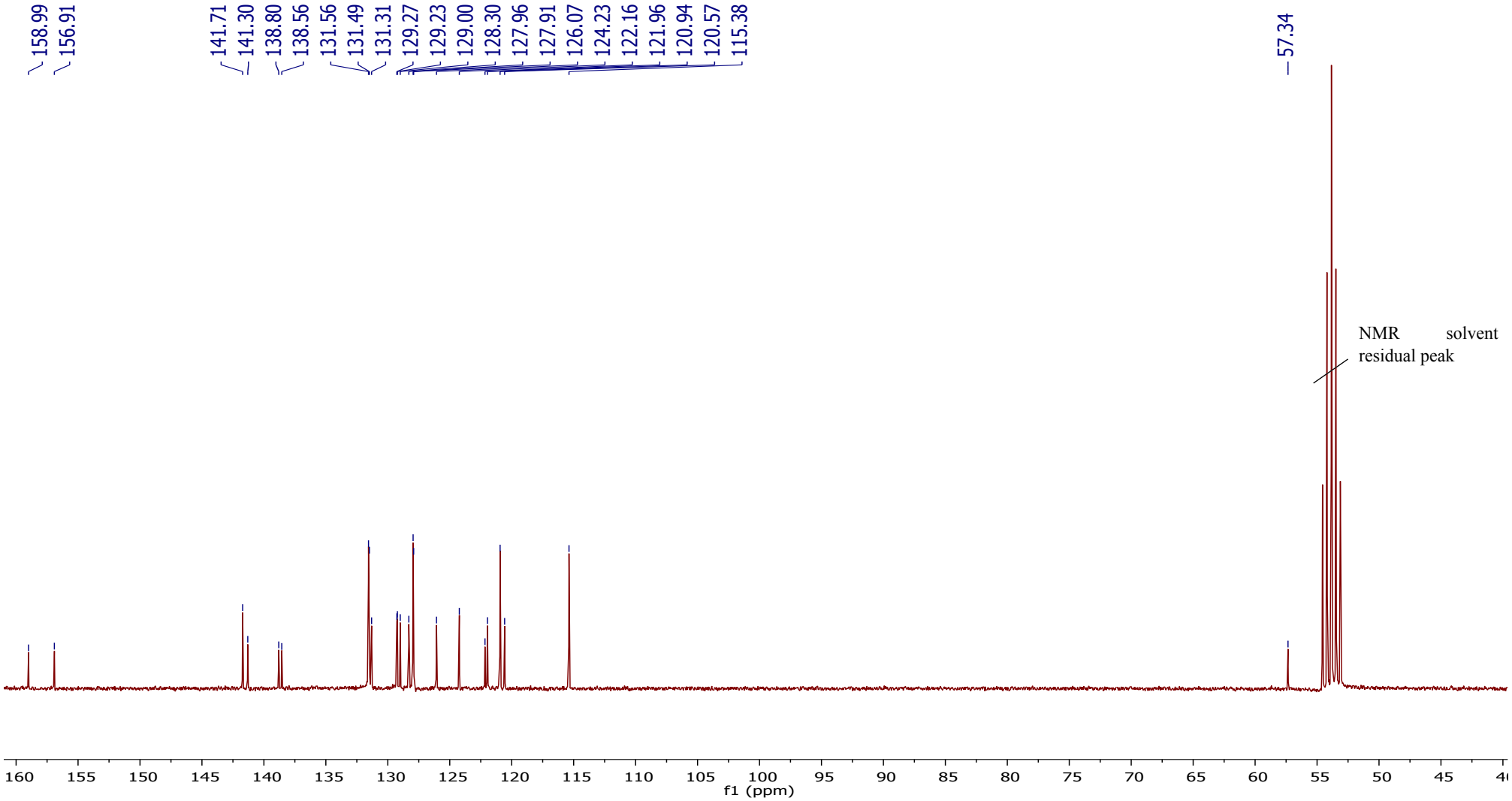

Figure S 58 ***SPA-2-FBr*** *– ^{13}C – CD_2Cl_2*

8.6 **SPA-2-FBr** – ^{13}C – DEPT135 – CD_2Cl_2

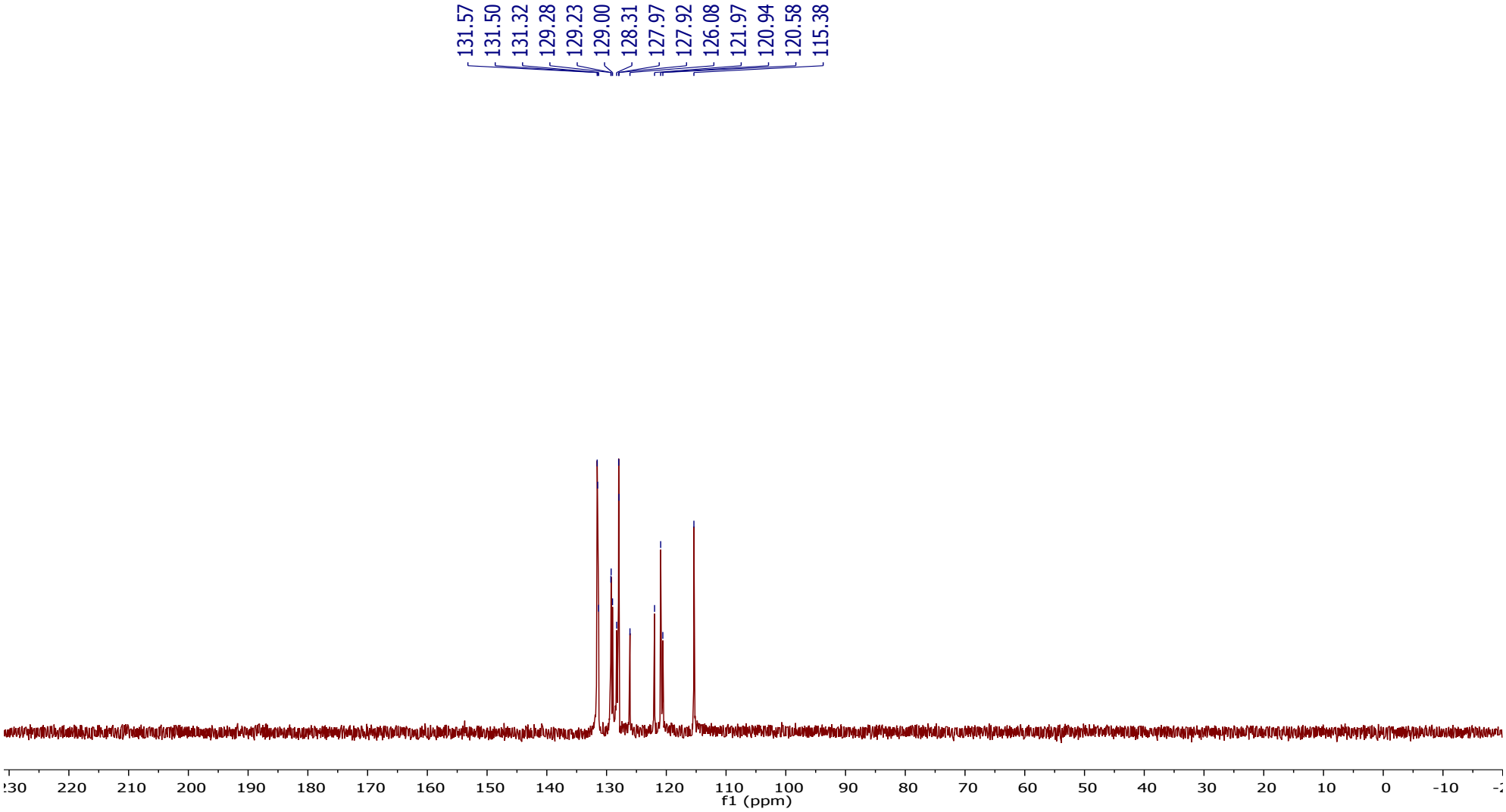

Figure S 59 ***SPA-2-FBr*** *– ^{13}C – DEPT135 – CD_2Cl_2*

8.7 **SPA-2,7-FBr$_2$** – ^{1}H – CD_2Cl_2

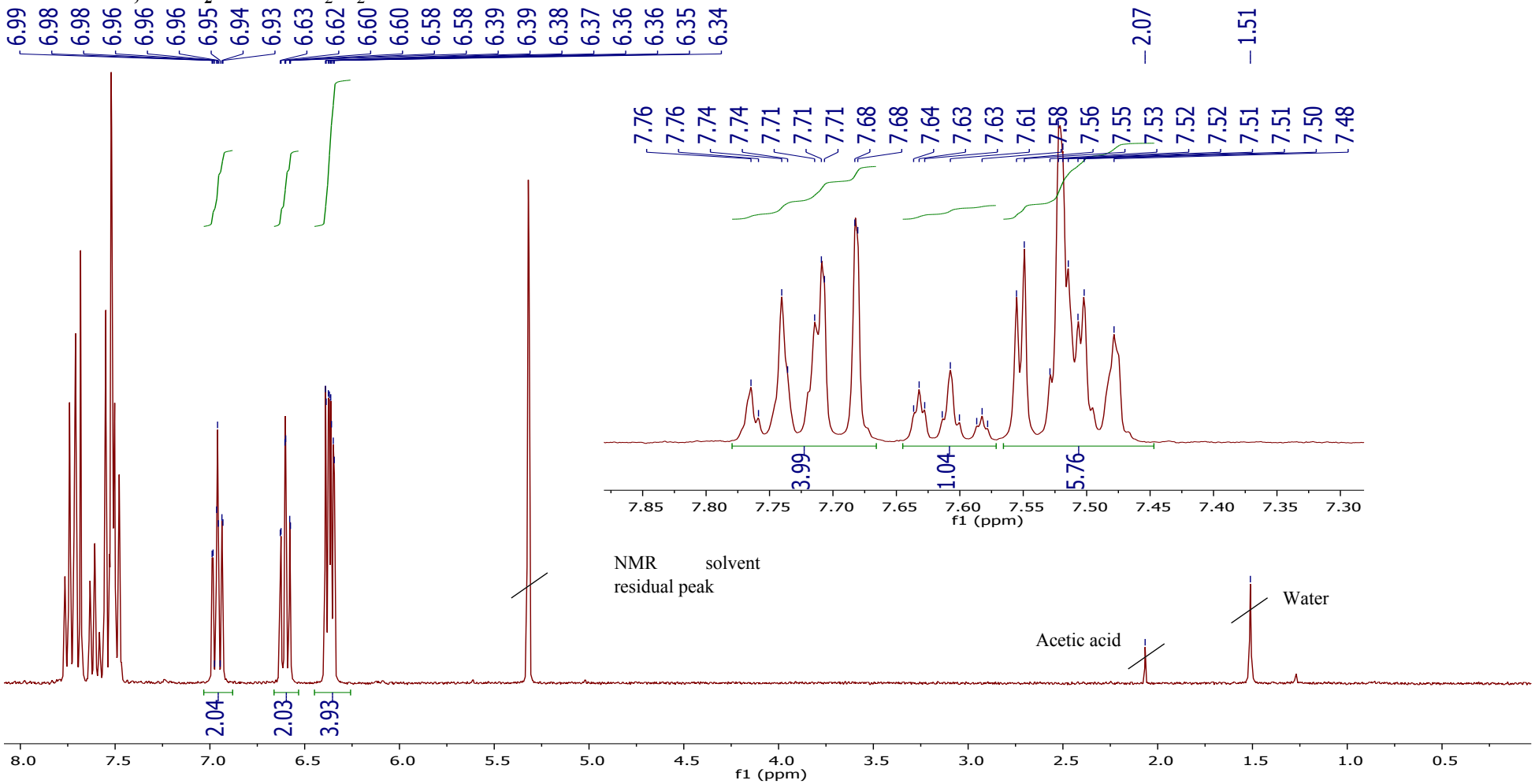

Figure S 60 ***SPA-2,7-FBr$_2$*** *– ^{1}H – CD_2Cl_2*

8.8 **SPA-2,7-FBr$_2$** – ^{13}C – CD_2Cl_2

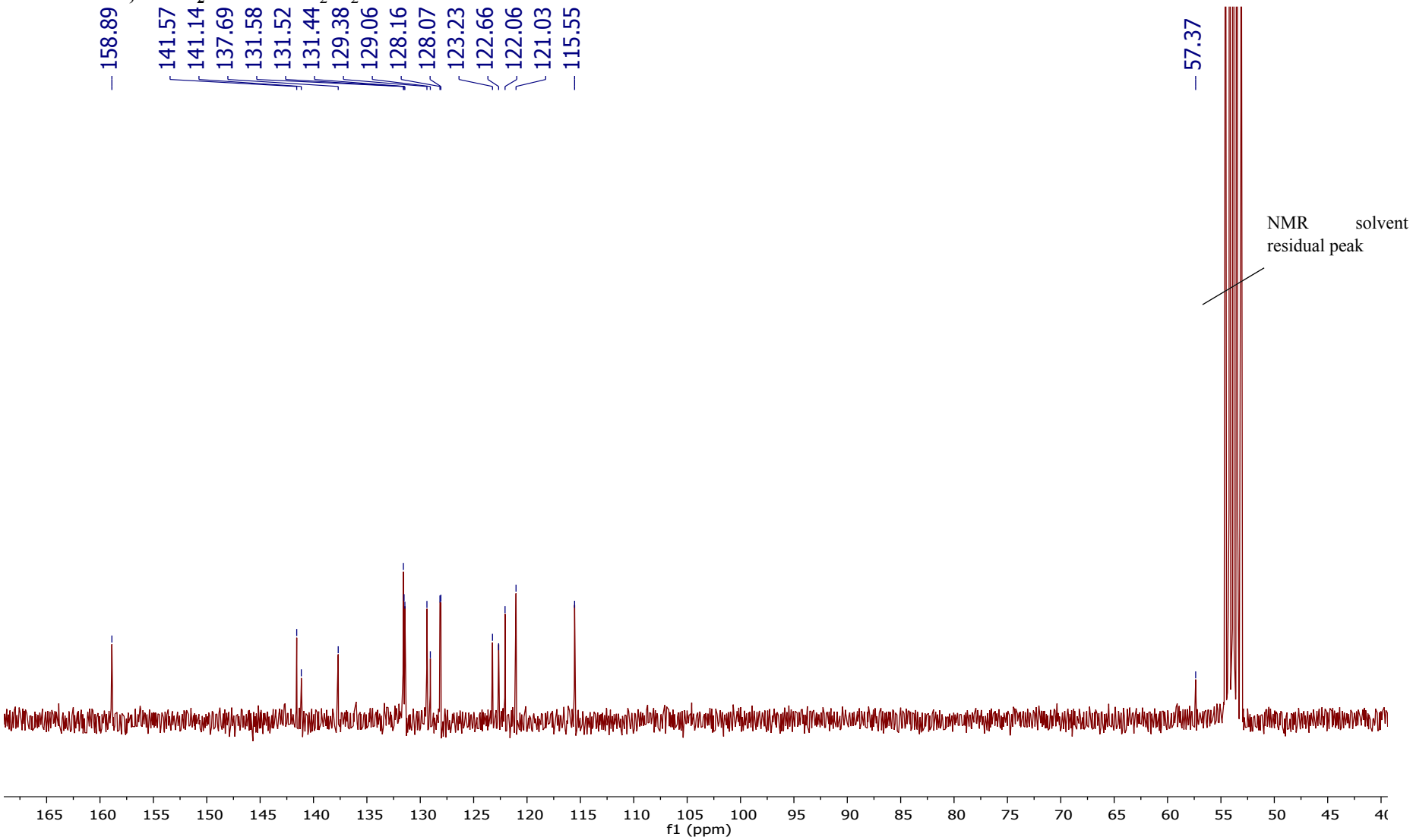

Figure S 61 ***SPA-2,7-FBr$_2$*** *– ^{13}C – CD_2Cl_2*

8.9 **SPA-2,7-FBr$_2$** – ^{13}C – DEPT135 – CD_2Cl_2

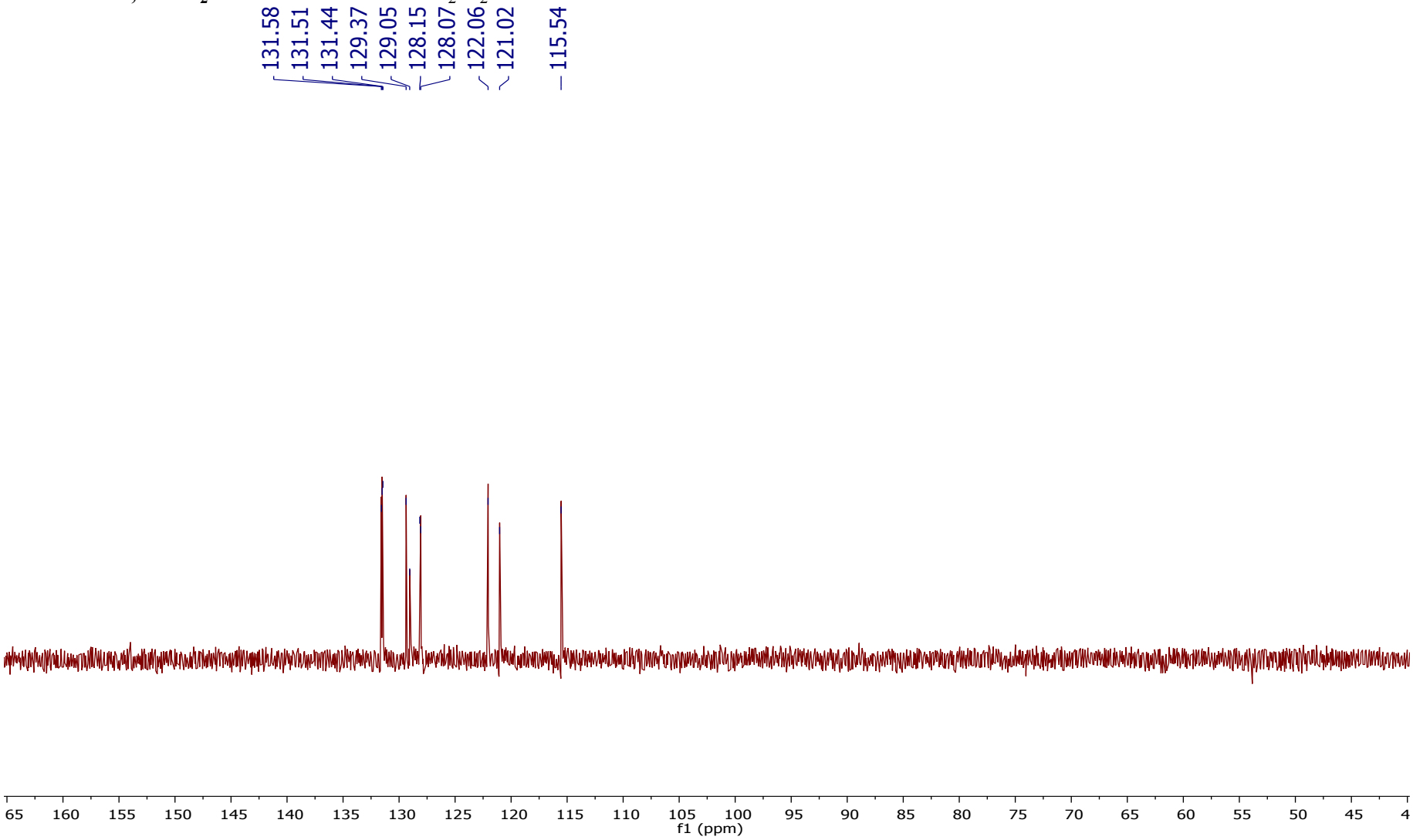

Figure S 62 ***SPA-2,7-FBr$_2$*** *– ^{13}C – DEPT135 – CD_2Cl_2*

8.10 **SPA-3,6-FBr$_2$** – ^{1}H – CD_2Cl_2

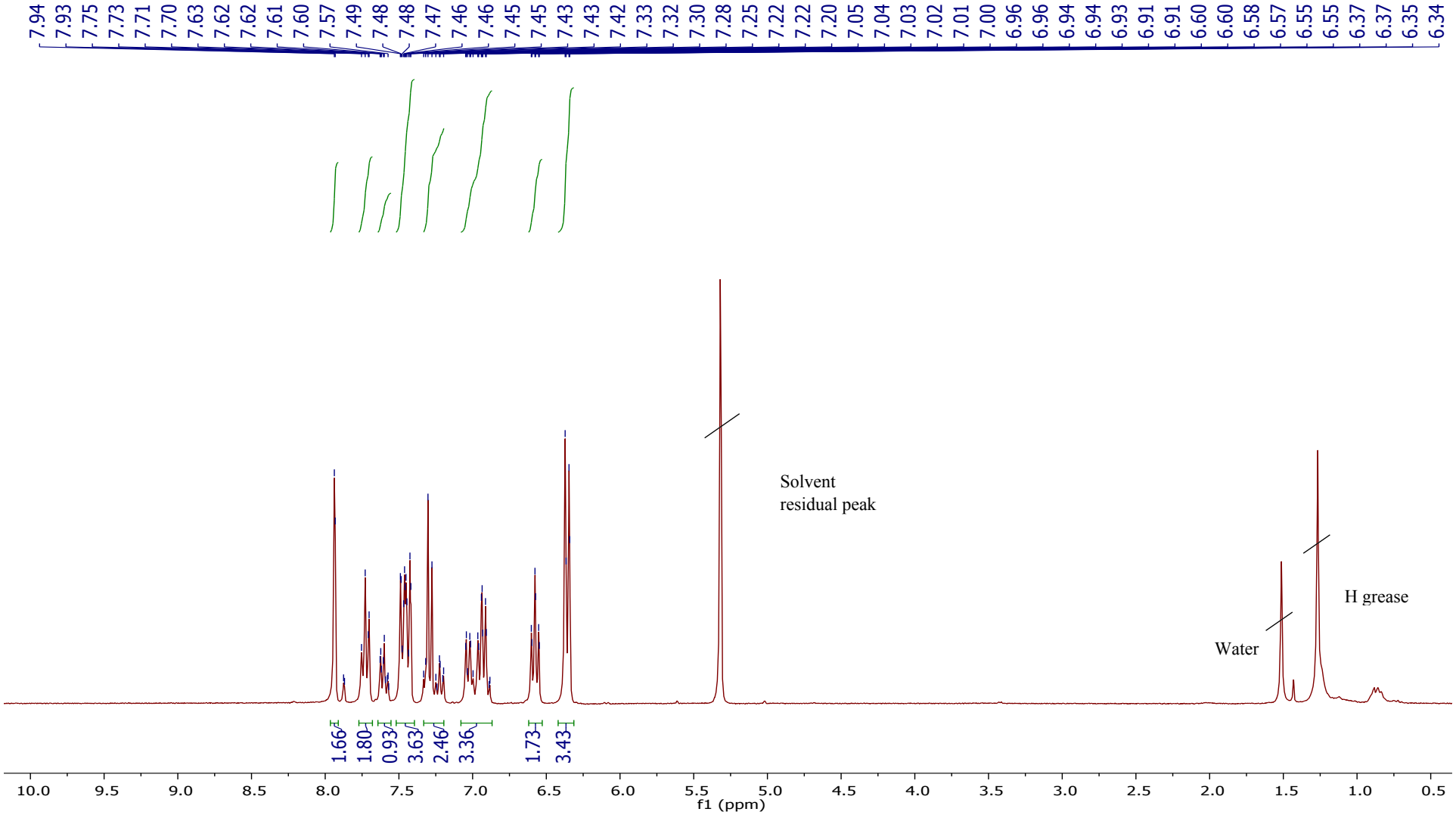

Figure S 63 ***SPA-3,6-FBr$_2$*** *– ^{1}H – CD_2Cl_2*

8.11 **SPA-3,6-FBr$_2$** – ^{13}C – CD_2Cl_2

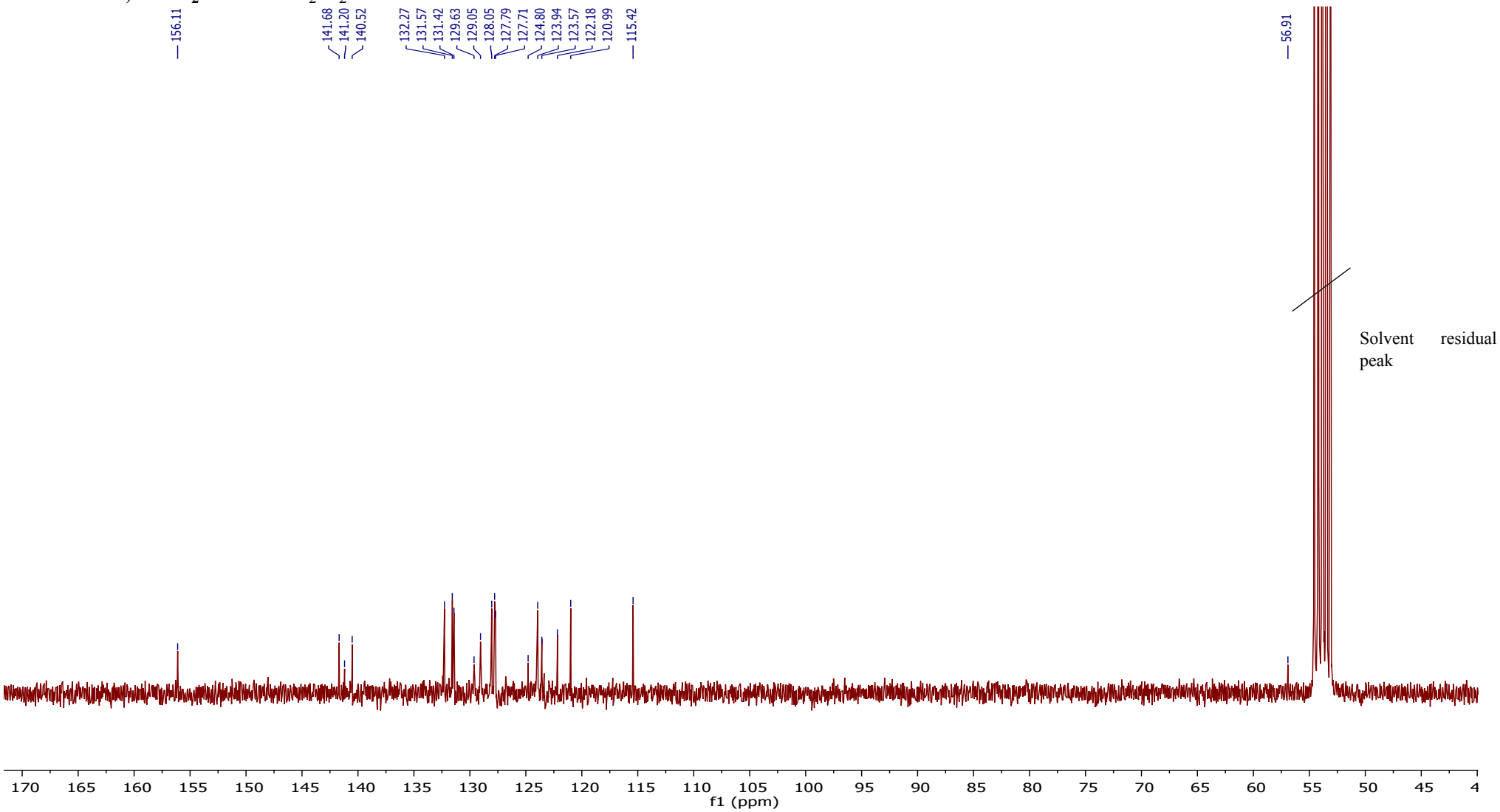

Figure S 64 ***SPA-3,6-FBr$_2$*** *– ^{13}C – CD$_2$Cl$_2$*

8.12 **SPA-3,6-FBr$_2$** – ^{13}C – DEPT135 – CD$_2$Cl$_2$

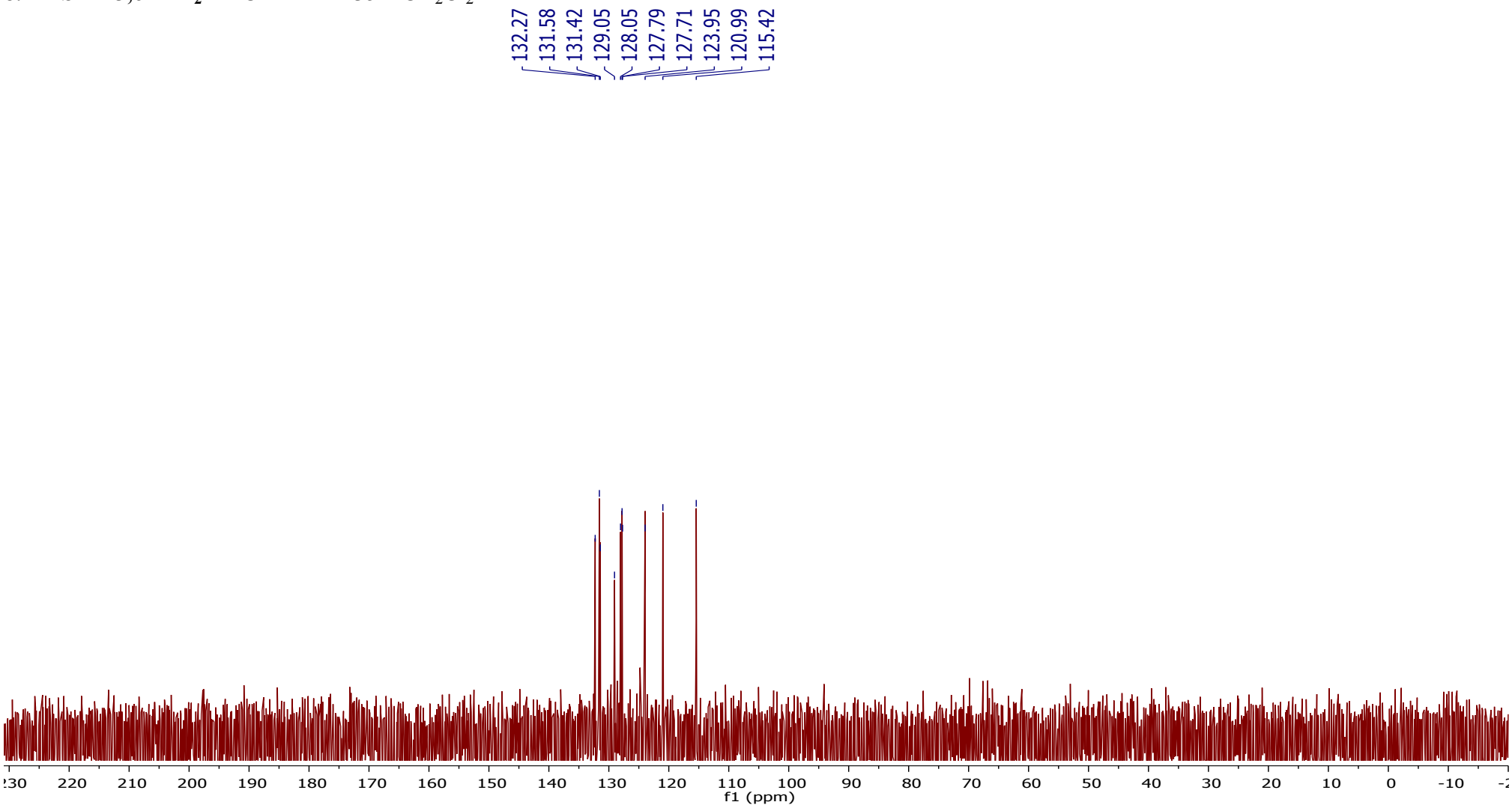

Figure S 65 ***SPA-3,6-FBr$_2$*** *– ^{13}C – DEPT135 – CD$_2$Cl$_2$*

8.13 **SPA-2-FPOPh$_2$** – ^{1}H – CD$_2$Cl$_2$

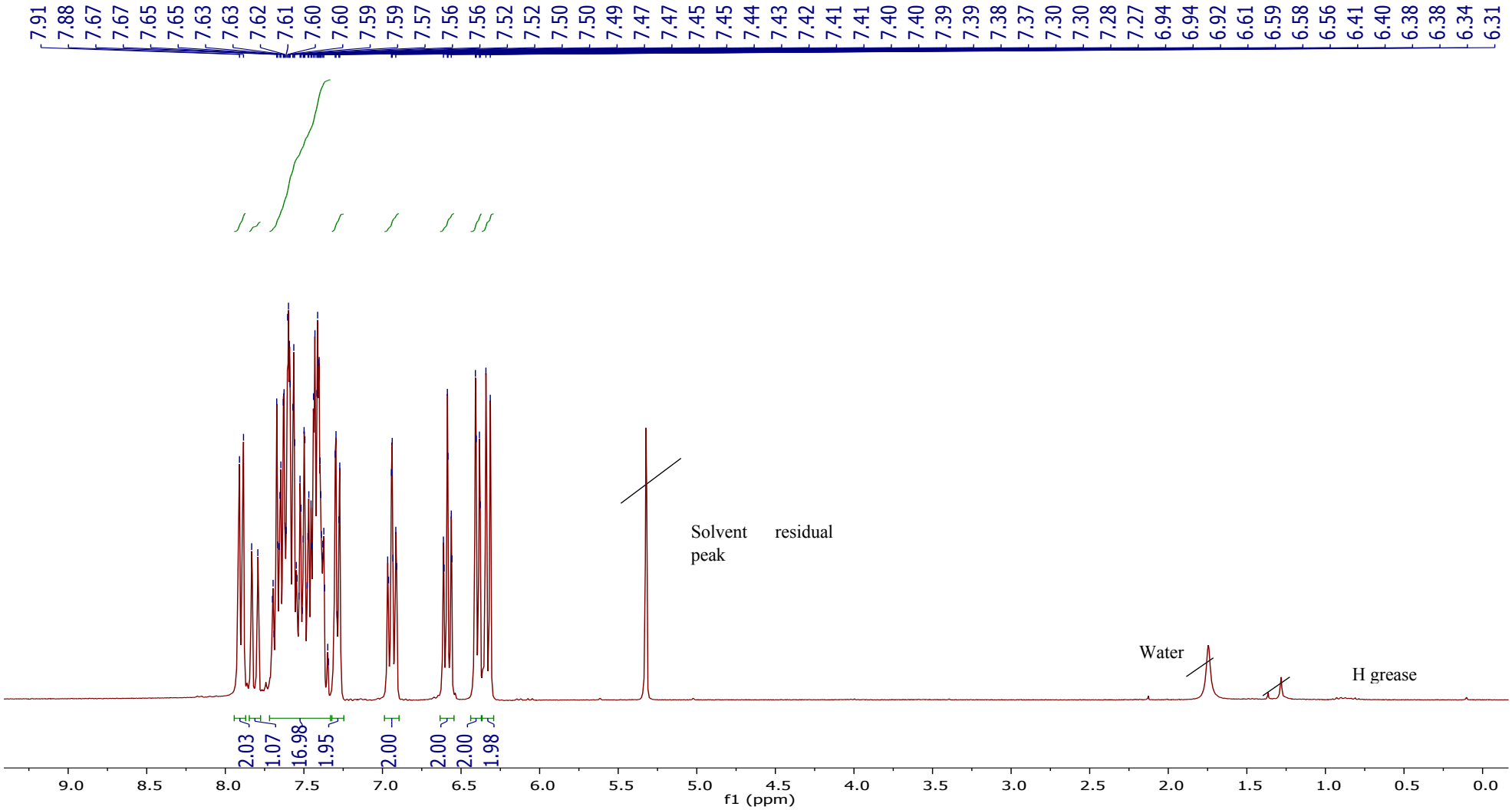

Figure S 66 ***SPA-2-FPOPh$_2$*** *– ^1H – CD_2Cl_2*

8.14 **SPA-2-FPOPh$_2$** – ^{13}C – CD_2Cl_2

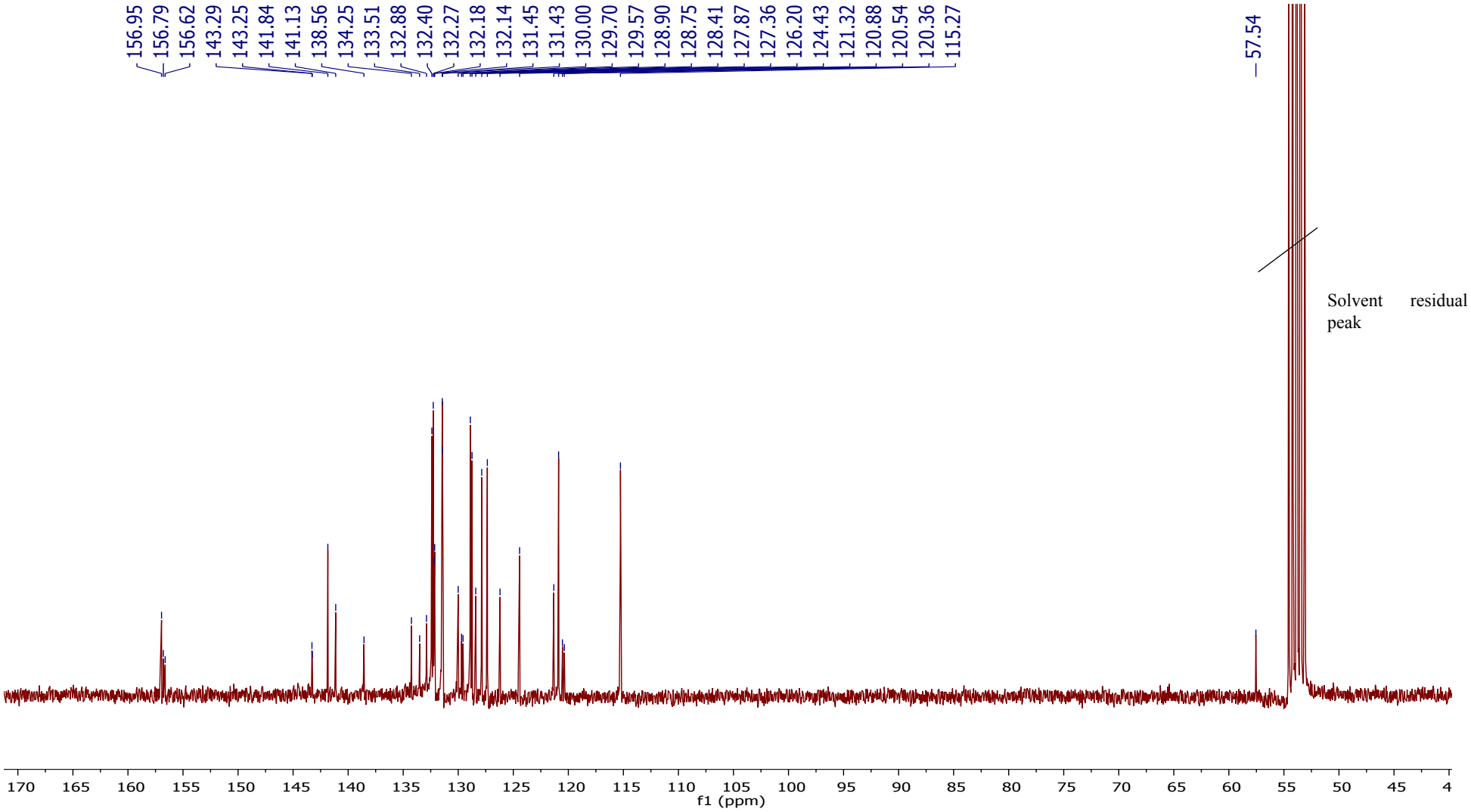

Figure S 67 ***SPA-2-FPOPh$_2$*** *– ^{13}C – CD_2Cl_2*

8.15 **SPA-2-FPOPh$_2$** – ^{13}C – DEPT135 – CD_2Cl_2

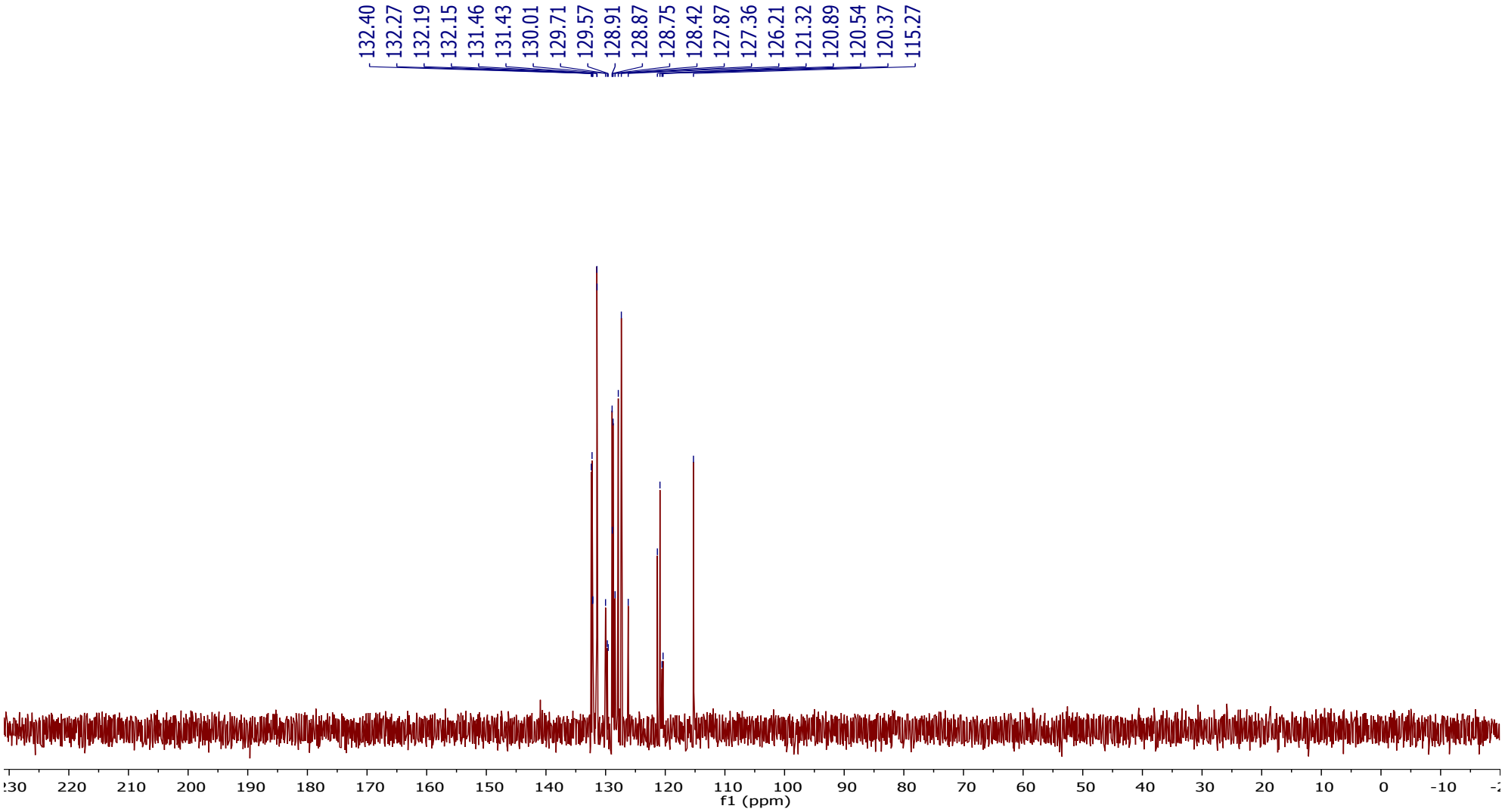

Figure S 68 ***SPA-2-FPOPh$_2$*** *– ^{13}C – DEPT135 – CD_2Cl_2*

8.16 **SPA-2-FPOPh$_2$** – ^{31}P decoupled– CD_2Cl_2

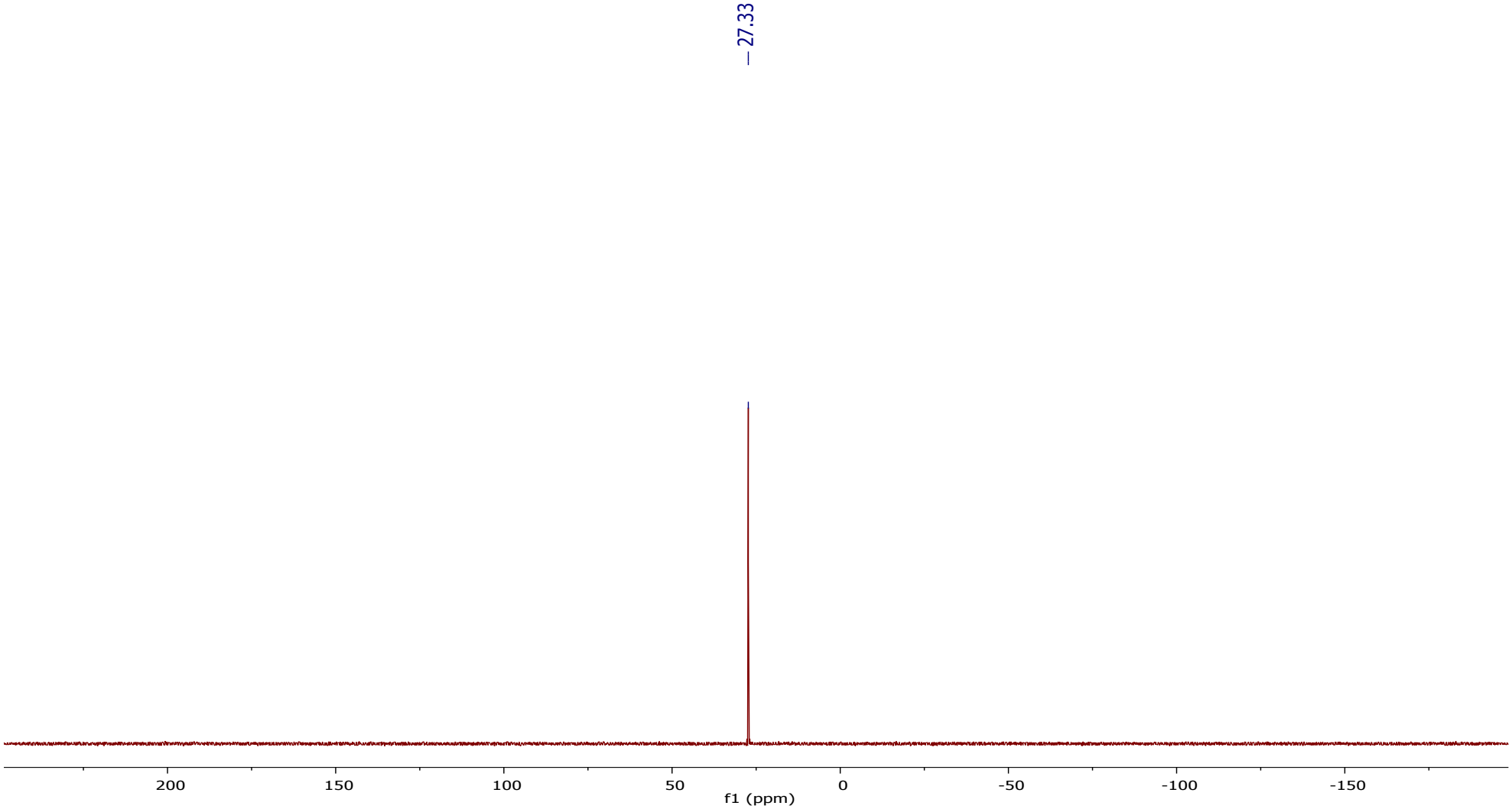

Figure S 69 ***SPA-2-FPOPh$_2$*** *– ^{31}P decoupled– CD_2Cl_2*

8.17 **SPA-2,7-F(POPh$_2$)$_2$** – ^{1}H – CD_2Cl_2

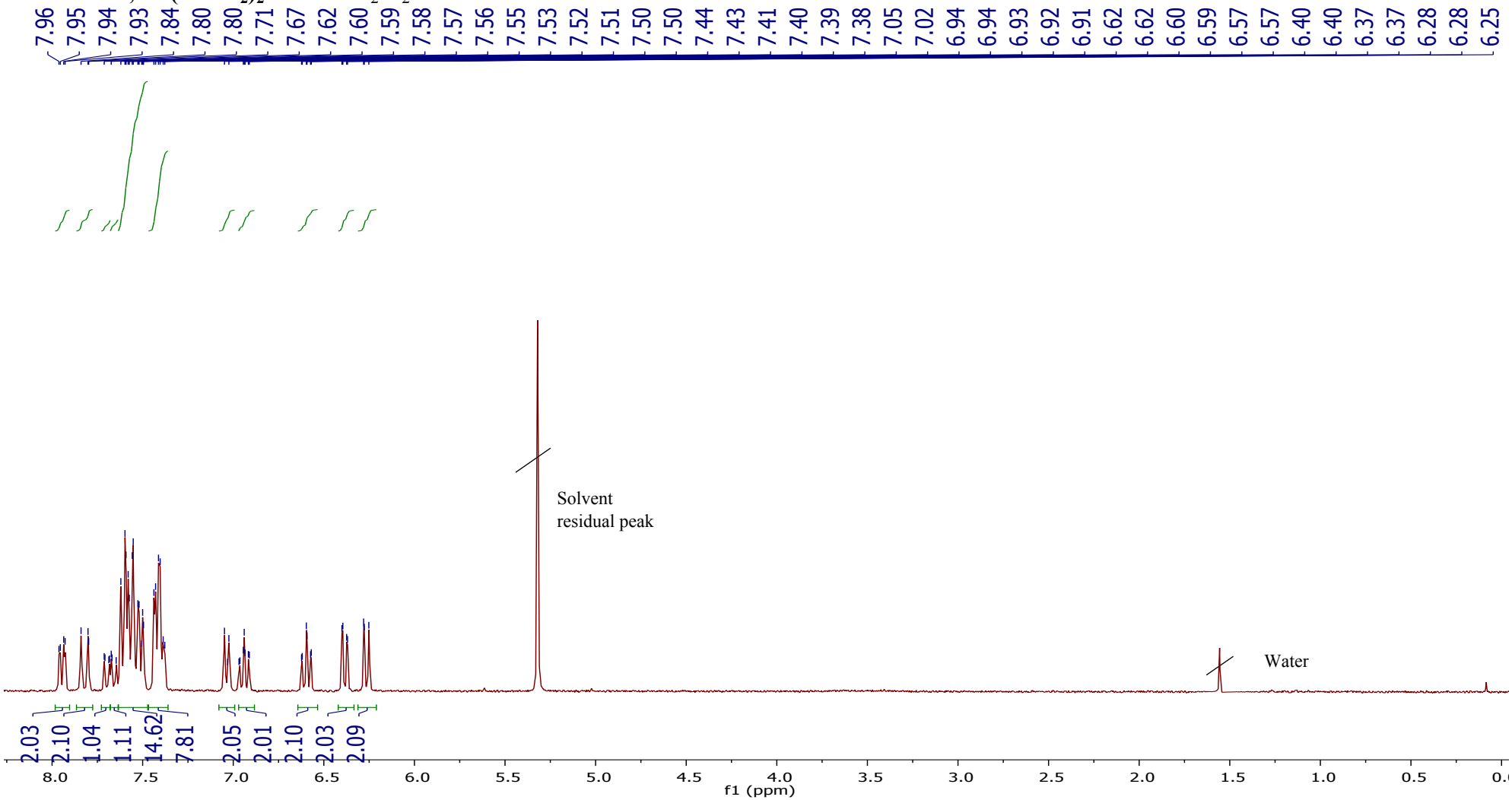

Figure S 70 ***SPA-2,7-F(POPh$_2$)$_2$*** *– ^{1}H – CD_2Cl_2*

8.18 **SPA-2,7-F(POPh$_2$)$_2$** – ^{13}C – CD_2Cl_2

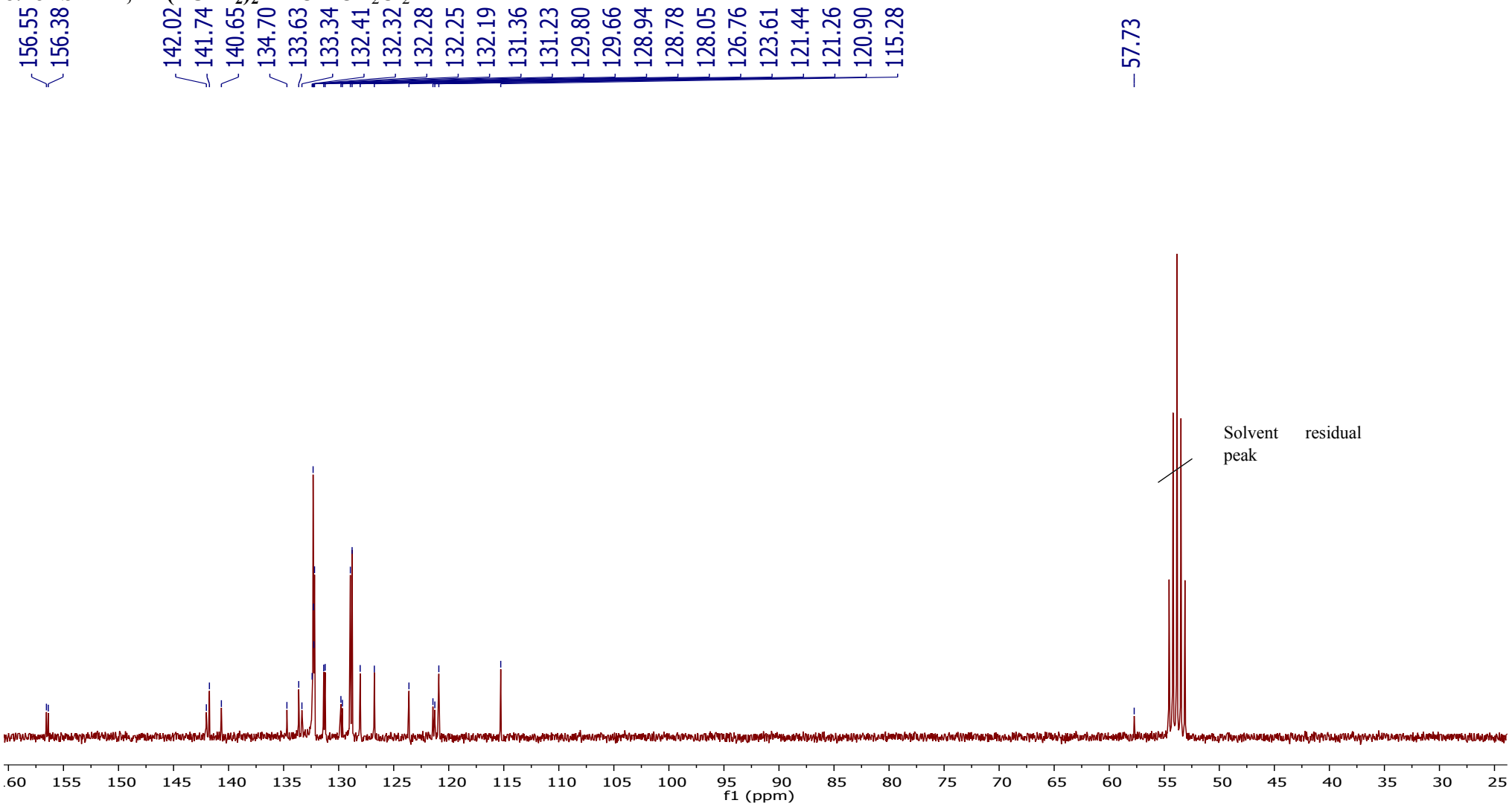

Figure S 71 ***SPA-2,7-F(POPh$_2$)$_2$*** *– ^{13}C – CD_2Cl_2*

8.19 **SPA-2,7-F(POPh$_2$)$_2$** – ^{13}C – DEPT135 – CD_2Cl_2

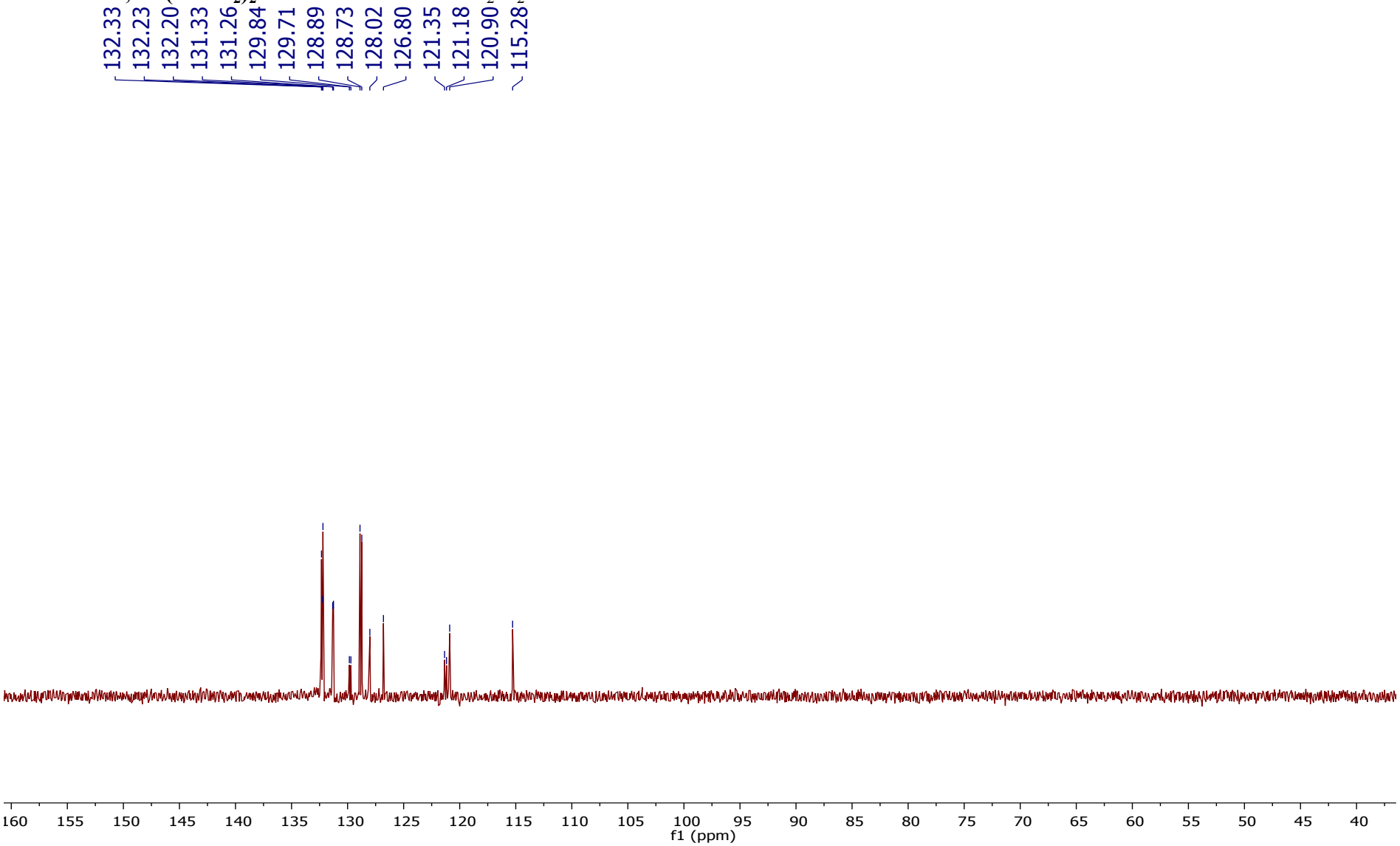

Figure S 72 ***SPA-2,7-F(POPh$_2$)$_2$*** *– ^{13}C – DEPT135 – CD_2Cl_2*

8.20 **SPA-2,7-F(POPh$_2$)$_2$** – ^{31}P decoupled– CD_2Cl_2

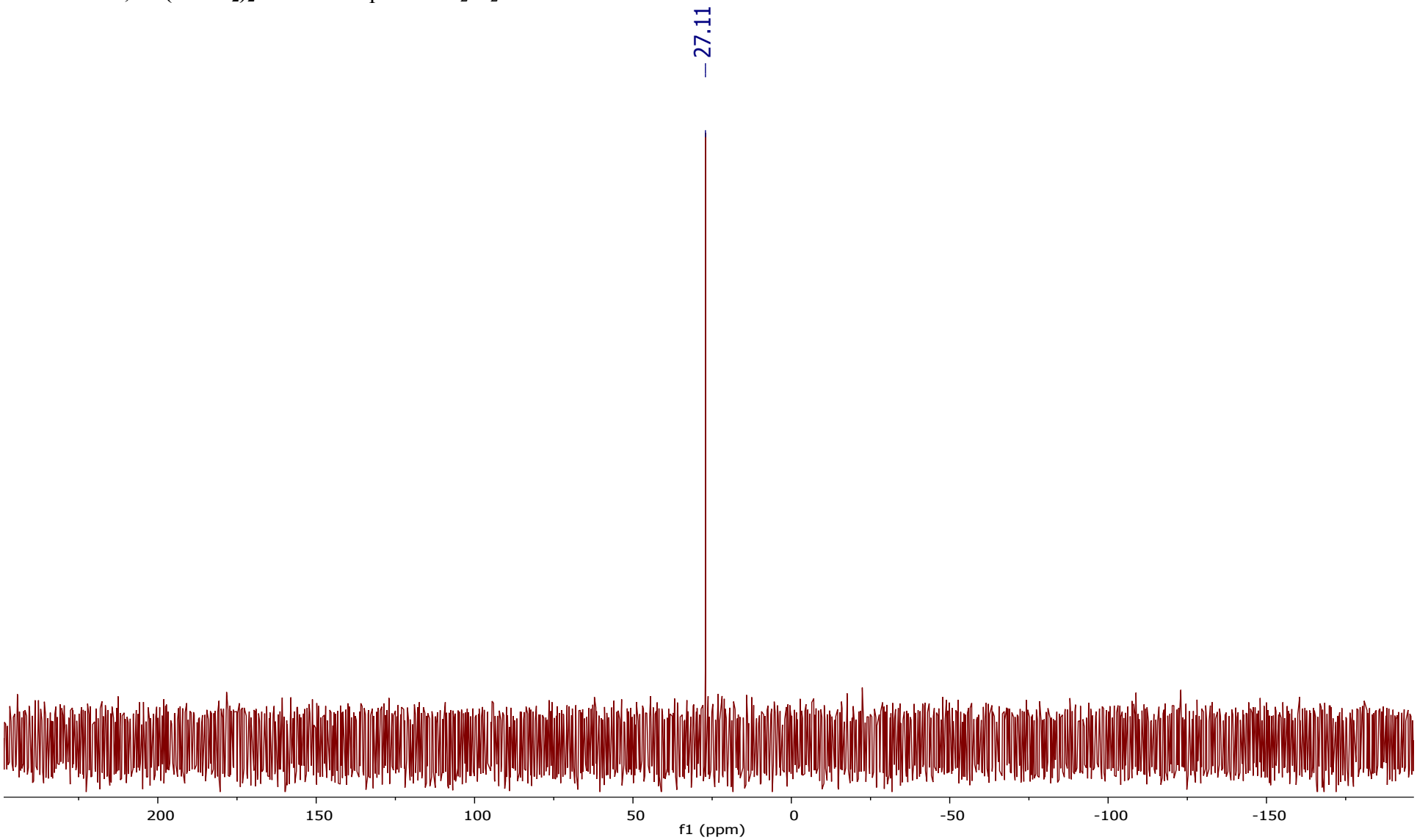

Figure S 73 ***SPA-2,7-F(POPh$_2$)$_2$*** *– ^{31}P decoupled– CD_2Cl_2*

8.21 **SPA-2,7-F(POPh$_2$)$_2$** – ^{1}H – CD_2Cl_2

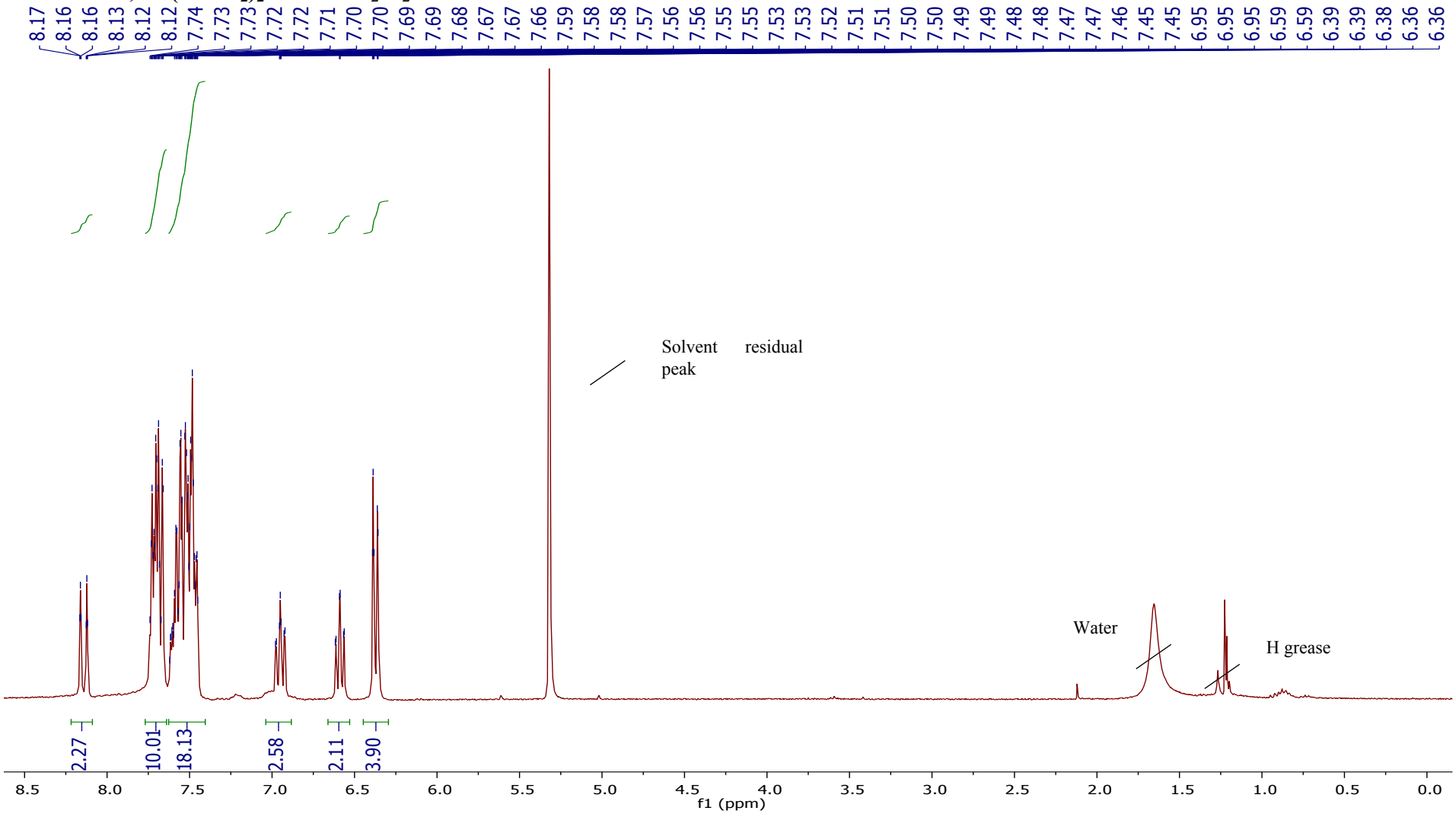

Figure S 74 ***SPA-2,7-F(POPh$_2$)$_2$*** *– ^{1}H – CD_2Cl_2*

8.22 **SPA-2,7-F(POPh$_2$)$_2$** – ^{13}C – CD_2Cl_2

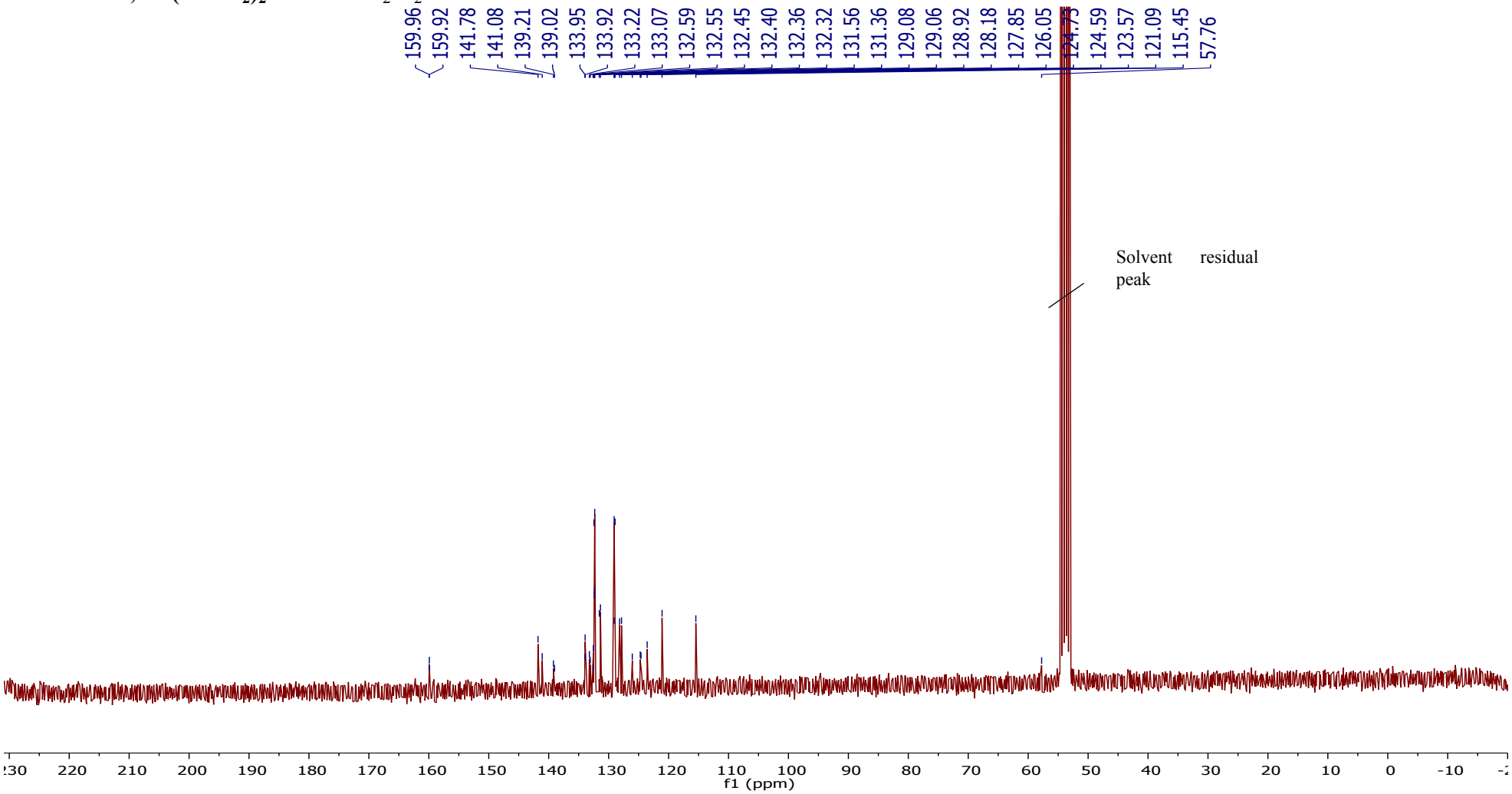

Figure S 75 ***SPA-2,7-F(POPh$_2$)$_2$*** *– ^{13}C – CD_2Cl_2*

8.23 **SPA-2,7-F(POPh$_2$)$_2$** – ^{13}C – DEPT135 – CD_2Cl_2

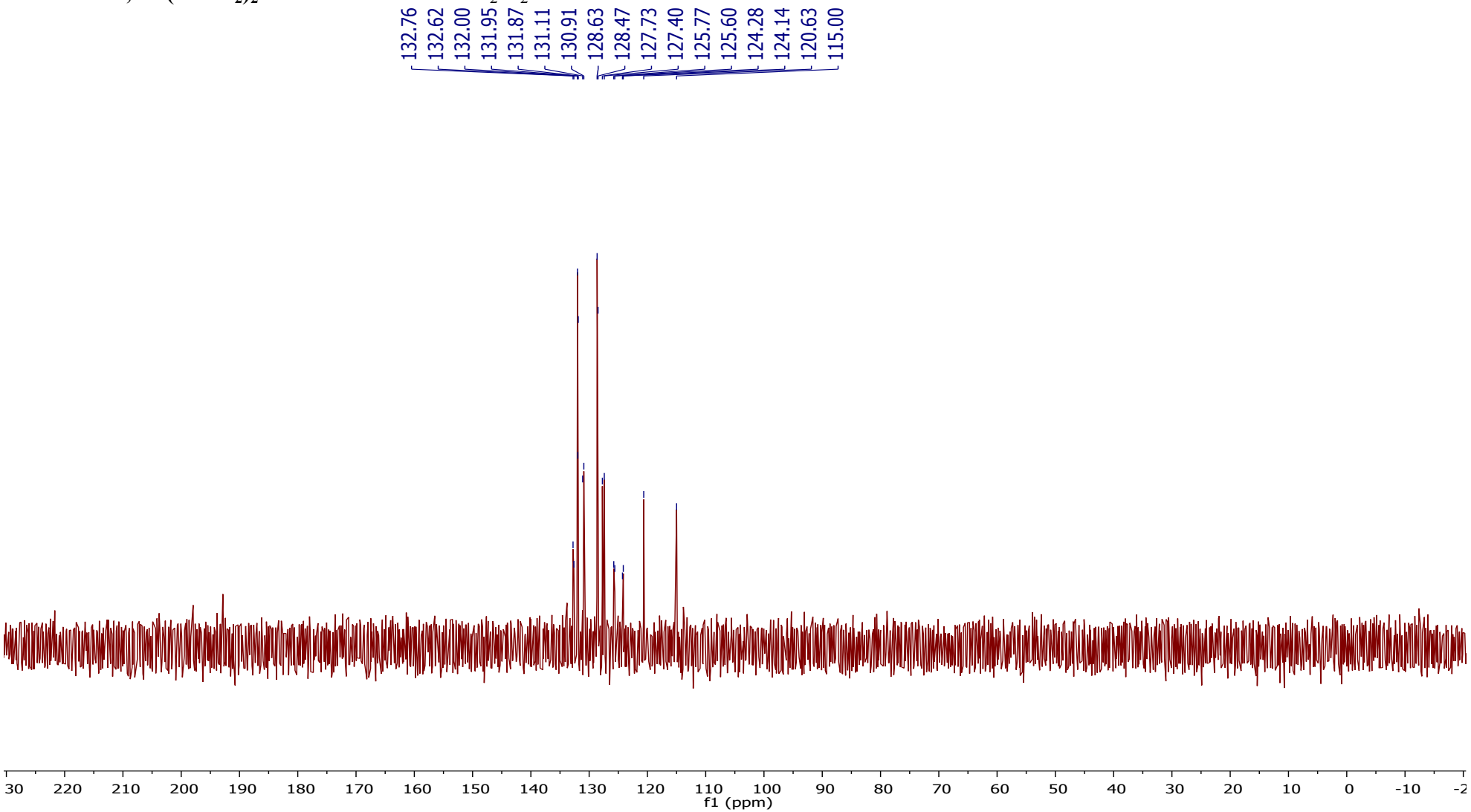

Figure S 76 ***SPA-2,7-F(POPh$_2$)$_2$*** *– ^{13}C – DEPT135 – CD_2Cl_2*

8.24 **SPA-2,7-F(POPh$_2$)$_2$** – ^{31}P decoupled– CD_2Cl_2

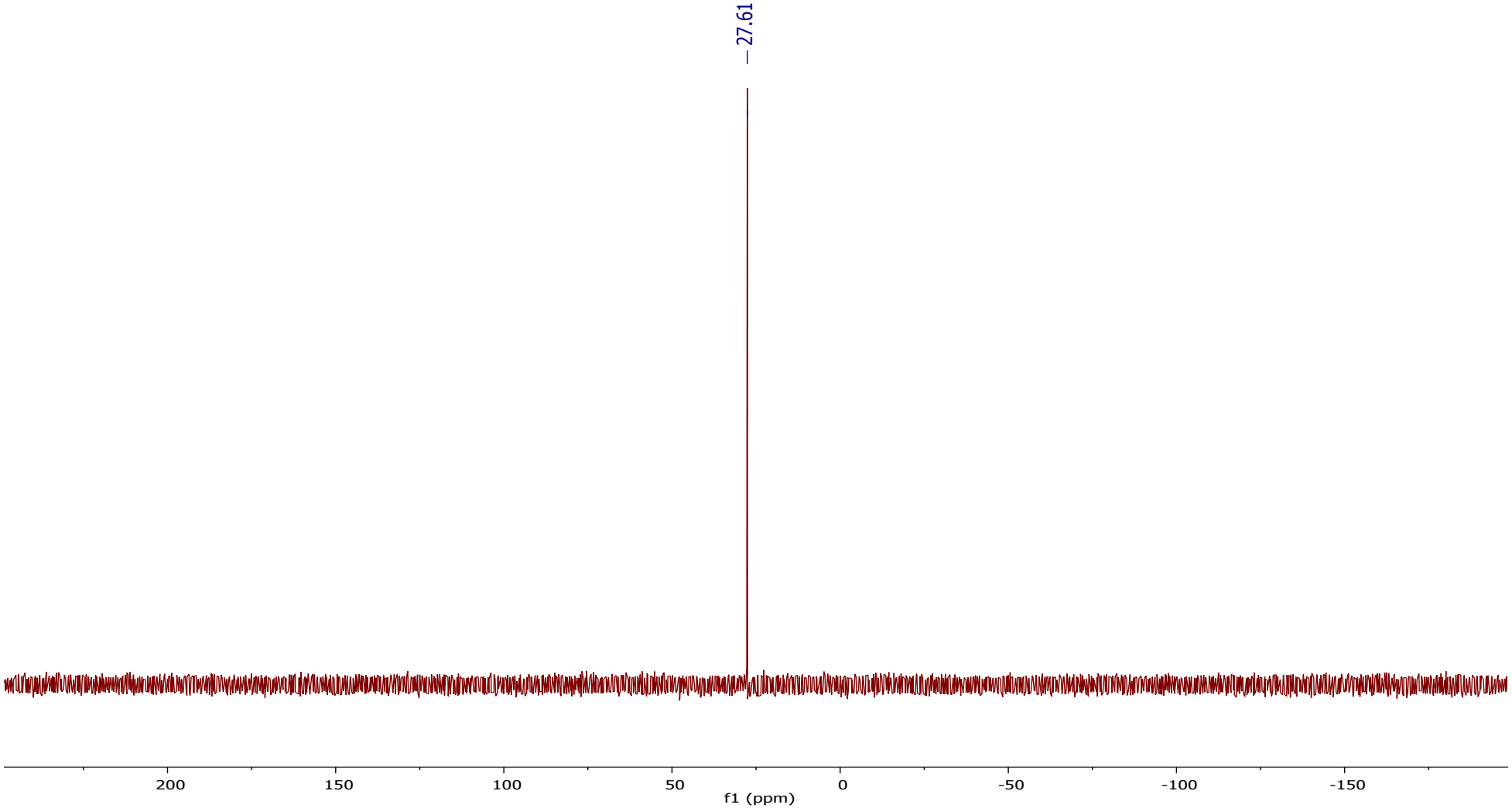

Figure S 77 ***SPA-2,7-F(POPh$_2$)$_2$*** *– ^{31}P decoupled– CD_2Cl_2*

9 Copy of high resolution mass spectroscopy spectra

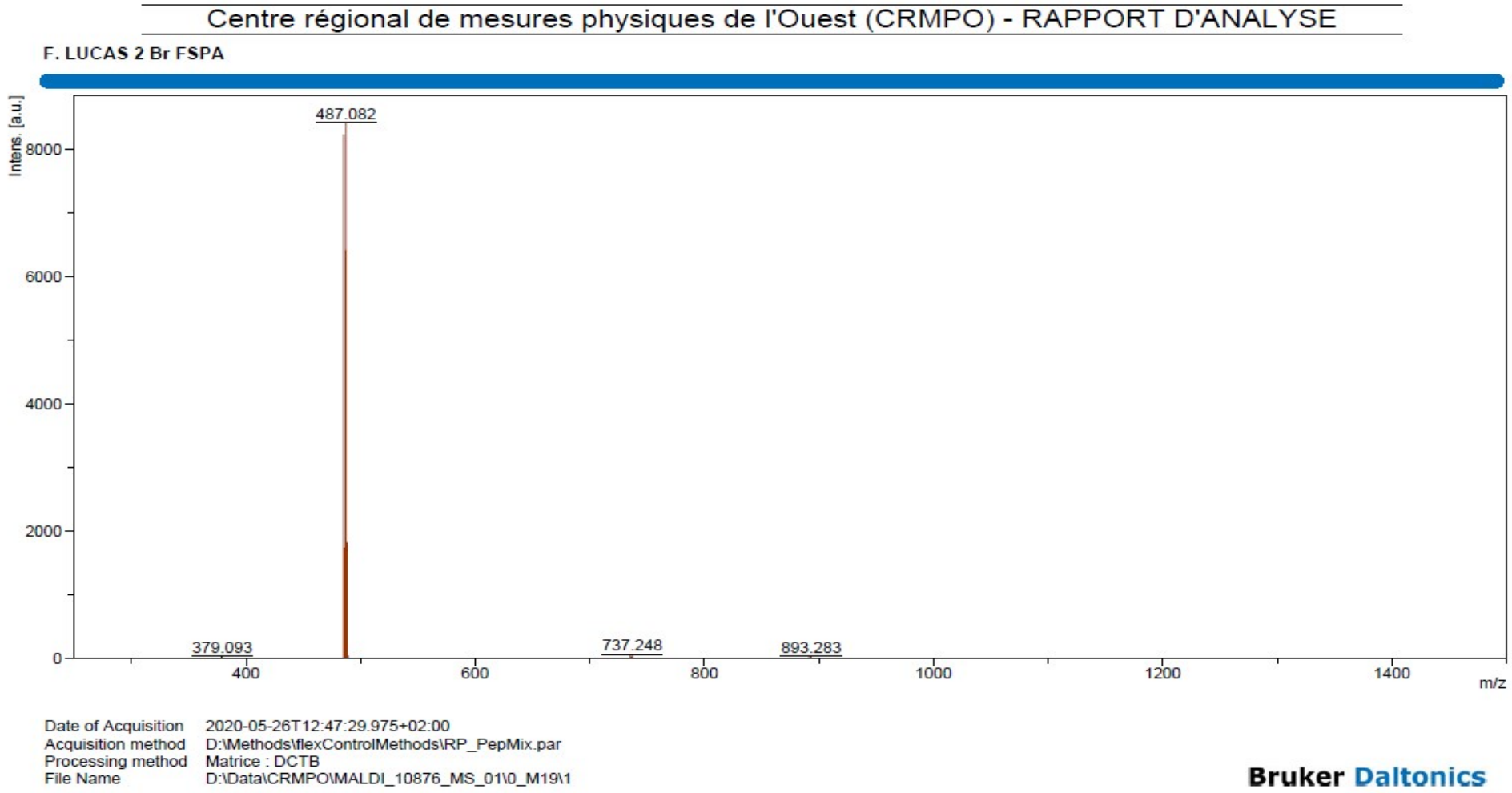

Figure S 78 HRMS spectrum of SPA-2-FBr

Centre régional de mesures physiques de l'Ouest (CRMPO) - RAPPORT D'ANALYSE

Analysis Info

Analysis Name	D:\Data\CRMPO\ASAP_9948_MS_01.d	Acquisition Date	06/21/2019 3:04:30 PM
Method	ASAP_CRMPO_tune_low.m	Operator	Fabian LAMBERT
Sample Name	FL Vol 1-112	Instrument	maXis
Comment	F. LUCAS FL Vol 1-112 Température : 220°C		

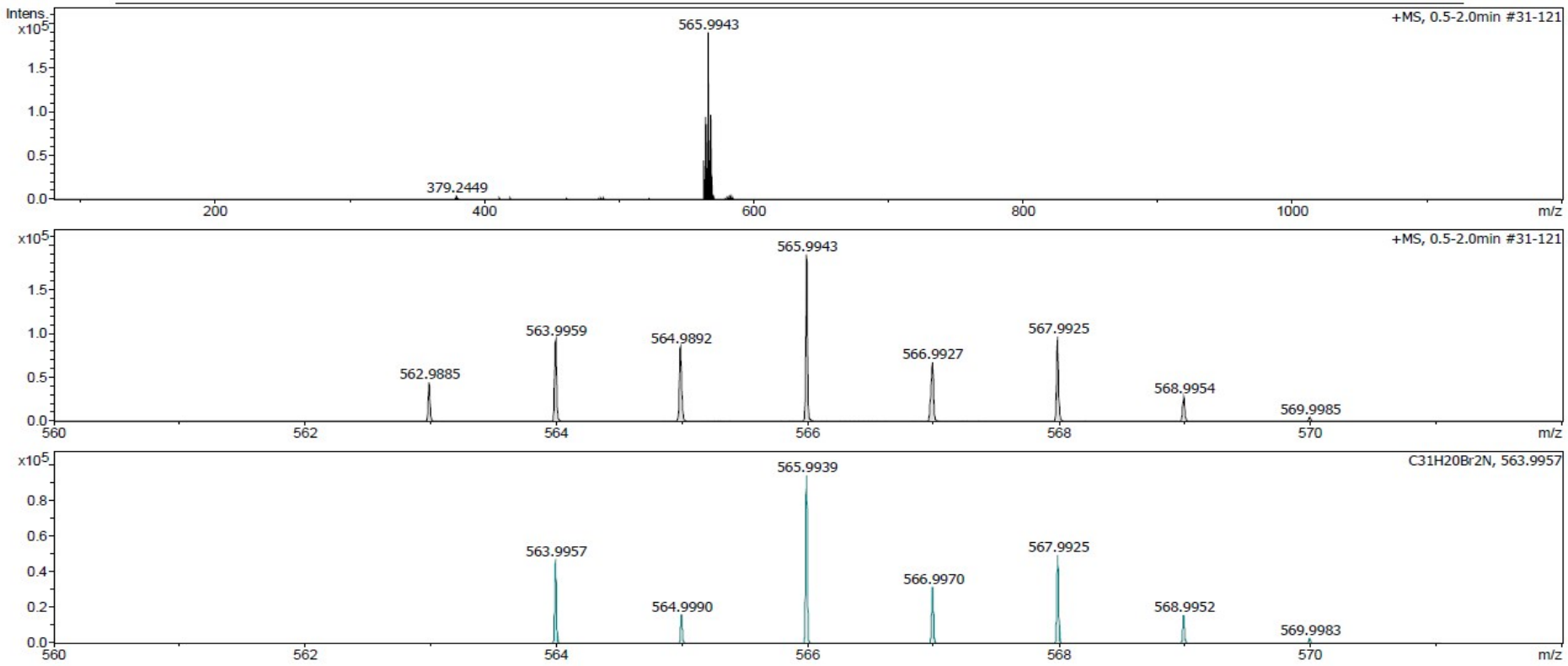

Figure S 79 HRMS spectrum of SPA-2,7-FBr$_2$

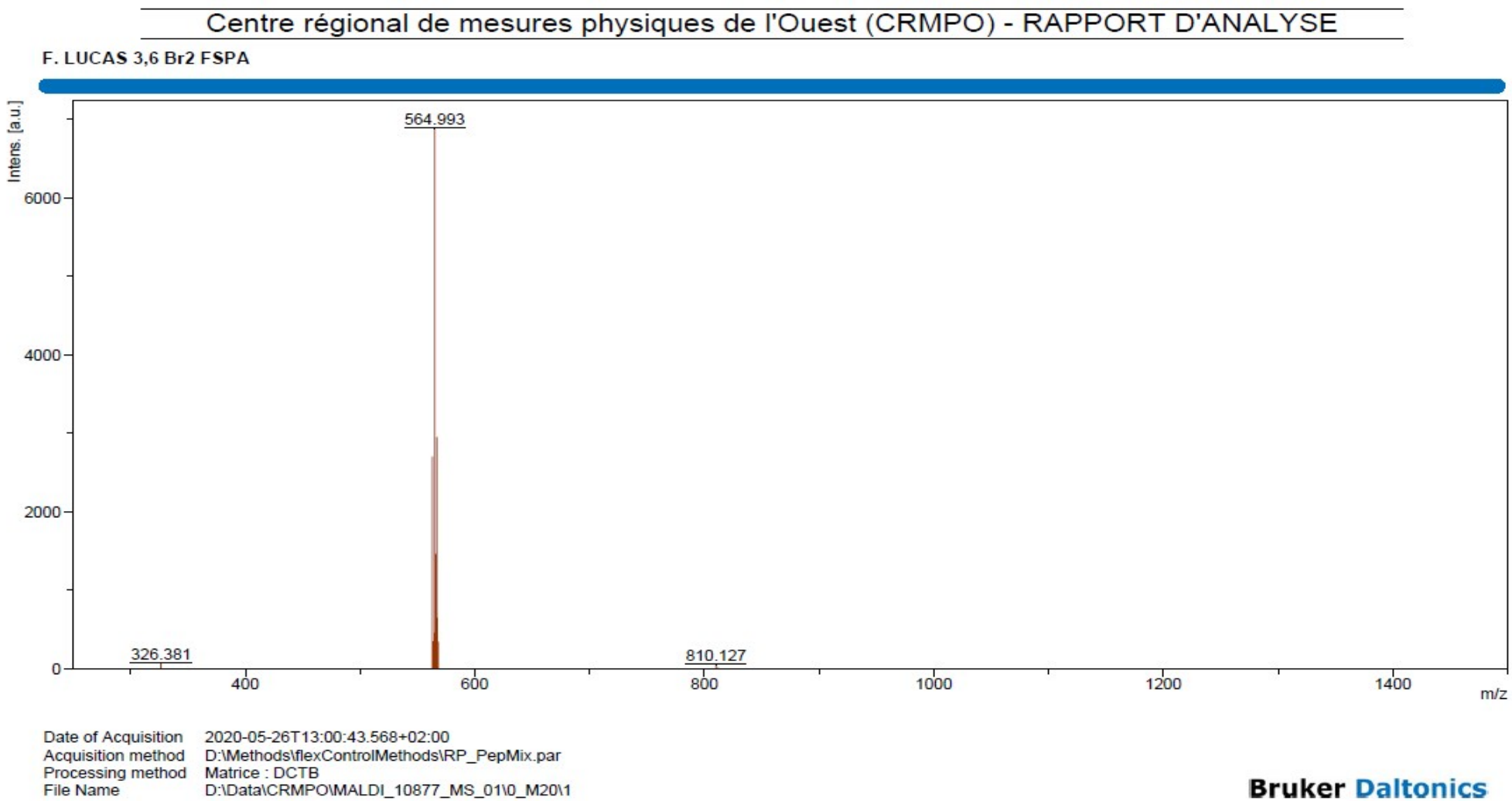

Figure S 80 HRMS spectrum of SPA-3,6-FBr$_2$

Centre régional de mesures physiques de l'Ouest (CRMPO) - RAPPORT D'ANALYSE

Analysis Info

Analysis Name	D:\Data\CRMPO\ASAP_9644_MS_01.d	Acquisition Date	04/10/2019 4:25:00 PM
Method	ASAP_CRMPO_tune_low.m	Operator	Fabian LAMBERT
Sample Name	FL Vol 1-128	Instrument	maXis
Comment	F. LUCAS FL Vol 1-128 Température : 180°C		

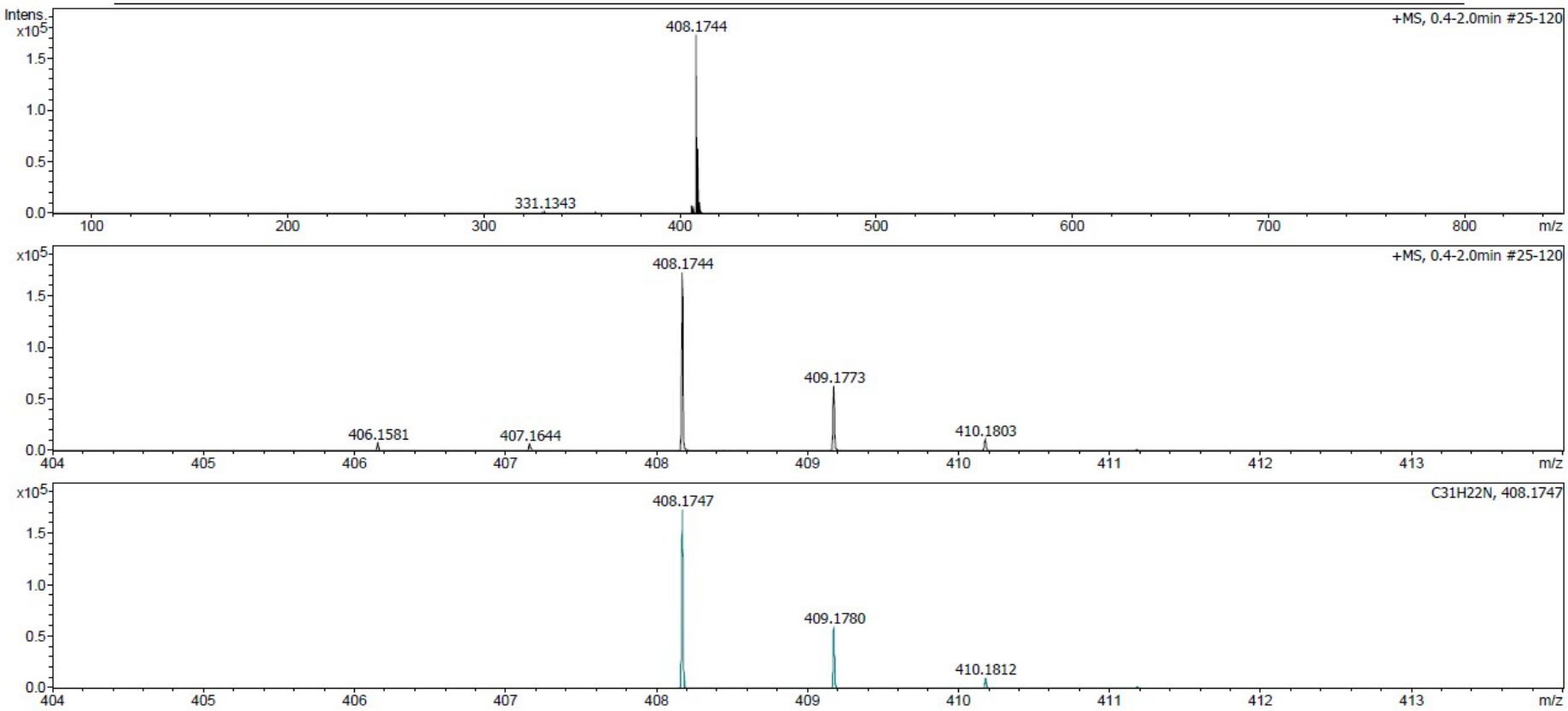

*Figure S 81 HRMS spectrum of **SPA-F***

Centre régional de mesures physiques de l'Ouest (CRMPO) - RAPPORT D'ANALYSE

Analysis Info

Analysis Name	D:\Data\CRMPO\ASAP_9643_MS_01.d	Acquisition Date	04/10/2019 4:52:28 PM
Method	ASAP_CRMPO_tune_low.m	Operator	Fabian LAMBERT
Sample Name	FL Vol 1-116	Instrument	maXis
Comment	F. LUCAS FL Vol 1-116 Température : 320°C		

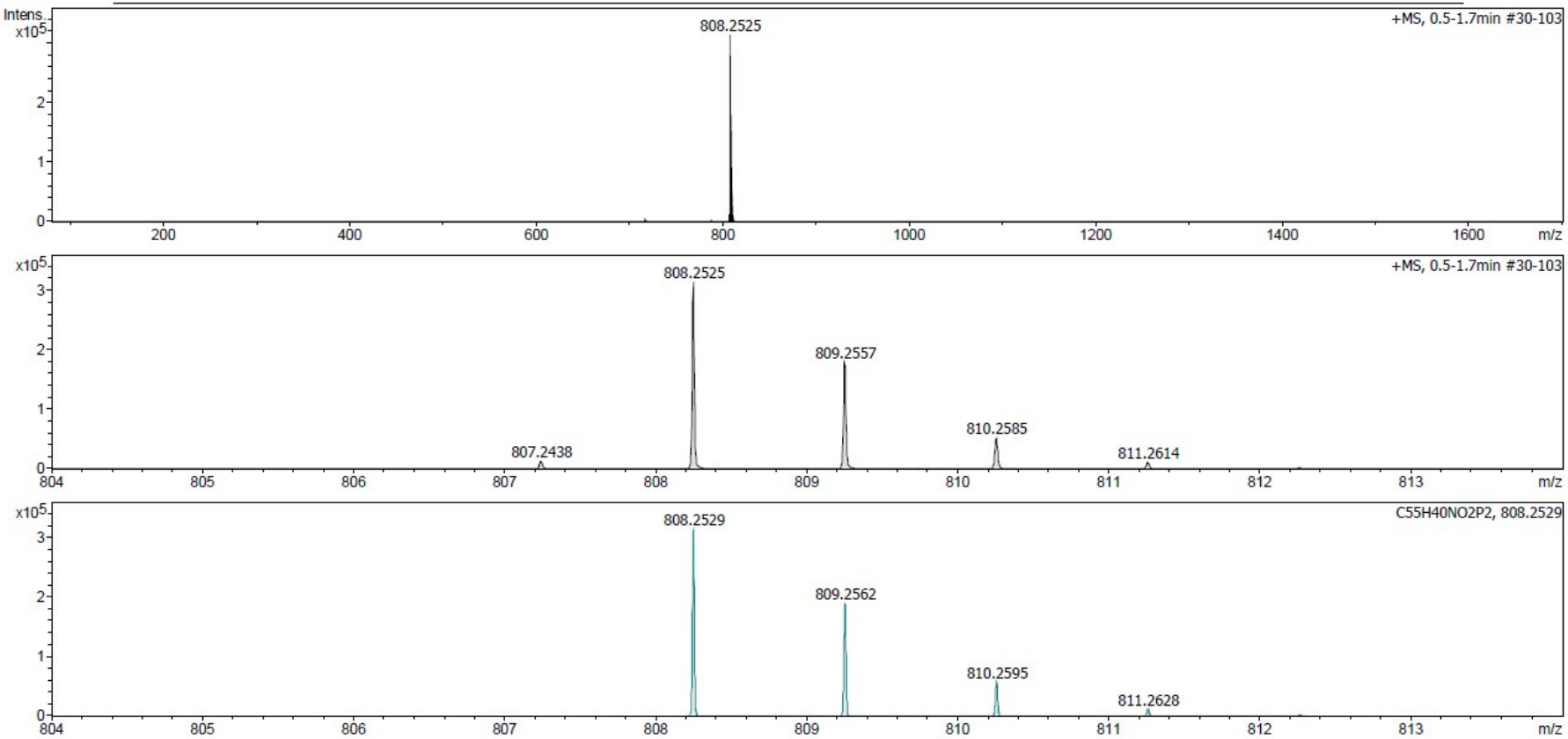

Figure S 82 HRMS spectrum of ***SPA-2,7-F(POPh$_2$)$_2$***

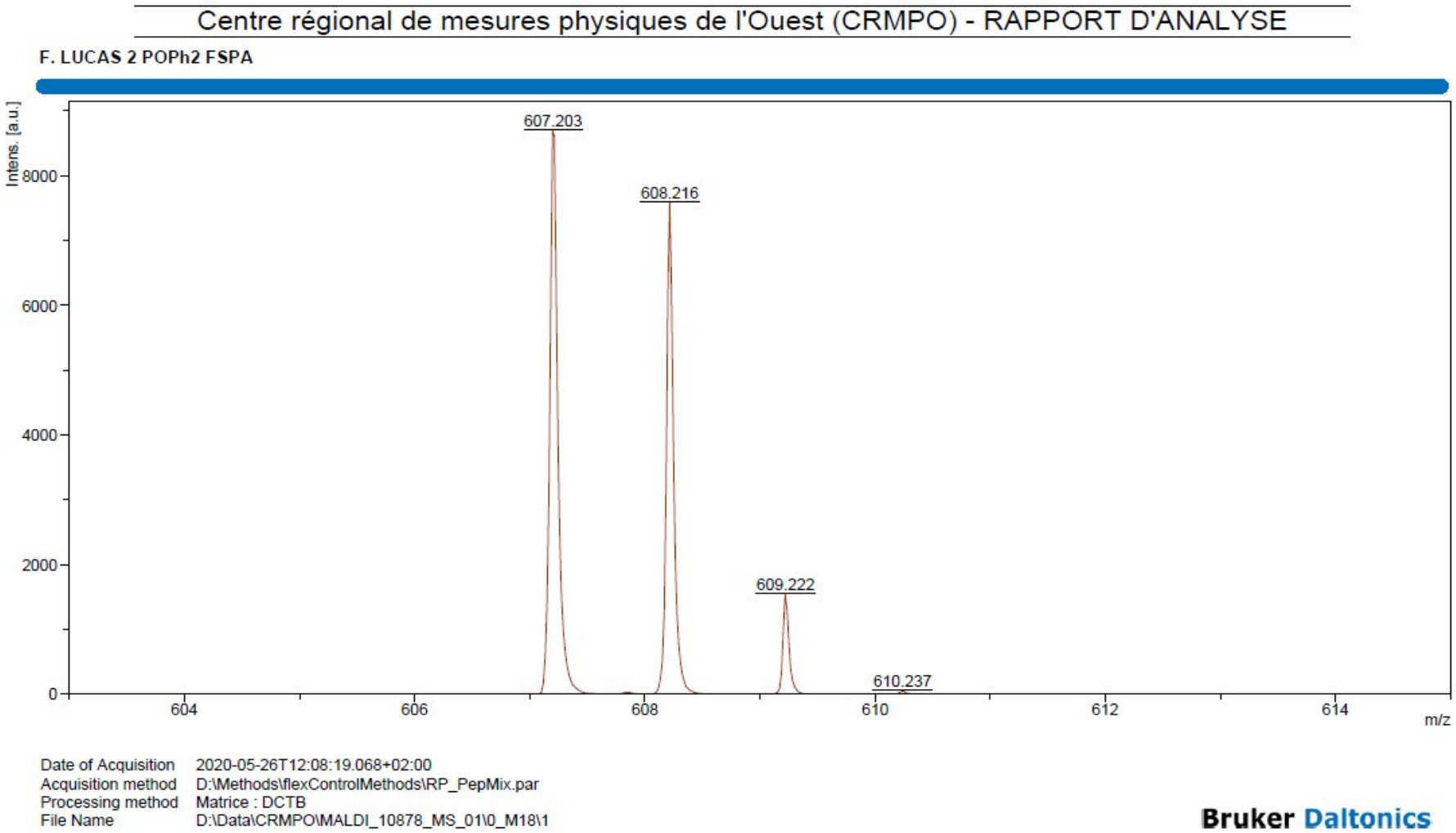

Figure S 83 ***SPA-2-FPOPh$_2$***

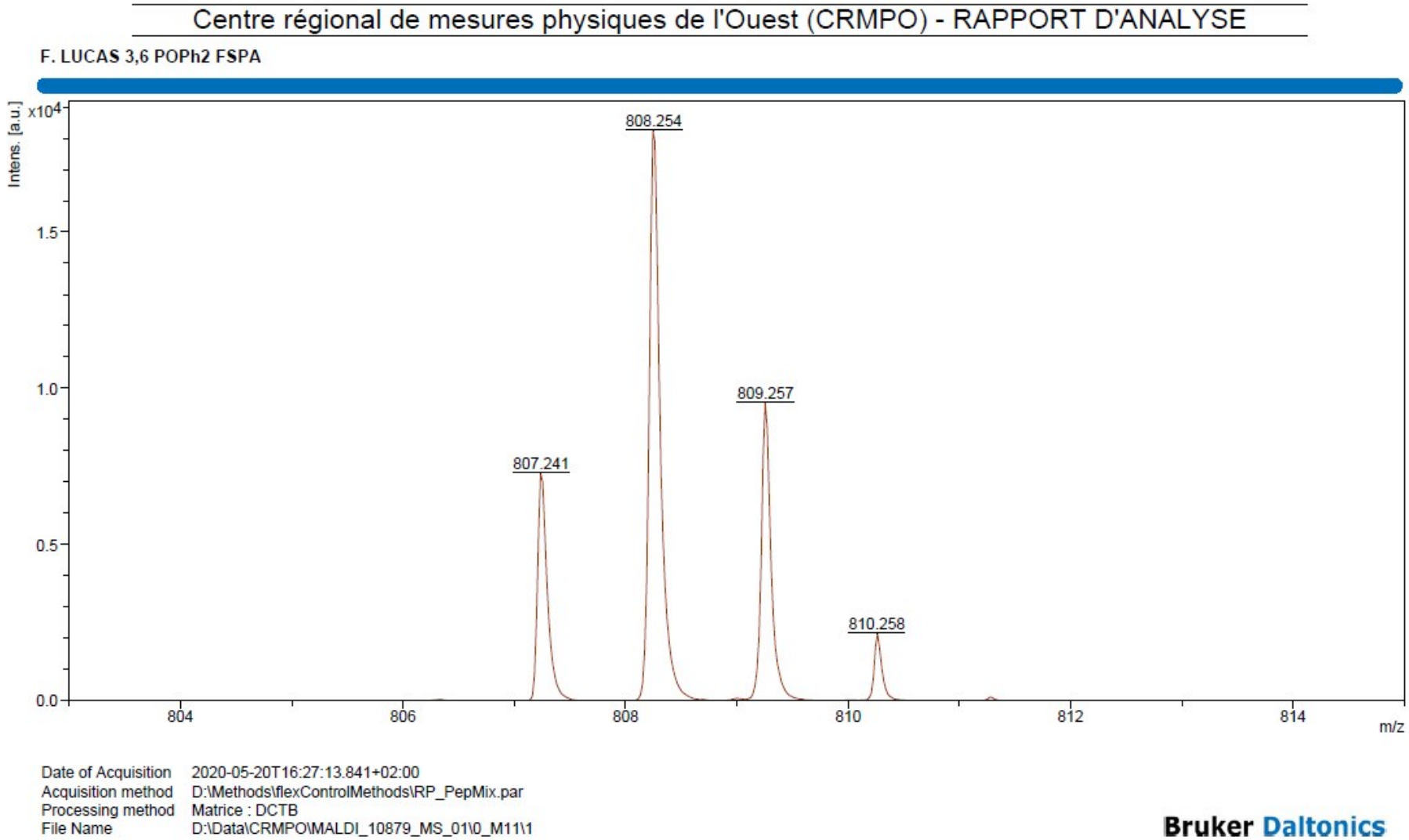

Figure S 84 HRMS spectrum of ***SPA-3,6-F(POPh$_2$)$_2$***

10 References

1. G. R. Fulmer, A. J. M. Miller, N. H. Sherden, H. E. Gottlieb, A. Nudelman, B. M. Stoltz, J. E. Bercaw and K. I. Goldberg, *Organometallics*, 2010, **29**, 2176-2179.
2. A. P. Kulkarni, C. J. Tonzola, A. Babel and S. A. Jenekhe, *Chemistry of Materials*, 2004, **16**, 4556-4573.
3. P. H. a. W. Kohn, *Phys. Rev.*, **136**, B864.
4. J.-L. Calais, *Int. J. Quant. Chem.*, 1993, **47**, 101.
5. A. D. Becke, *Phys. Rev. A*, 1988, **38**, 3098.
6. A. D. Becke, *J. Chem. Phys.*, 1993, **98**, 1372.
7. A. D. Becke, *J. Chem. Phys.*, 1993, **98**, 5648.
8. Y. W. a. R. G. P. Lee C., *phys. rev. B*, 1988, **37**, 785.
9. G. W. T. M. J. Frisch, H. B. Schlegel, G. E. Scuseria, M. A. Robb, J. R. Cheeseman, G. Scalmani, V. Barone, B. Mennucci, G. A. Petersson, H. Nakatsuji, M. Caricato, X. Li, H. P. Hratchian, A. F. Izmaylov, J. Bloino, G. Zheng, J. L. Sonnenberg, M. Hada, M. Ehara, K. Toyota, R. Fukuda, J. Hasegawa, M. Ishida, T. Nakajima, Y. Honda, O. Kitao, H. Nakai, T. Vreven, J. A. J. Montgomery, J. E. Peralta, F. Ogliaro, M. Bearpark, J. J. Heyd, E. Brothers, K. N. Kudin, V. N. Staroverov, T. Keith, R. Kobayashi, J. Normand, K. Raghavachari, A. Rendell, J. C. Burant, S. S. Iyengar, J. Tomasi, M. Cossi, N. Rega, J. M. Millam, M. Klene, J. E. Knox, J. B. Cross, V. Bakken, C. Adamo, J. Jaramillo, R. Gomperts, R. E. Stratmann, O. Yazyev, A. J. Austin, R. Cammi, C. Pomelli, J. W. Ochterski, R. L. Martin, K. Morokuma, V. G. Zakrzewski, G. A. Voth, P. Salvador, J. J. Dannenberg, S. Dapprich, A. D. Daniels, O. Farkas, J. B. Foresman, J. V. Ortiz, J. Cioslowski, D. J. Fox, 2010, Gaussian 09, Revision B.01, Gaussian, Inc., Wallingford CT, 2010.